CATALYSIS BY BOVINE PANCREATIC RIBONUCLEASE A- ENERGETICS AND CONTRIBUTIONS FROM THE ACTIVE-SITE HISTIDINES

by

James E. Thompson

A dissertation submitted in partial fulfillment of the requirements for the degree of

Doctor of Philosophy

(Biochemistry)

at the

UNIVERSITY OF WISCONSIN-MADISON

1995

Acknowledgments

Al Hengge (W.W. Cleland lab) and Marcus Kallesse (L. Keissling lab) aided me in synthesizing UpA and Up(4-nitrophenol) (Chapter 5). Fernando Venegas contributed to both the studies involving ^{31}P NMR (Chapter 2) and cosolvent effects on catalysis (Chapter 3). Michael Schuster, Tatiana Kutateladze, gathered most of the data involving cosolvent effects and the uncatalyzed rate of RNA cleavage (Chapter 3) and June Messmore provided the K41A RNase A used as a control in these studies. Paula Wittmayer and Barbra Templer helped overcome technical obstacles to doing fluorescence polarization anisotropy studies (Chapter 4). Dave Quirk and Brad Kelemen provided their expertise during the titrations of the active site groups as monitored by ^{1}H NMR (Chapter 4). Ron Raines provided good advice, the opportunity to do good science and showed patience with my developing skills. All members of the Raines lab, past and present, provided a pleasant work environment and were both effective critics and sources of scientific ideas. M. Thomas Record and W. Wallace Cleland provided useful input on Chapters 3 and 4 respectively. The National Institutes of Health and the Department of Biochemistry provided support in the form of fellowships.

I must thank my parents and sister for their support and interest as well as for their sympathy. The most constant and important source of support during my time in Madison has been my wife, Brenda Dater. Thanks to my faithful reenactments, no one knows more about my frustrations with failed experiments or successful experiments that yielded only pedestrian findings; no one has more consistently lessened the sting of these frailties that are intrinsic to research.

Abstract

Ribonucleases catalyze the hydrolysis of the P–$O_{5'}$ bond in RNA. This reaction occurs in two steps: *cleavage* of the RNA strand by transphosphorylation to a 2′,3′-cyclic phosphodiester intermediate, and *hydrolysis* of this intermediate to a 3′-phosphomonoester. Chapter 1 discusses the reaction and the particular ribonuclease that we study, RNase A.

^{31}P NMR spectroscopy was used to monitor the accumulation of the 2′,3′-cyclic phosphodiester intermediate during the cleavage and hydrolysis reactions catalyzed by various ribonucleases and by small molecules. In addition, a trapping experiment was used to assess the throughput of the reaction catalyzed by RNase A. Only 0.1% of the RNA substrate was found to be both transphosphorylated and hydrolyzed without dissociating from the enzyme. These results suggest that ribonucleases have evolved primarily to catalyze RNA cleavage and not RNA hydrolysis. These results are discussed in Chapter 2.

We measured the variation of the RNase A specificity constant k_{cat}/K_m with glycerol and found a non-zero dependence. In contrast, the k_{cat}/K_m of a sluggish mutant ribonuclease A showed little dependence on glycerol. These data suggest that catalysis of RNA cleavage by RNase A is limited by a non–chemical step, such as product release or substrate encounter, and not by the conversion of the enzyme–bound substrate to enzyme–bound products. We have also set a lower limit on the rate enhancement of UpA cleavage by RNase A by measuring the rate of UpA cleavage in water which shows that the rate enhancement of RNA cleavage by RNase A is 10^{12}-fold. These results are discussed in Chapter 3.

The active site of bovine pancreatic ribonuclease A (RNase A) contains two histidines, histidine 12 (H12) and histidine 119 (H119). Site–directed mutagenesis was used to replace either H12 or H119 with an alanine residue. Kinetic characterization of the mutants data provides direct evidence that H119 acts as an acid catalyst during cleavage and indicate that each active-site histidine residue can stabilize the transition state by >5 kcal/mol. The pK_a's of the mutant enzymes' active-site histidines were measured in the presence and absence of inhibitor, which showed that the histidines act synergistically to bind the inhibitor. The interactions of the mutant enzymes with a substrate analog were measured, and removal of H12 or H119 was shown to decrease the enzyme's affinity for the inhibitor. These studies are described in Chapter 4.

Table of Contents

List of Figures

List of Tables

List of Schemes

List of Abbreviations

A; adenosine

A>p; adenosine 2′,3′ cyclic monophosphate

3′-AMP; adenosine 3′-monophosphate

5′–AMP; adenosine 5′–monophosphate

CpA; cytidylyl (3′→ 5′) adenosine

Cp (methoxy); cytidine 3′-methoxyphosphate

C>p; cytidine 2′,3′ cyclic monophosphate

DEPC; diethylpyrocarbonate

H12; histidine 12

H119; histidine 119

HEPES; *N*-(2-hydroxyethyl)piperazine-*N*′-(2-ethanesulfonic acid)

MES; 2-(*N*-morpholino)ethanesulfonic acid

3′-NMP; 3′ ribonucleoside monophosphate

NMR; nuclear magnetic resonance

N>p; ribonucleoside 2′,3′ cyclic monophosphate

NpN; RNA phosphodiester

poly(C); polycytidilic acid

polyU; polyuridylic acid

PEI; poly(ethylenimine)

RNase; ribonuclease

RNase A; bovine pancreatic ribonuclease A

SDS; sodium dodecyl sulfate

TBAP; tetrabutylammonium phosphate

TLC; thin-layer chromatography

UpA; uridylyl(3′→ 5′)adenosine

U>p; uridine 2′,3′-cyclic phosphate

U>v; uridine 2′,3′-cyclic vanadate

2′-UMP; uridine 2′–monophosphate

3′-UMP; uridine 3′-monophosphate

Up (4–nitrophenol); Uridine 3′- (4–nitrophenylphosphate)

Chapter 1
Introduction

In studying living systems, nothing can appeal to the chemist as do enzymes. The protein catalysts that guide most chemical reactions in every living system are capable of large rate accelerations; ornithine monophosphate decarboxylase is the highest measured to date at 10^{17}-fold faster than the uncatalyzed reaction (Radzicka, A. 1995). Enzymes are also highly specific catalysts. Valyl-tRNA synthetase binds valine 100–200 times tighter than threonine, which is isosteric to valine (Fersht, A. 1985). With enzymes, living organisms control virtually every reaction that occurs within them so that metabolism can be regulated to adapt to a wide variety of environments (Hochachka, P.W. 1984). Reactions as simple as the hydration of carbon dioxide are catalyzed, and hence controlled, by enzymes. It is the ultimate goal of enzymology to understand the structural features that imbue enzymes with their catalytic efficiency and specificity.

Bovine pancreatic ribonuclease A (RNase A; E.C. 3.1.27.5) has been studied with these goals in mind since the 1940's. The enzyme is purified from bovine pancreas, a readily available and rich source of the enzyme (Kunitz, M. 1939). RNase A catalyzes the hydrolysis of the P–$O_{5'}$ bond of RNA. It does so by catalyzing two reactions. The *cleavage* reaction is a transphosphorylation in which the 2′ oxygen attacks the phosphate and the P–$O_{5'}$ bond is broken (Figure 1.1a). Both enzymatic and nonenzymatic reactions benefit from base (𝔹) catalyzed deprotonation of the attacking 2′–OH and acid (𝔸–ℍ) catalyzed protonation of the 5′–OH leaving group. The cleavage reaction yields a 2′,3′-cyclic phosphodiester (N>p) and a free 5′–OH. The *hydrolysis* reaction is an attack of water on the N>p, which yields a 3′-monophosphate (Figure 1.1b). The roles for acid and base catalysis are opposite to those played in the cleavage reaction; there is base assisted attack of water and acid assisted departure of the 2′–OH leaving group. Figure

1.1 describes the net bond making and breaking during the two reactions, and it also describes the simplest mechanism consistent with all kinetic data available for RNase A. However, the mechanism of small molecule catalysis of these reactions by has been proposed to go through a stable phosphorane (Breslow, R. 1989) and there are a number of proposals for the enzymatic mechanism (Witzel, H. 1963; Breslow, R. 1989; Gerlt, J.A. 1993), which continue to be vigorously debated (Menger, F.M. 1991; Herschlag, D. 1994).

RNase A is active as a monomer of 13,788 amu and requires no cofactors to catalyze the degradation of RNA. It is also active in a dimeric and trimeric form, but is purified most often as a monomer (Crestfield, A.M. 1962; Kim, J.-S. 1993). The "A" form is the unglycosylated form of the enzyme. Barnard noted that in ruminal animals, the pancreatic RNase was present at roughly 0.2 – 1 mg/g of pancreatic tissue compared to 1 μg/g in man and other non-ruminants. *In vivo*, RNase A is secreted into the rumen, and Barnard concluded that RNase A serves to degrade ingested RNA in a pathway that yields phosphate to fulfill the nutritional needs of ruminal bacteria (Barnard, E.A. 1969).

To evaluate RNase A as a candidate for experiments exploring enzyme structure–function relationships, it seems self-evident that both structure and function must be defined as well as possible. Structurally, RNase A is well characterized. There are dozens of structures of the enzyme currently available and they include the free enzyme (Nachman, J. 1990), the enzyme complexed with phosphate (Wlodawer, A. 1981), with substrate analogs (Aguilar, C.F. 1992; Fontecilla–Camps, J.C. 1995), products (Zegers, I. 1994), and transition state analogs at (Borah, B. 1985). The resolution of these structures is as high as 1.5 Å (Aguilar, C.F. 1992), but this list is not comprehensive.

The function of RNase A has been probed mainly by measurement of steady-state kinetic parameters. The pH, salt and temperature dependence of the hydrolysis reaction have been characterized (Findlay, D. 1961; Eftink, M.R. 1983). Pre-steady state kinetics have been measured for the substrate association in the hydrolysis reaction (Erman, J.E. 1966). The kinetic parameters (*i.e.*, k_{cat} and K_m) of the cleavage reaction have been measured with a variety of substrates (Richards, F.M. 1971; Davis, A.M. 1988), under a variety of pH's (Richards, F.M. 1971). The plethora of structural and functional data available makes RNase A an ideal candidate for enzyme structure – function correlation.

The goals of the research reported here may be divided into two categories. First, we seek to better define the function of wild–type RNase A. Second, we seek to perturb the structure of RNase A and to characterize the function of the altered enzymes. In doing so, we hope to better understand the structural determinants of the catalytic activity of RNase A and to generate catalysts with new properties.

Defining the function of RNase A. Although there is an abundance of data on the function of RNase A, there are still gaps in the functional characterization that warrant attention. For instance, although the cleavage and hydrolysis reactions are extensively characterized individually, there is no definitive data on the behavior of RNase A when carrying out both reactions simultaneously. The two reactions shown in Figure 1.1 form a full catalytic cycle, but there is evidence that some N>p might dissociate from the enzyme (Markham, R. 1952; Cozzone, P.J. 1977; Day, A.G. 1992). Chapter 2 details our experiments that define quantitatively the kinetic linkage of the cleavage and hydrolysis reactions. We also compare the relative energetics of enzymatically and non-

enzymatically catalyzed cleavage and hydrolysis reactions which illustrates functional differences between the two types of catalysts.

Also, two key pieces of functional information are missing from descriptions of RNase A as a catalyst of the cleavage reaction. The uncatalyzed rate of RNA cleavage is not known, and so the absolute value of RNase A as a catalyst cannot be determined. The other vital gap in the characterization of the cleavage reaction is the nature of the rate–limiting step. Organisms can gain an advantage over competing organisms if their enzymatic catalysts are more efficient (Burbaum, J.J. 1989). The molecular evolution afforded by selective pressure has yielded many enzymes that catalyze reactions at rates that are no longer limited by the chemical conversion of bound substrate to bound products. Instead they are limited by substrate association or product release (Cleland, W.W. 1975; Blacklow, S.C. 1988). The nature of the rate limiting step in RNase A-catalyzed cleavage of RNA has never been determined. In order to understand the changes in enzyme function engendered by structural perturbation, it is important to know the rate-limiting step and the overall rate enhancement. Chapter 3 addresses both of these concerns for RNase A-catalyzed cleavage.

Structural perturbation and functional characterization Recombinant DNA technology has provided a useful method to explore enzyme structure – function relationships: one perturbs the structure of the enzyme by site-directed mutagenesis and characterizes the functional change that results (Knowles, J.R. 1987). Recombinant forms of RNase A have only recently become available, which reflects the difficulties inherent in cloning and expressing the enzyme. Expression of synthetic and native

RNase A genes was attempted in a variety of systems which suffered from low yields and undesirable modifications of the enzyme (for a review see del Cardayré et al., 1994). A breakthrough came when del Cardayré *et. al.* found that expression of the RNase A gene fused with a *pelB* leader sequence under the control of the T7 promoter in *E. coli* yielded wild-type sequence RNase A in insoluble inclusion bodies at 50 mg/l of culture (delCardayré, S.B. 1995). The insolubility of RNase A solved an anticipated problem: an overexpressed ribonuclease would probably be cytotoxic. RNase A is a protein that can be refolded easily (Anfinsen, C.B. 1973; McGeehan, G.M. 1989), so purification of the enzyme from the insoluble misfolded aggregate was successful (delCardayré, S.B. 1995).

With the expression system in place, the primary obstacle to manipulation of the primary sequence of RNase A was overcome. Candidate residues for protein engineering were selected on the basis of their conservation across the family of sequenced pancreatic ribonucleases and also by their position in the enzyme. To date, work in the Raines lab has focused on residues in or near the RNase A active site. Figure 1.2 shows the active-site of RNase A complexed with uridine vanadate (U>v), a putative transition state analog (Borah, B. 1985). This structure shows that the side chains of Lys41, His12, His119, and Gln11 are in positions to interact with U>v. It also shows that the mainchain amide of Phe120 can interact with U>v.

Lys41 is close to the phosphate, but actually forms a hydrogen bond with the 2′–oxygen. Lys41 could serve as an electrostatic catalyst during RNA cleavage, stabilizing the buildup of negative charge on phosphorus with its positive charge. Alternatively, Lys41 could polarize the substrate 2′–OH to facilitate deprotonation by His12. Lys41 has been altered by site–directed mutagenesis and also by replacement with different covalent

adducts of a K41C mutant (Messmore, J.M. 1995). The functional characterization of these mutants shows that eliminating Lys41 causes a 10^5-fold drop in catalytic efficiency, verifying the residue's importance in stabilizing the transition state of the cleavage reaction. In addition, the loss of catalytic efficiency correlates inversely with pK_a of the side chain, which suggests that the purpose of Lys41 is to donate a hydrogen bond to the transition state. This result is consistent with either of the proposed mechanistic roles of Lys41 suggested above.

The side chain of Gln11 is found in a hydrogen bond with a nonbridge oxygen in the complex with U>v (Borah, B. 1985). This interaction could stabilize the transition state. However, there was only a small effect on catalysis upon mutation of Gln11. Characterization of mutants at Gln11 with a variety of substrates showed that elimination of the Gln11 sidechain caused a drop in both k_{cat} and K_m (delCardayré, S.B. 1995). These results show that Gln11 can prevent nonproductive binding of substrate. It is interesting that the overall effect on k_{cat}/K_m seen on eliminating Gln11 is only twofold. Gln11 is absolutely conserved through the sequenced pancreatic ribonucleases, yet has only the modest effect described on RNase A function.

Asp121 forms a hydrogen bond with His119 in most crystal structures. Although it does not directly contact the substrate, Asp121 is conserved and forms a "catalytic dyad" when hydrogen bonded to His119. The "catalytic dyad' terminology was coined to highlight the similarity to the active-site of the serine proteases, where the active features an aspartate:histidine:serine network that acts to increase the nucleophilicity of the serine. This comparison is particularly interesting when considering the hydrolysis reaction, as His119 is thought to deprotonate a water molecule for attack on the

phosphate. In this case, water is activated in a way analogous to activation of serine in the serine proteases. This may be an example of convergent evolution. However, the effects of mutating Asp121 on enzyme function are small; less than a twofold drop in k_{cat}/K_m is observed on changing this residue to alanine (Quirk, D.J. 1995).

Study of the active-site residues has clarified the roles of these residues in the function of RNase A. Other studies have also yielded enzymes with novel properties. For example, structures of the enzyme complexed with uridine monophosphates showed that the side-chain of Thr45 made noncovalent contacts with uracil; Thr45 is absolutely conserved throughout pancreatic ribonucleases. RNase A has a 10^4-fold preference (as measured by k_{cat}/K_m) for pyrimidines 3′ to the scissile phosphodiester. On mutation of Thr45 to alanine or glycine, the preference for pyrimidines is reversed, establishing that Thr45 mediates the 3′ pyrimidine specificity (delCardayré, S.B. 1994). In addition, this enzyme cleaves a long strand of polyadenylic acid in a processive manner, instead of binding and releasing after cleavage.

The residues under scrutiny in this work are the two active-site histidines. His12 and His119 have been identified as important for catalysis by a variety of experimental approaches. RNase A that had been chemically modified with haloacetic acids was shown to have greatly reduced activity; modification of His12 or His119 was sufficient to nearly inactivate the enzyme (Crestfield, A.M. 1963). In addition, the pH dependence of k_{cat}/K_m for RNase A-catalyzed cleavage of the dinucleotide substrates UpA and CpA is bell-shaped with a maximum at about pH 6. This dependence is consistent with an active site that contains two residues of pK_a ~6, one of which must be protonated and the other

unprotonated for catalysis to occur. The residues in the active site that are most likely to have these properties are His12 and His119.

Histidines 12 and 119 could serve as general acids and bases during catalysis by RNase A. General acid/base catalysis is often observed when abstraction or donation of a proton is likely to be rate limiting (Jencks, W.P. 1987). Since the cleavage reaction requires removal of a proton from a secondary alcohol ($pK_a \sim 14$) it is a candidate for general base catalysis. Also, the leaving group is a primary alkoxide whose conjugate acid has $pK_a \sim 14.8$ (Ballinger, P. 1960) and whose departure would be facilitated by general acid catalysis. For an amino acid side-chain to act as a general acid/base catalyst, it must be in the correct protonation state. For example, to deprotonate a high pK_a moiety it would be effective to employ a base of higher pK_a than histidine, such as lysine. However, at physiological pH, the ε–amino group of lysine is mostly protonated and cannot serve as a general base. The imidazole side chain of histidine is in a mixed protonation state at physiological pH and serves as a general acid or base in a variety of enzymes, such as mandelate racemase and triose phosphate isomerase (Gerlt, J.A. 1993). Chapter 4 contains the results of structural perturbations at His12 and His119 on enzyme function, affinity for the substrate analog and on the charge structure of the RNase A active site.

* * *

Work on RNase A has provided much insight into enzymatic catalysis, protein folding, and structural stability. Two Nobel prizes have been awarded to researchers who used RNase A as a subject for their research. Anfinsen, Stein and Moore shared a prize after elucidating the primary structure of RNase A and showing that the primary structure

determined the tertiary structure, and hence the function of RNase A (Anfinsen, C.B. 1973). The second Nobel prize involving RNase A was awarded to Merrifield for complete chemical synthesis of the enzyme. The research described in this thesis is unlikely to be the third body of work to receive such recognition. However, we have been successful in characterizing the rate-limiting step and the overall rate enhancement of the RNase A-catalyzed cleavage of RNA. The protein engineering we have carried out provides some new information about the roles of the active-site histidines in catalysis by RNase A and has yielded an enzyme with novel catalytic properties. In the final analysis, we understand RNase A a little better for having carried out these studies, which is as much as a young researcher can ask.

Figure 1.1

The two reactions catalyzed by RNase A: cleavage (**A**) and hydrolysis (**B**). This figure describes the overall changes in bonding during the reactions and is also the simplest mechanism consistent with all kinetic data available on catalysis by RNase A. Based on structural and kinetic data, His12 is proposed to be $\mathbb{B}$ and His119 to be $\mathbb{A}$.

A

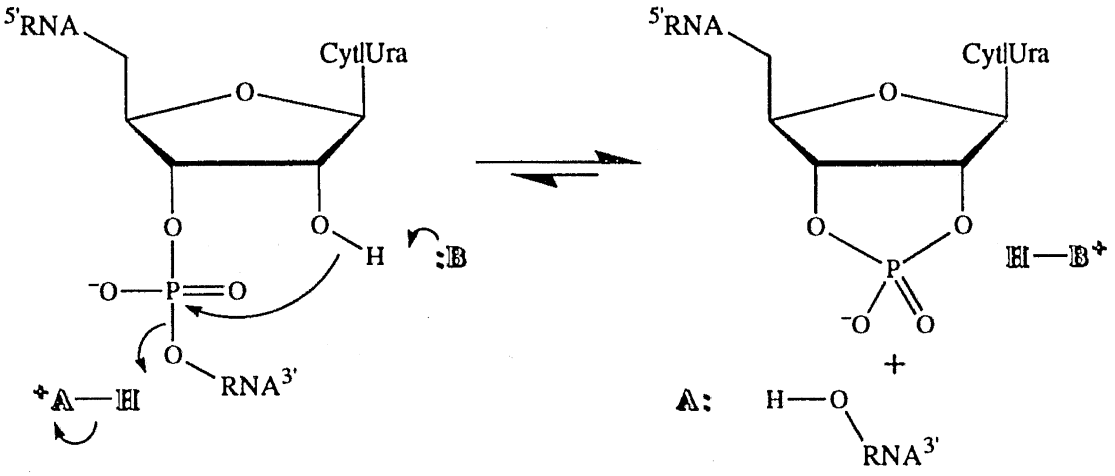
5'RNA
Cyt|Ura
O
O
O
H
:B
⁻O—P═O
O
RNA3'
+A—H
5'RNA
Cyt|Ura
O
O
O
P
⁻O
O
H—B+
+
A:
H—O
RNA3'

B

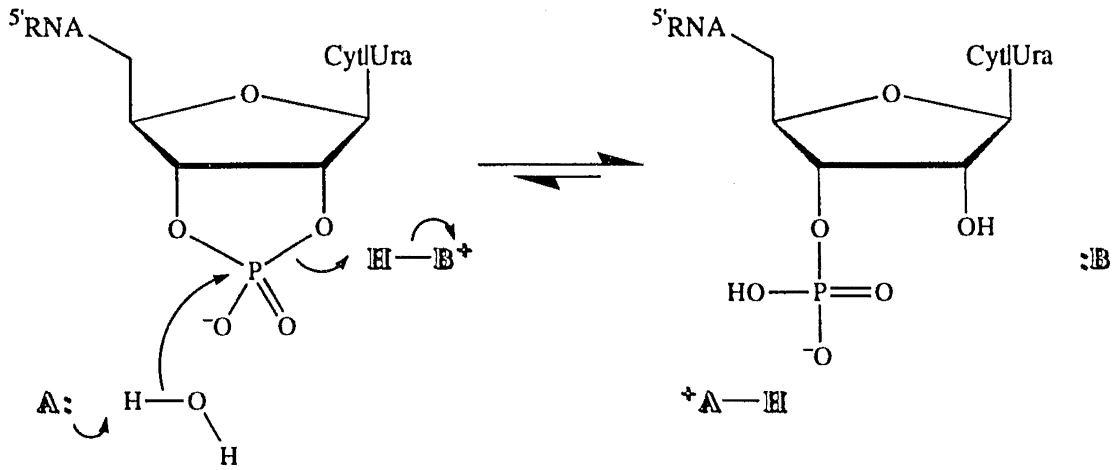
5'RNA
Cyt|Ura
O
O
O
P
⁻O
O
H—B+
A:
H—O
H
5'RNA
Cyt|Ura
O
OH
O
HO—P═O
⁻O
:B
+A—H

Figure 1.2

The structure of the RNase A active-site complexed with U>v (Borah, B. 1985).

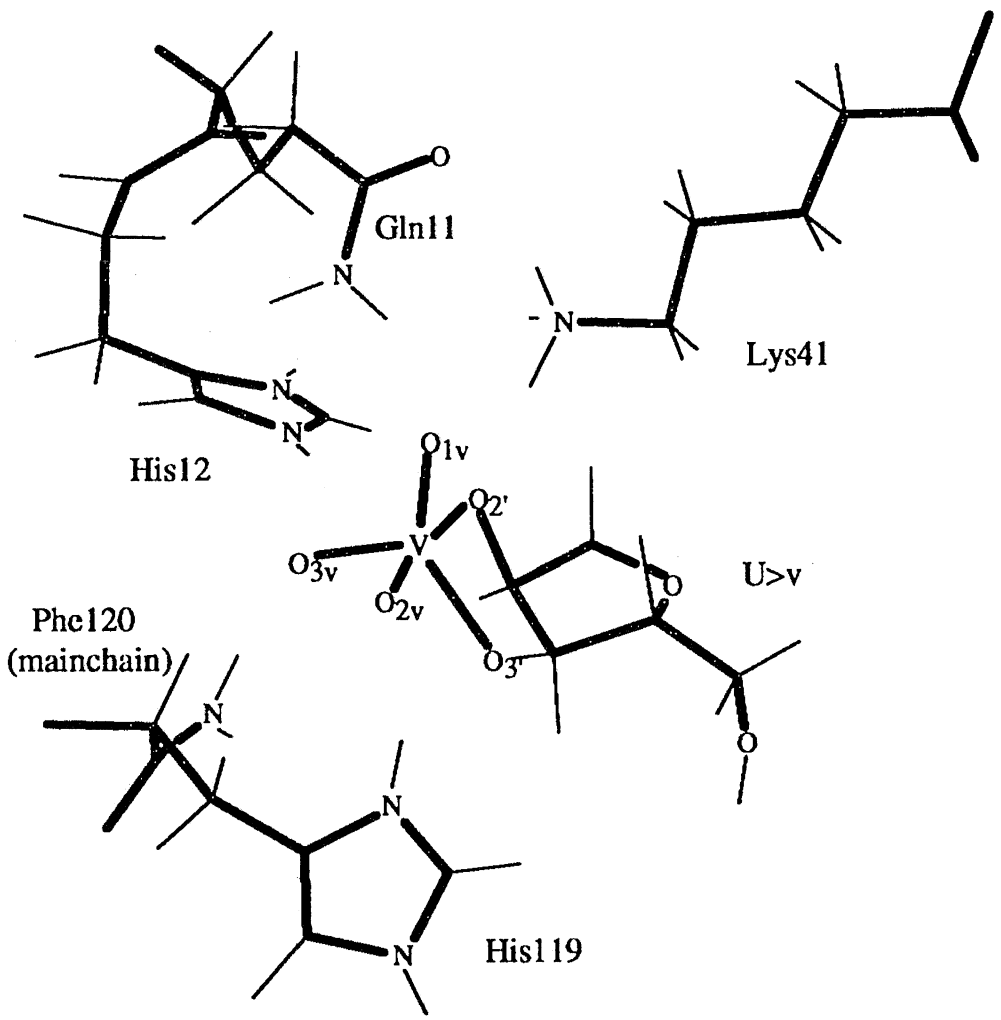
Gln11
Lys41
His12
O1v
O2'
V
O3v
O2v
O3'
U>v
Phe120
(mainchain)
His119

Chapter 2

Fate of the 2′,3′-cyclic phosphodiester intermediate

Published as: James E. Thompson, Fernando D. Venegas, Ronald T. Raines (1994) Energetics of Catalysis by Ribonucleases: Fate of the 2′,3′-cyclic phosphodiester intermediate. *Biochemistry*, **33**, 7408–7414.

Summary

Ribonucleases catalyze the hydrolysis of the P–$O_{5'}$ bond in RNA. This reaction occurs in two steps: *cleavage* of the RNA strand by transphosphorylation to a 2′,3′-cyclic phosphodiester intermediate, and *hydrolysis* of this intermediate to a 3′-phosphomonoester. ^{31}P NMR spectroscopy was used to monitor the accumulation of the 2′,3′-cyclic phosphodiester intermediate during the cleavage and hydrolysis reactions catalyzed by various ribonucleases and by small molecules. The intermediate was found to accumulate during catalysis by monomeric bovine pancreatic ribonuclease A (RNase A), a dimer and trimer of RNase A, bovine seminal ribonuclease, RNase T_1, barnase, and RNase I. These enzymes, which are of widely disparate phylogenetic origin, released rather than hydrolyzed most of the intermediate formed by cleavage of RNA. In contrast, the intermediate did not accumulate during catalysis by hydroxide ion or imidazole buffer. In the presence of these small molecules, hydrolysis is faster than cleavage. A trapping experiment was used to assess the throughput of the reaction catalyzed by RNase A. [5,6-^{3}H]UpA was incubated with RNase A in the presence of excess unlabeled U>p, which dilutes the specific radioactivity of any released cyclic intermediate. Only 0.1% of the RNA substrate was found to be both transphosphorylated and hydrolyzed without dissociating from the enzyme. These results suggest that ribonucleases have evolved primarily to catalyze RNA cleavage and not RNA hydrolysis.

Introduction

Bovine pancreatic ribonuclease A (RNase A) and other RNases catalyze the hydrolysis of the P–$O_{5''}$ bond of ribonucleic acids (RNA). It has long been known that the reaction catalyzed by RNase A proceeds by a two–step mechanism: cleavage of the RNA by transphosphorylation to form a 2′,3′-cyclic phosphodiester intermediate and hydrolysis of this cyclic intermediate to form a 3′-phosphomonoester (3′ NMP) (Figure **1.x)** (Markham, R. 1952; Brown, D.M. 1953).

Model chemistry performed by Westheimer and coworkers (Kumamoto, J. 1956) showed that cyclic phosphodiesters are cleaved at 10^8–fold faster than linear phosphodiesters. Originally the increased reaction rate was attributed to the relief of strain in the trigonal bipyramidal transition state of cyclic phosphate hydrolysis. This explanation has been challenged by theoretical work suggesting that favorable solvation of the transition state is the source of the rate enhancement (Dejaegere, A. 1993). However, Westheimer's experimental results stand and suggest that the hydrolysis reaction may occur faster than cleavage in the absence of catalysts.

To understand the energetics and mechanism of catalysis by RNases, the kinetic linkage of the two reactions must be determined. In other words, after cleavage, how does the enzyme-bound N>p partition between hydrolysis and dissociation? Researchers and textbook authors have presumed that the reactions catalyzed by RNases yield 3′-NMPs, an assumption that may not be valid (Cuchillo, C.M. 1993). We report here an investigation of the accumulation of N>p during the hydrolysis of RNA as catalyzed by a variety of enzymes and small molecules. We also quantify the amount of substrate that remains bound to the enzyme through both steps of RNase A-catalyzed hydrolysis of the dinucleotide UpA. These results provide a quantitative measure of the kinetic linkage of

the cleavage and hydrolysis reactions and illuminate energetic features of catalysis by RNases.

Results

^{31}P NMR Analysis. Phosphorus exists in three chemical states (NpN, N>p, and 3′-NMP) during the ribonuclease–catalyzed degradation of RNA. The ^{31}P NMR chemical shifts of these states are: –0.5 ppm for NpN (starting material), 19.1 ppm for N>p (intermediate product), and 3.4 ppm for 3′-NMP (final product). ^{31}P NMR spectroscopy was used to follow the time-course for the hydrolysis of RNA.

The time-course for the degradation of poly(U) as catalyzed by hydroxide ion showed that poly(U) was converted to 3′-UMP without the accumulation of U>p (Figure 2.1). The reaction catalyzed by imidazole buffer (data not shown) gave a similar result. In contrast the time course of RNase A–catalyzed degradation of poly(U), showed that a large fraction of the poly(U) was converted to U>p before any 3′-UMP was detected (Figure 2.2). At short times, the U>p produced was heterogeneous, as evidenced by the multiple resonances between δ 19.1 and δ 19.5. The downfield resonance has a chemical shift identical to that of authentic U>p. The upfield resonance is likely to be from the cyclic phosphodiester in poly(U)U>p [that is, U>p at the 3′-end of poly(U)], which has a more shielded phosphorous atom. At long times, the poly(U)U>p was converted to U>p, which was eventually hydrolyzed to 3′-UMP. The reactions catalyzed by dimeric RNase A, trimeric RNase A, dimeric bovine seminal ribonuclease, RNase T_1, barnase, and RNase I gave time-courses (data not shown) similar to that shown in Figure 2.2. The RNase A-catalyzed hydrolysis of UpA showed complete conversion of UpA to U>p before any 3′-UMP was detected (data not shown). No 2′,3′-cyclic phosphodiester intermediate was detected in RNA hydrolysis catalyzed by staphylcoccal nuclease, which

is believed not to produce such an intermediate (Cotton, F.A. 1979). No poly(U) cleavage was detected after 2 days in 2.5 M NaCl at 70 °C, nor was any DNA cleavage detected after 1 h in 0.2 M NaOH at 25 °C.

Synthesis of [5,6 -^{3}H]UpA. The synthesis of [5,6 -^{3}H]UpA was successful by the following criteria. Synthetic [5,6-^{3}H]UpA was a single peak by PEI cellulose TLC (R_f 0.04, system C). Treatment of this material with RNase A produced initially a radiolabeled product that co-migrated during TLC with U>p (R_f 0.37, system C). This material was eventually converted to a product that co-migrated during TLC with Up (R_f 0.67, system C).

Throughput Experiment. RNase A catalyzes the cleavage of [5,6-^{3}H]UpA to form labeled U>p and unlabeled A. The resulting enzyme-bound U>p can have two fates: release from the enzyme into solvent or hydrolysis by the enzyme to form 3′-UMP. The throughput experiment was designed to measure the partitioning between these two possible fates. In this experiment, RNase A catalyzes the cleavage of labeled UpA in the presence of a large pool of unlabeled U>p. This large pool traps any labeled U>p released from the enzyme by diluting its specific radioactivity. Under these conditions, rebinding and hydrolysis of labeled U>p is insignificant. Labeled 3′-UMP will only be formed if labeled U>p (from cleavage of labeled UpA) suffers hydrolysis rather than release to solvent, as shown in Scheme 2.1.

Elution profiles for the throughput experiment are shown in Figure 2.3 and the resulting radiochemical analyses are shown in the inset of Figure 2.4. A plot of the time-course of the labeled 3′-UMP:labeled U>p ratio is also shown in Figure 2.4. The shape of this particular plot reports on the ability of unlabeled U>p to trap any labeled U>p that is released during catalysis. Complete trapping would yield a line of slope zero. Since

the labeled 3′-UMP:labeled U>p ratio increased only slowly during the time-course of the experiment, the pool of unlabeled U>p was apparently effective at competing with labeled U>p for re-binding to the enzyme.

The *y*-intercept of the plot in Figure 2.4 describes the fate of the U>p produced during the initial turnover of UpA by RNase A. Any labeled 3′-UMP formed during this turnover can only derive from the throughput of labeled UpA, since no labeled U>p is present. In theory, the intercept in Figure 2.4 can range from zero (for no throughput) to infinity (for complete throughput). Although the intercept is unaffected by the degree of trapping, it can be estimated more accurately if the trap is effective so that the labeled 3′-UMP:labeled U>p ratio is constant. An exponential fit of the data in Figure 2.4 gives an intercept of approximately $1x10^{-3}$, which indicates that labeled U>p was released by RNase A $1x10^{3}$ times more often than it was hydrolyzed. A control reaction containing no RNase A was unchanged over the time–course of the experiment.

Discussion

The kinetic linkage of cleavage and hydrolysis. Studies of phosphodiester cleavage showed that hydrolysis of ethylene phosphate is 10^{8}–fold faster than that of dimethyl phosphate (Kumamoto, J. 1956). A key deficiency of dimethyl phosphate as a model for RNA is the lack of an intramolecular nucleophile analogous to the 2′–OH of RNA. The hydrolysis of dimethylphosphate is intermolecular whereas the cleavage of RNA is intramolecular, a difference that will mean faster rates of cleavage of RNA.

The rates of linear phosphodiesters cleavage by RNase A vary widely compared to the rates of cyclic phosphodiester hydrolysis. The value of k_{cat} for cleavage is 1- to 10^{3}-fold greater than that for hydrolysis depending on the substrate [CpA is the fastest

and Cp (methoxy) the slowest substrate for cleavage (Richards, F.M. 1971)]. These kinetic parameters suggest that the cyclic intermediate may dissociate from the enzyme. Qualitative support for this hypothesis can be found in the early RNase A literature. For instance, Markham and Smith were able to isolate N>p from yeast RNA that had been exposed to RNase A (Markham, R. 1952). Also, the products of the RNase A–catalyzed reaction with polyadenylic acid were monitored by ^{31}P NMR and shown to proceed only to A>p (Cozzone, P.J. 1977). The subsequent slow hydrolysis of the A>p to 3′-AMP was assumed to be non-enzymatic. Recently, the bacterial ribonuclease barnase was shown to yield product mixtures containing only N>p (Day, A.G. 1992).

^{31}P NMR is a useful tool for monitoring the relative rates of cleavage and hydrolysis of RNA. RNA, N>p, and 3′-NMP have well dispersed chemical shifts and can be monitored simultaneously. The accumulation of N>p indicates that cleavage occurs faster than hydrolysis. Several RNase catalyzed reactions were monitored and all were found to accumulate N>p, indicating that the rate of hydrolysis is slower than the rate of cleavage. The RNases surveyed were of disparate phylogenetic origin and cellular location. RNase A, its multimers and bovine seminal ribonuclease are bovine enzymes (*bos taurus*) that are secreted into the gut and seminal fluid respectively. RNase 1 is produced by *E. Coli* and is maintained in the cell. Barnase is from *bacillus amyloliquefaciens* and RNase T1 is from *Aspergillus oryzae*, a fungus. These enzymes all catalyze cleavage to a greater extent than hydrolysis.

The results of the ^{31}P NMR experiments imply that the value of k_{cat}/K_m for the cleavage of RNA is greater than k_{cat}/K_m for the hydrolysis of the 2′,3′-cyclic phosphodiester (Raines, R.T. 1988). For RNase A, this finding is consistent with steady-

state kinetic parameters. Under the conditions used here, the value of k_{cat}/K_m [= $2.3x10^6$ $M^{-1}s^{-1}$ (delCardayré, S.B. 1995)] for cleavage of UpA is 10^3–fold higher than that [= $1.7x10^3$ $M^{-1}s^{-1}$ (delCardayré, S.B. 1994)] for hydrolysis of U>p. As predicted from these values, little 3′-UMP is detected by ^{31}P NMR spectroscopy (data not shown) or TLC (Figures 2.3 and 2.4) until all of the UpA has been converted to U>p. In contrast, 3′-UMP is detected before poly(U) is transphosphorylated completely by RNase A (Figure 2.2). This result is also consistent with steady-state parameters, since the value of k_{cat}/K_m [= $3.88x10^4$ $M^{-1}s^{-1}$; (del Rosario, E.J. 1969)] for the cleavage of UpU is only 10–fold higher than that for the hydrolysis of U>p. The steady-state parameters were measured for the cleavage and hydrolysis reactions separately, and the NMR experiment monitored both reactions simultaneously. The agreement between the NMR data and the steady-state data suggest that RNase A catalyzes cleavage and hydrolysis as kinetically discrete steps.

The energetics of enzymatic and small molecule catalysis of RNA degradation. Since no U>p accumulates on degradation of poly(U) at 0.2 M NaOH, cleavage must limit the rate of this reaction (Figure 2.1). Single stranded DNA shows no cleavage at all under identical conditions, so the 2′–OH of RNA is required for reaction with hydroxide; this suggests U>p forms and is quickly hydrolyzed. Poly(U) degraded by imidazole shows a similar product mixture (data not shown). We conclude that the free energy barriers to catalysis of RNA degradation by RNases are qualitatively different than the barriers to catalysis by small molecules (illustrated in Figure 2.5). Because RNase A has two active-site histidines essential for catalysis, comparison with the imidazole data is particularly salient. Free imidazole experiences the barriers to catalysis shown by the

dashed lines, but the same functionality positioned in the RNase A active-site as histidine experiences completely different barriers shown by the solid lines (Figure 2.5). The additional catalytic machinery of RNase A inverts the relative barrier heights.

Mechanistic implications of the partitioning of the RNase A•U>p complex. The ^{31}P NMR data suggest all RNases release N>p as product and that these products rebind and are hydrolyzed in a separate slower step. The throughput experiment provides a quantitative value for the partitioning of the enzyme bound U>p between release and hydrolysis. This experiment is powerful because the partition ratio $k_{through}/k_{off}$ is obtained only for a RNase A that has just transphosphorylated UpA (Figure 1.1), rather than for RNase A's of mixed active-site protonation states. The ratio $(k_{through}/k_{off})_{t=0}$= 0.001 indicates that after RNase A catalyzes cleavage of UpA, the bound U>p dissociates from the enzyme 1 x 10^3 times for every one time that it remains bound to the enzyme and is hydrolyzed. According to scheme 2.1, $k_{through}$ is equal to $k_{cat}^{U>p}$ [= 2.9 s^{-1} (delCardayré, S.B. 1995)]. Since $k_{through}/k_{off}$ = 1 x 10^{-3}, $k_{off}^{U>p}$= 2.6 x 10^3 s^{-1}, which is close to that of k_{cat}^{UpA} [= 1.4 x 10^3 s^{-1} (delCardayré, S.B. 1994)]. Erman and Hammes measured a $k_{off}^{U>p}$ four-fold higher (10^4 s^{-1}) (Erman, J.E. 1966); but under different experimental conditions. Thus, release of U>p may partially limit the rate of cleavage of UpA by RNase A.

The throughput experiment also has implications for the mechanism of enzyme recycling. The active-sites of RNases typically contain two residues with side chains that can function as general acid/base catalysts. In RNase A, these residues are His12 and His119 (Crestfield, A.M. 1963; Thompson, J.E. 1994). The imidazole group of His12 is postulated to act as a general base in the cleavage reaction and a general acid in the

hydrolysis reaction. The imidazole group of His119 is postulated to have a complementary role, acting as a general acid in the cleavage reaction and a general base in the hydrolysis reaction. After catalysis of cleavage, each histidine residue in the active-site of RNase A is protonated appropriately for catalysis of hydrolysis of the bound N>p. After hydrolysis of this substrate, each histidine residue is returned to its initial protonation state, completing the catalytic cycle (Figure 1.1). But RNase A interrupts this cycle by releasing rather than hydrolyzing the cyclic intermediate. Thus, RNase A (and perhaps other ribonucleases) has an iso mechanism (Medwedew, G. 1937) in which protonation states of the unliganded enzyme are interconverted by a pathway that does not involve substrate molecules. Neither the cleavage nor the hydrolysis reaction show noncompetitive product inhibition (Rebholz, K.L. 1993), which is indicative of an mechanism where recycling to the active enzyme form is rate–limiting (Northrop, D.B. 1994).

Conclusions: RNases have evolved to catalyze cleavage of RNA as opposed to hydrolysis. Studies of substrate specificity suggest a molecular explanation for the rate enhancement of RNA cleavage over that of hydrolysis. Among the catalytically important features of RNase A are subsite interactions with the leaving group (the "B2" interactions). For example, the k_{cat} for CpA, CpU, and Cp(methoxy) are 3000 s^{-1}, 27 s^{-1}, and 0.5 s^{-1} (Richards, F.M. 1971) respectively, even though the different primary alcohol leaving groups are likely to have similar pK_a's. These data suggest that RNase A catalysis is greatly enhanced by B2 subsite interactions that favorably orient the phosphodiester for cleavage. For hydrolysis to occur, water must bind in the active-site. Interestingly, the loss of ~10^3 in k_{cat} in going from CpA to Cp(methoxy) as a substrate is

the same loss in catalytic efficiency as in going from UpA to U>p. The absence of interactions between water and the B2 pocket may be the reason that hydrolysis is catalyzed poorly relative to cleavage (Cuchillo, C.M. 1993).

Scheme 2.1

The throughput experiment. The large type U>p signifies a large pool of unlabelled U>p, which dilutes the specific activity of any dissociated [5,6 ^{3}H]U>p. The effect of this dilution is to eliminate rebinding of [5,6^{3}H]U>p, as shown by the dashed arrow.

scheme 1 will go here

Figure 2.1

The time-course of the reaction of poly(U) with 0.2 M NaOH. The reaction was monitored at 25° C.

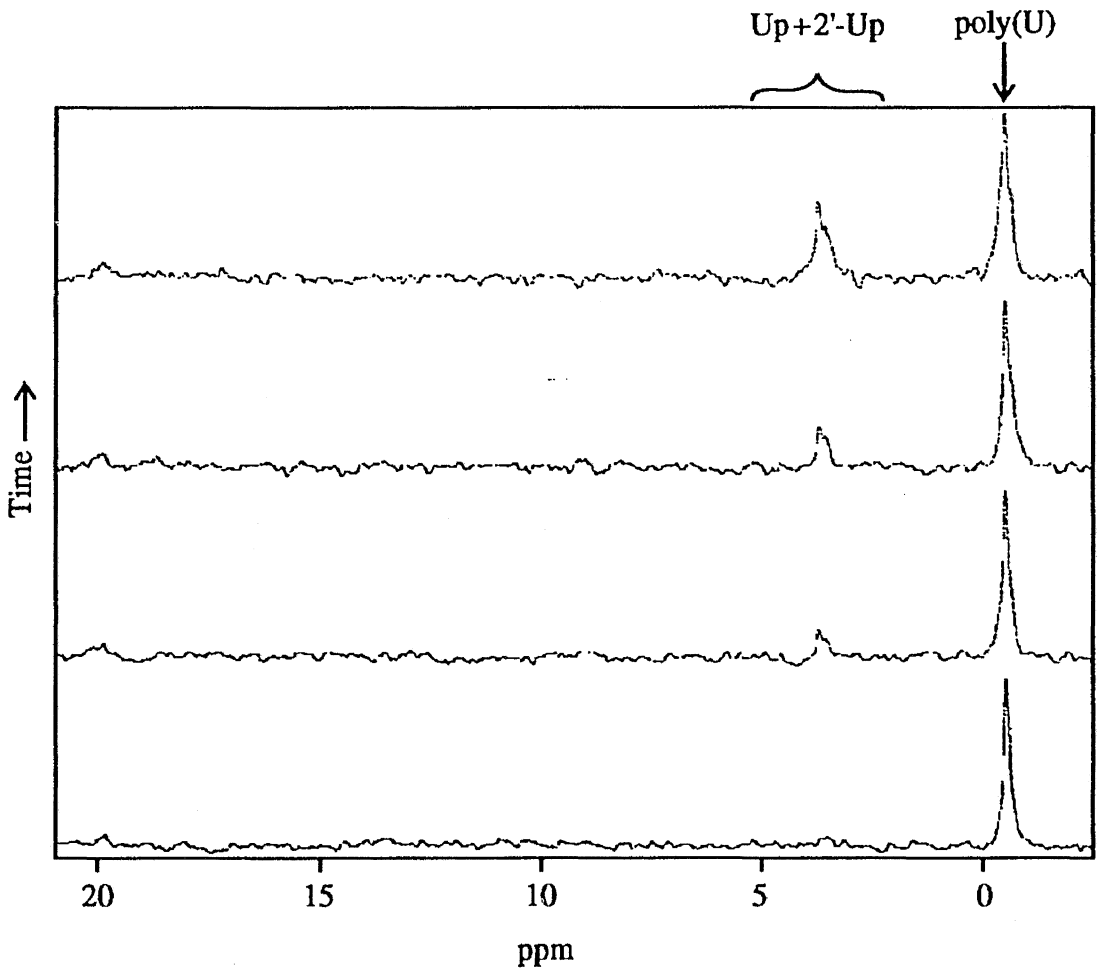
Up+2'-Up
poly(U)
Time
20
15
10
5
0
ppm

Figure 2.2

The time-course of the reaction of poly(U) with RNase A. The reaction was monitored at 25° C, in 0.10 mM imidazole•HCl buffer, containing 0.20 M NaCl.

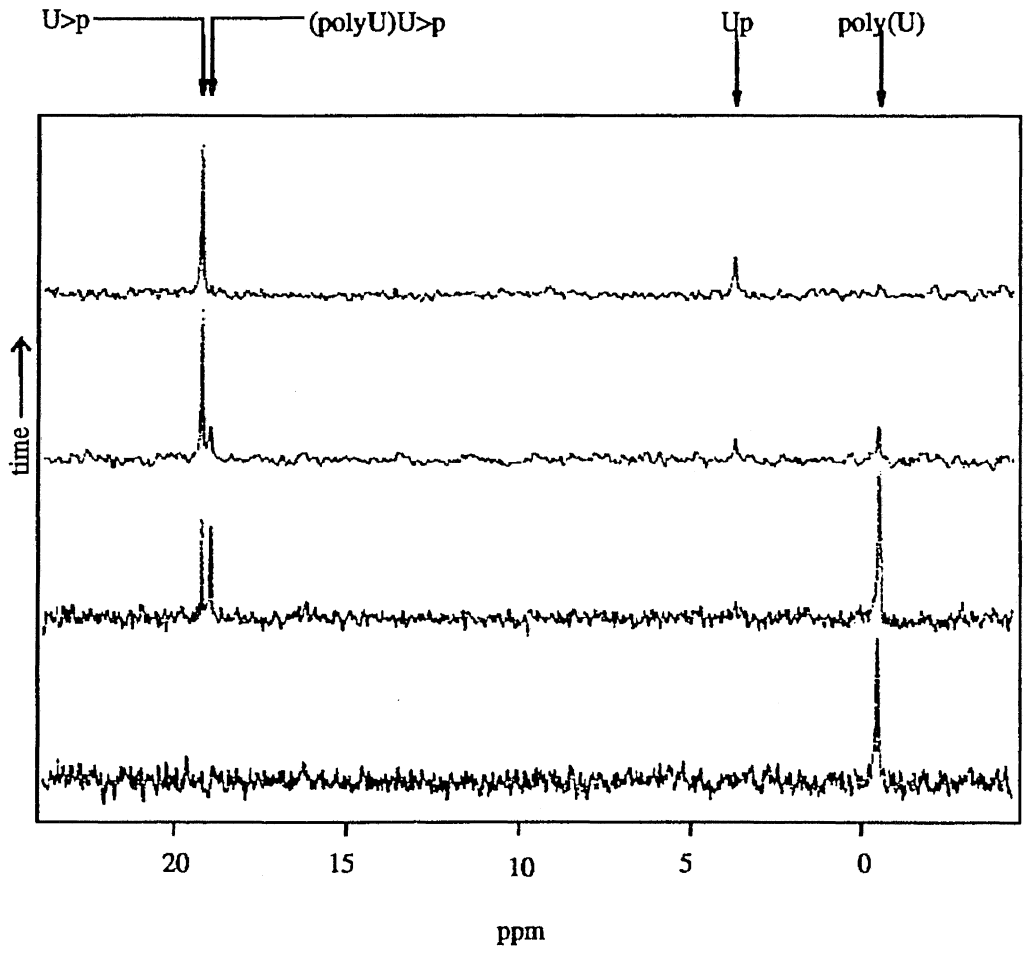
U>p
(polyU)U>p
Up
poly(U)
time
20
15
10
5
0
ppm

Figure 2.3

PEI–cellulose TLC elution profiles of [5,6 ^{3}H]UpA during the thoughput experiment.

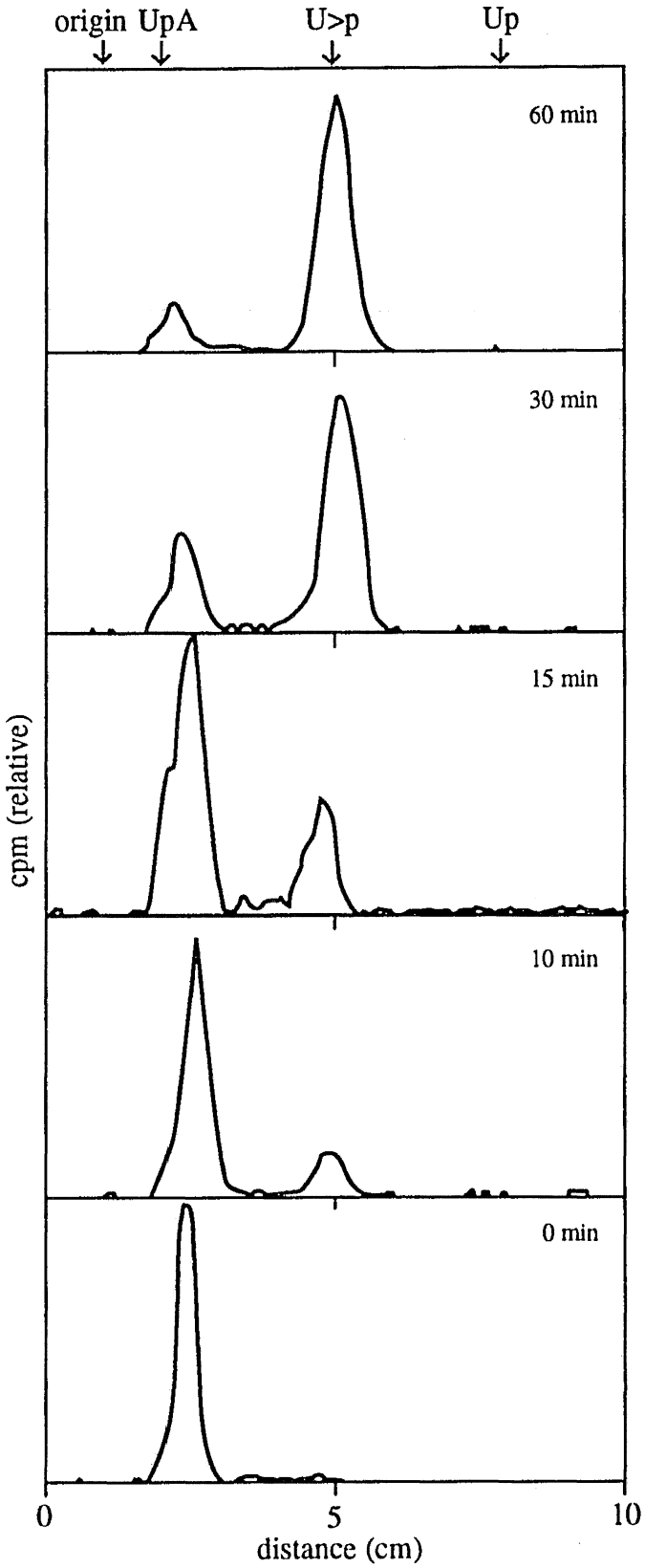
origin
UpA
U>p
Up
60 min
30 min
15 min
10 min
0 min
cpm (relative)
0
5
10
distance (cm)

Figure 2.4

Data from the throughput experiment. The inset shows the reaction progress with time, the large graph the ratio of counts in 3´-UMP vs the counts in U>p with time.

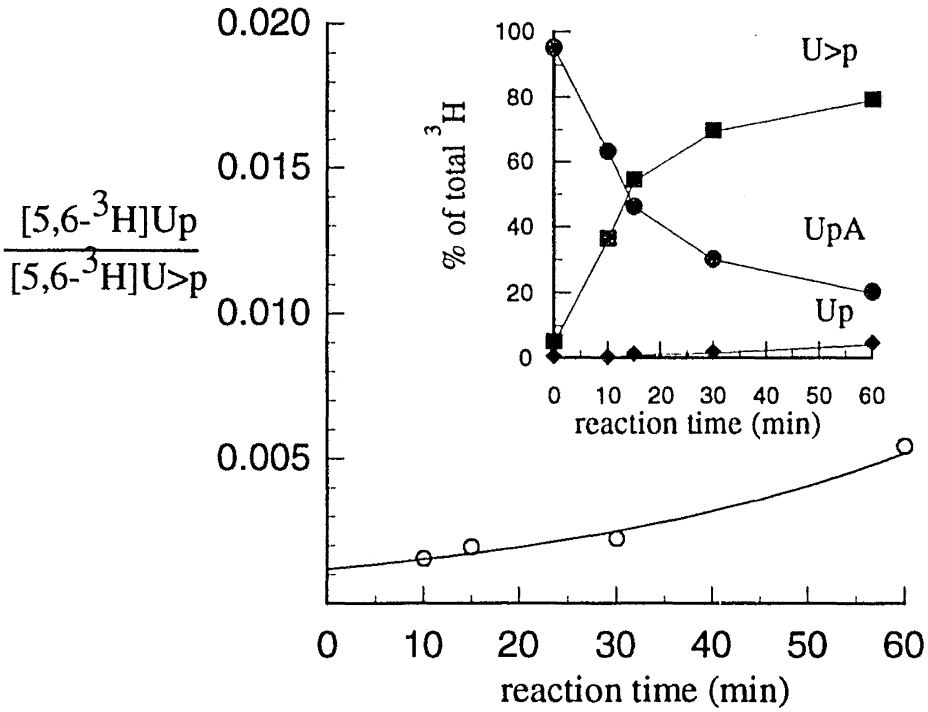
0.020
0.015
0.010
0.005
[5,6-3H]Up / [5,6-3H]U>p
0 10 20 30 40 50 60
reaction time (min)
100
80
60
40
20
0
% of total 3H
U>p
UpA
Up
0 10 20 30 40 50 60
reaction time (min)

Figure 2.5

The relative qualitative free energy barriers to catalysis by small molecules (dashed lines) and enzymatic RNases (solid lines).

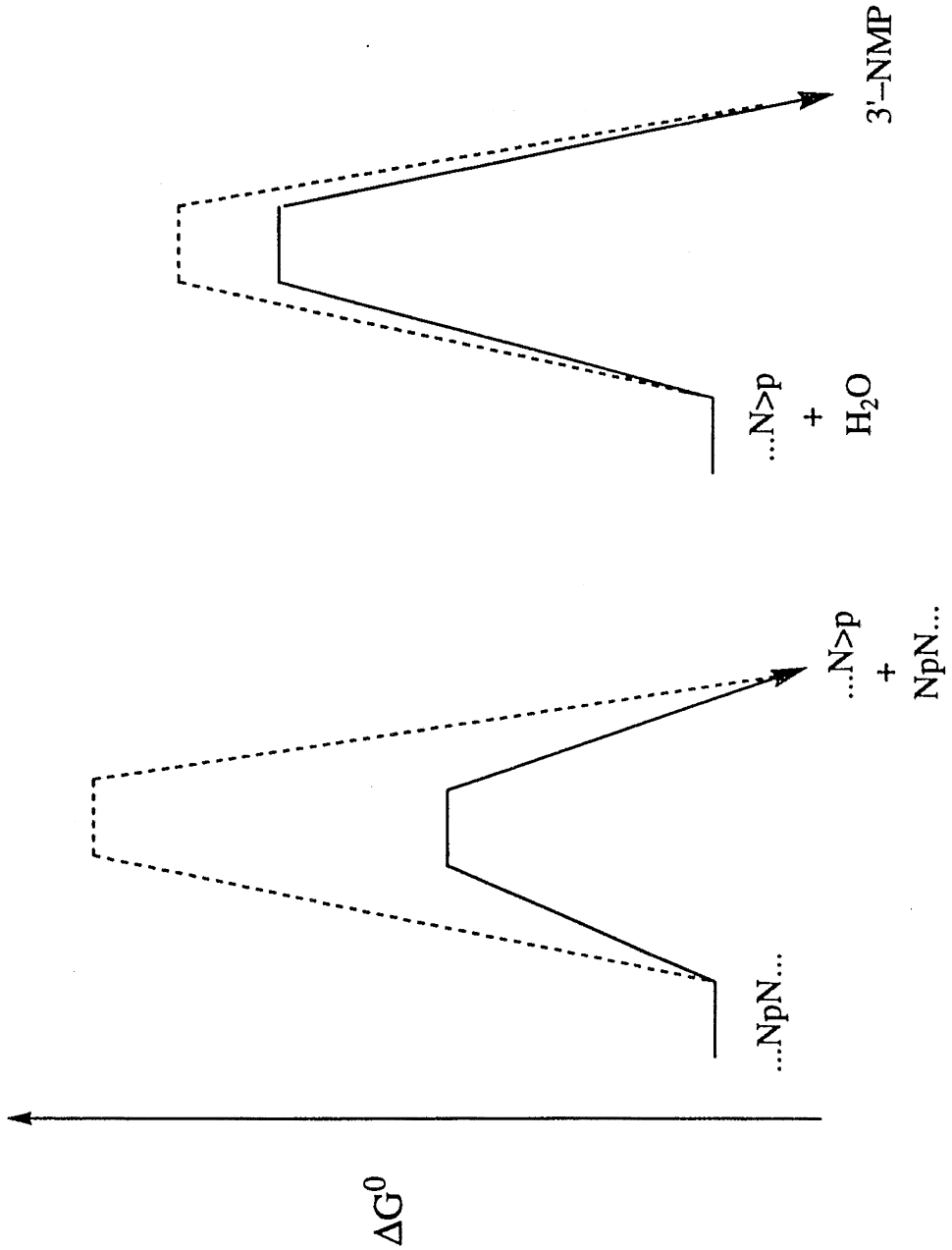
ΔG⁰
...NpN...
...N>p
+
NpN...
...N>p
+
H2O
3'-NMP

Chapter 3

Limits to Catalysis by Ribonuclease A

Published as: Thompson, J.E., Kutateladze, T.G., Schuster, M.C., Venegas, F. D., Messmore, J.M., Raines, R.T. (1995) *Bioorganic Chem.* in press.

Summary

Ribonuclease A catalyzes the cleavage of the P–$O_{5'}$ bond of RNA. We measured the variation of the RNase A specificity constant k_{cat}/K_m with glycerol and found a non-zero dependence. In contrast, the k_{cat}/K_m of a sluggish mutant ribonuclease A showed little dependence on glycerol. Since catalysis by the slow mutant is likely be limited by conversion of bound substrate to bound products, the data suggest that catalysis of RNA cleavage by RNase A is limited by a non–chemical step, such as product release or substrate encounter, and not by the conversion of the enzyme–bound substrate to enzyme–bound products. Thus, further evolutionary modifications of RNase A that affect only this chemical conversion cannot increase catalytic efficiency. We have also set a lower limit on the rate enhancement of UpA cleavage by RNase A by measuring the rate of UpA cleavage in water. [5,6-^{3}H] Up [3,5,8-^{3}H]A was incubated in buffered water and the reaction products analyzed by HPLC, which yielded a first order rate constant for RNA cleavage of 5×10^{-9} s^{-1} ($t_{1/2}$ = 4 years) and a rate enhancement of RNA cleavage by RNase A of 10^{12}-fold, which correspond to a transition state dissociation constant of K_d = 10^{-15} M and a transition state binding energy of 12 kcal/mol (1 μM standard state).

Introduction

Knowledge of the nature of the rate–limiting step in enzymatic catalysis is essential for quantitative comparison of different enzymes' catalytic activities. For example, if eliminating an enzymic active-site residue yields a mutant of lowered catalytic activity, quantifying the loss of activity as loss in transition state binding affinity is valid only if both the wild-type and mutant enzymes' catalytic activities are limited by conversion of enzyme–bound substrates to enzyme–bound products ("the chemical step" hereafter). This is not always (or even often) true (Cleland, W.W. 1975; Blacklow, S.C. 1988). If an enzyme's rate of chemical catalysis exceeds the rate of substrate binding or product release, then a mutant's observed loss of transition state affinity represents only a lower limit of the true loss.

Comparing two enzymes' catalytic activities is even more informative if the rate of the uncatalyzed reaction is known. One can calculate the transition state binding energies from the rate enhancements over background and more accurately assess catalytic efficiency (Wolfenden, R. 1976). For example, a mutant that is 10^3-fold less active than a wild –type enzyme may appear sluggish. But this mutant may have considerable catalytic activity if the wild-type enzyme accelerates the reaction 10^{12}–fold. Of course, to make such comparisons, one must show evidence that the catalyzed and uncatalyzed reactions take place by the same mechanism.

In the absence of catalysts, many enzyme catalyzed reactions take place at rates too slow to measure conveniently. Kahne and Still (Kahne, D. 1988) measured a background rate for peptide bond hydrolysis of 3×10^{-9} s^{-1} by covalently attaching a radioactive peptide to a solid support and measuring the amount of radiolabel liberated over time. They also analyzed the reaction products to ensure that peptide bond hydrolysis was the source of the radioactivity. We have performed a similar experiment

that measures the uncatalyzed rate of RNA phosphodiester bond cleavage at 25° C. We have also investigated the nature of the rate–limiting step in catalysis by RNase A. The results allow us to consider more quantitatively than was previously possible the catalytic efficiency of RNase A and its mutants.

Results

Cosolvent dependence of k_{cat}/K_m. The value of $k_{cat}/K_m = 2.3 \times 10^6\ M^{-1}s^{-1}$ (delCardayré, S.B. 1994) for the cleavage of UpA by wild–type RNase A is typical of that for substrate association (Fersht, A. 1985). In contrast, the value of $k_{cat}/K_m = 200\ M^{-1}s^{-1}$ for the cleavage of UpA by K41A RNase A (Messmore, J.M. 1995) is indicative of a reaction that is limited by a chemical transition state. As shown in Figure 3.1, the value of k_{cat}/K_m for the cleavage of UpA by wild–type but not K41A RNase A was inversely related to glycerol concentration. The glycerol-dependence of k_{cat}/K_m for the cleavage of poly(C) by wild–type RNase A is within error for that of the cleavage of UpA (data not shown). If catalysis by the sluggish mutant enzyme is indeed limited by a chemical transition state, then the glycerol-dependent change in the value of k_{cat}/K_m for catalysis of the chemical step limits the rate of catalysis.

The value of $k_{cat}/K_m = 5.7 \times 10^4\ M^{-1}s^{-1}$ (Thompson, J.E. 1994) for the RNase A-catalyzed cleavage of Up(4-nitrophenol) is approximately 40-fold lower than that for the cleavage of UpA. As shown in Figure 3.1, added glycerol had little effect on the value of k_{cat}/K_m for the cleavage of Up(4-nitrophenol) by wild–type RNase A. Again, the lack of a glycerol-dependence indicates that the rate of this slow reaction is limited by a chemical transition state.

In contrast, to the results with glycerol, the sucrose-dependence of k_{cat}/K_m is identical for wild–type RNase A and K41A RNase A. Thus, the rate-limiting transition state for catalysis by wild–type RNase A is altered differently by glycerol and sucrose. This finding indicates that catalysis by the wild–type enzyme is not limited by diffusion, since the addition of glycerol or sucrose have similar effects on solution microviscosity (Blacklow, S.C. 1988). Rather, since glycerol but not sucrose is known to interact with

single stranded nucleic acids [(Ganguly, S. 1993) and references therein], the data in Figure 3.1 indicates that the cleavage of UpA is limited by substrate desolvation.

Success of [5,6-^{3}H]Up[3,5,8-^{3}H]A synthesis and purification: A portion of the purified [5,6-^{3}H]Up[3,5,8-^{3}H]A was separated from its degradative products. 99.44% of the total ^{3}H measured was attributable to [5,6-^{3}H]Up[3,5,8-^{3}H]A. Also, the purified [5,6-^{3}H]Up[3,5,8-^{3}H]A was a single spot by TLC.

The uncatalyzed rate of RNA phosphodiester bond cleavage at pH 6. The six possible phosphodiester bond cleavage products were separated from [5,6-^{3}H]Up[3,5,8-^{3}H]A and analyzed; U>p and adenosine increased most dramatically at pH 6. Less than 1% of the [5,6-^{3}H]Up[3,5,8-^{3}H]A was consumed over 20 days. Two independently measured rate constants were extracted by plotting the loss of [5,6-^{3}H]Up[3,5,8-^{3}H]A (Figure 3.2) and the increase in U>p and adenosine (Figure 3.3). The first-order rate constant measured for disappearance of UpA at pH 6.0 and 25 ° C was $k = 6 \times 10^{-9}$ s^{-1} ($t_{1/2}$ = 3.5 years) which is in reasonable agreement with value of determined by appearance of U>p and adenosine at pH 6.0 and 25 °C, $k = 5 \times 10^{-9}$ s^{-1} ($t_{1/2}$ = 4.8 years). Breslow has measured a rate constant for cleavage of UpU at 8.35 by extrapolation from higher temperatures, $k = 2.4 \times 10^{-9}$s^{-1} (Breslow, R. 1995), which agrees well with the directly measured value. The pH differences preclude close comparison, however.

The other degradative products of P–O bond cleavage of UpA (*e.g.* 5′-AMP, uridine) did not correlate with UpA disappearance. The appearance of U>p and A is consistent with (but is not proof of) the uncatalyzed reaction following the same mechanism as in RNase A-catalyzed cleavage.

The uncatalyzed rate of RNA phosphodiester bond cleavage at pH 12. 2′ and 3′-UMP and adenosine were dominant in the products of the reaction at pH 12 (Figure 3.4), consistent with ^{31}P NMR characterization of the specific base catalyzed reaction (Chapter

2). The [5,6-^{3}H]Up[3,5,8-^{3}H]A was completely consumed over 20 days at pH 12. Extracting a rate constant for cleavage of UpA from these data is difficult, as the reaction was 87% complete when the second data point was taken. Assuming that the rate of UpA disappearance was linear over this time yields a rate constant $k = 10^{-4}$ s^{-1}.

Discussion

Cosolvent addition experiments. The rate of RNase A-catalyzed cleavage (Figure 1.1) of UpA is not limited by chemical conversion of bound UpA to bound products. This is also the true of the RNase A-catalyzed cleavage of poly(C), a macromolecular substrate. RNase A joins the family of "perfect enzymes" (Blacklow, S.C. 1988; Burbaum, J.J. 1989); evolutionary pressure has optimized these enzymes to convert bound substrate into bound product to the point that the conversion is no longer rate–limiting. This is not the case, however, when Up(4–nitrophenol) is the substrate. As might be expected from its slower rate, the cleavage of Up(4-nitrophenol) is limited by the chemical step.

The pH-independent k_{cat}/K_m of 10^7 for cleavage of UpA (Chapter 4) is low compared to the rate of encounter of proteins by small molecules, which is generally given as 10^8-10^{10} $M^{-1}s^{-1}$(Chou, K.C. 1982). This apparent inconsistency is not uncommon in the case of substrates associating with enzymes, as substrate binding is a complex process that often involves changes in noncovalent interactions of substrate and enzyme. Additionally, enzymes exist in multiple protonation and conformational states in solution. If any of these states do not lead to catalysis, the effect will be a lower apparent rate of association (Blacklow, S.C. 1988). Measured association constants for substrate and enzyme usually fall in the range of $10^6 - 10^8$ $M^{-1}s^{-1}$ [Fersht(1985), and references therein], and it should be noted that the term "diffusion limited" may not be strictly correct for the lower association rates. Rather, these rates might be referred to as "not limited by the chemical step". The association rate of UpA has not been measured, but the k_{on} for U>p binding to RNase A is 1 x 10^7 $M^{-1}s^{-1}$ (del Rosario, E.J. 1970), which is in close agreement with the pH–independent k_{cat}/K_m of 1.6 x 10^7 $M^{-1}s^{-1}$ for cleavage of UpA (Chapter 4).

Uncatalyzed rate of phosphodiester bond cleavage. According to the scheme of Wolfenden (Scheme 3.1), comparing the k_{cat}/K_m of the enzymatic reaction to the rate constant of uncatalyzed reaction quantifies an enzyme's affinity for the transition state {Wolfenden, 1976 #613}. This analysis assumes that the transition state decays at the same rate whether or not it is bound to the enzyme; thus the rate is limited by the rate at which the transition state is achieved and eq 3.1 is the result (where $K_E^{\ddagger}$ = equilibrium constant for activation for the enzyme; $K_{NE}^{\ddagger}$ is the equilibrium constant for activation in the absence of catalysts; K_{TX} is the dissociation constant for the enzyme binding to the transition state; k_{NE} = the rate of the uncatalyzed reaction).

$$K_{TX} = K_{NE}^{\ddagger}/K_E^{\ddagger} = k_{NE}/(k_{cat}/K_m) \qquad 3.1$$

RNase A catalyzes the transphosphorylation of UpA with a k_{cat}/K_m of 2 x 10^6 $M^{-1}s^{-1}$ under the conditions used to measure the uncatalyzed rate of [5,6-^{3}H]Up[3,5,8-^{3}H]A transphosphorylation (delCardayré, S.B. 1994). The binding constant for the association of RNase A with the transition state is found to be $K_{TX} \leq 2 \times 10^{-15}$ M. We may also convert the rate constants of the catalyzed and uncatalyzed reactions into free energies of activation using eq 3.2 (where k is the rate constant, h is Planck's constant, and k_b is Boltzmann's constant, R is the gas constant and T is temperature).

$$\Delta G^{\ddagger} = RT\ln\,[kh/(k_bT)] \qquad 3.2$$

The values of k_{cat}/K_m and our value for k_{uncat} indicate that the barrier to the RNase A-catalyzed cleavage of UpA is 18 kcal/mol, whereas the barrier to the uncatalyzed reaction is 30 kcal/mol. It should be noted that eq. 3.2 is most valid for gas-phase reactions, and it

assumes a uniform rate of transition state decay. However, the rate of transition state decay may be different in solution, and so $\Delta G^{\ddagger}$ calculated from eq. 3.2 for enzymatic solutions may not be accurate. Irrespective of this qualification, we may consider differences between similar reactions ($\Delta\Delta G^{\ddagger}$) in the same solvent with confidence. If we assign a 1 μM standard state in the case of the enzymatically-catalyzed reaction, then RNase A provides a $\Delta\Delta G^{\ddagger}$ of 12 kcal/mol relative to the uncatalyzed reaction.

Energy Barriers to RNase A catalysis. A quantitative free energy profile of the barriers to degradation of UpA by RNase A may be constructed using our data (Figure 3.5). The barriers for the hydrolysis reaction are taken from the data of Eftink and Biltonen (Eftink, M.R. 1983) and constructed using eq 3.2.

It is interesting to note that the uncatalyzed barriers to cleavage and hydrolysis are similar. Cleavage of the P–$O_{2'}$ or P–$O_{3'}$ bond of U>p and the P–$O_{5'}$ bond of UpA both occur 10^5–fold faster than does cleavage of the phosphodiester linkage of DNA (Kumamoto, J. 1956; Bunton, C.A. 1960). This similarity implies that either cyclizing a phosphodiester or introducing a 2′ nucleophile affects P–O bond cleavage equally. Cyclizing accelerates cleavage by strain (Kluger, R. 1990) or poor ground state solvation (Dejaegere, A. 1993); the 2′-OH accelerates cleavage by providing an intramolecular nucleophile. RNase A and other ribonucleases (Chapter 2) are more efficient at cleavage than hydrolysis. This disparity in catalytic efficiency suggests that a biological role for ribonucleases may be to destroy the genetic information carried by polymeric RNA—to do this the enzyme need only be efficient at cleavage.

The mutant K41A may be regarded in the context of the quantified energetics (Figure 3.5). The elimination of Lys41 removes a positively charged hydrogen bond

donor from the active-site of the enzyme. Recent studies suggest that it is the hydrogen bonding capacity of Lys41 that effects catalysis rather than its positive charge {Messmore, 1995 #521}. The loss of ≥5 kcal/mol of transition state binding energy on truncation of Lys–41 is considerable, but the remaining enzyme still stabilizes the transition state by 7 kcal/mol compared to the uncatalyzed reaction.

The catalytic value of the B2 subsite of RNase A may also be quantified using our data. This subsite interacts with the base of the residue 5′ to the scissile phosphodiester bond and is thought to be composed of Gln69, Asn71, and Glu111 (Parés, X. 1991). The rates of RNase A-catalyzed transphosphorylation of substrates with different leaving groups are related as follows; (leaving group =) adenosine > guanosine > cytidine > uridine > methoxy (Richards, F.M. 1971). If one considers CpA to have the best interactions with the B2 pocket and Cp (methoxy) to have no interactions, then one may convert the "lost" interactions with the B2 pocket into lost transition state stabilization energy. CpA is transphosphorylated by RNase A with a k_{cat}/K_m of 3 x 10^6 $M^{-1}s^{-1}$, Cp (methoxy) with a k_{cat}/K_m of 250 $M^{-1}s^{-1}$ (Witzel, H. 1962). This corresponds to a transition state stabilization energy ≥4.7 kcal/mol provided by the B2 subsite. Assuming the uncatalyzed rates of transphosphorylation of CpA and Cp(methoxy) are similar to that of UpA, we also observe that the enzyme is able to provide 7.3 kcal/mol transition state stabilization energy without using the B2 subsite.

Biopolymer stability. The rate of cleavage of a peptide bond at pH 6 in water is 3 x 10^{-9} s^{-1} (Kahne, D. 1988). This value is very similar to the uncatalyzed rate of 5 x 10^{-9} s^{-1} for ribonucleotide phosphodiester cleavage under similar conditions. RNA and protein are the two biopolymers in the fundamental DNA → RNA → protein pathway

that are most frequently degraded. Although a dilute solution does not mimic intracellular conditions, it is nonetheless interesting to note that protein and RNA have similar rates of degradation under these conditions.

Figure 3.1

Relative k_{cat}/K_m for the cleavage reaction plotted against percent cosolvent (w/v). With glycerol as the cosolvent: UpA cleaved by wild-type RNase A (○); Up(4–nitrophenol) cleaved by wild-type RNase A (△); UpA cleaved by K41A (●). Relative k_{cat}/K_m plotted against the relative viscosity for cleavage of UpA by wild-type RNase A using sucrose as the viscogen (◆), corrected for the dependence of k_{cat}/K_m of K41A. The superscript ^{0} indicates a value measured in the absence of viscogen. Assays were carried out at pH 6.0, in 50 mM MES-HCl buffer containing 0.10 M NaCl at 25 °C.

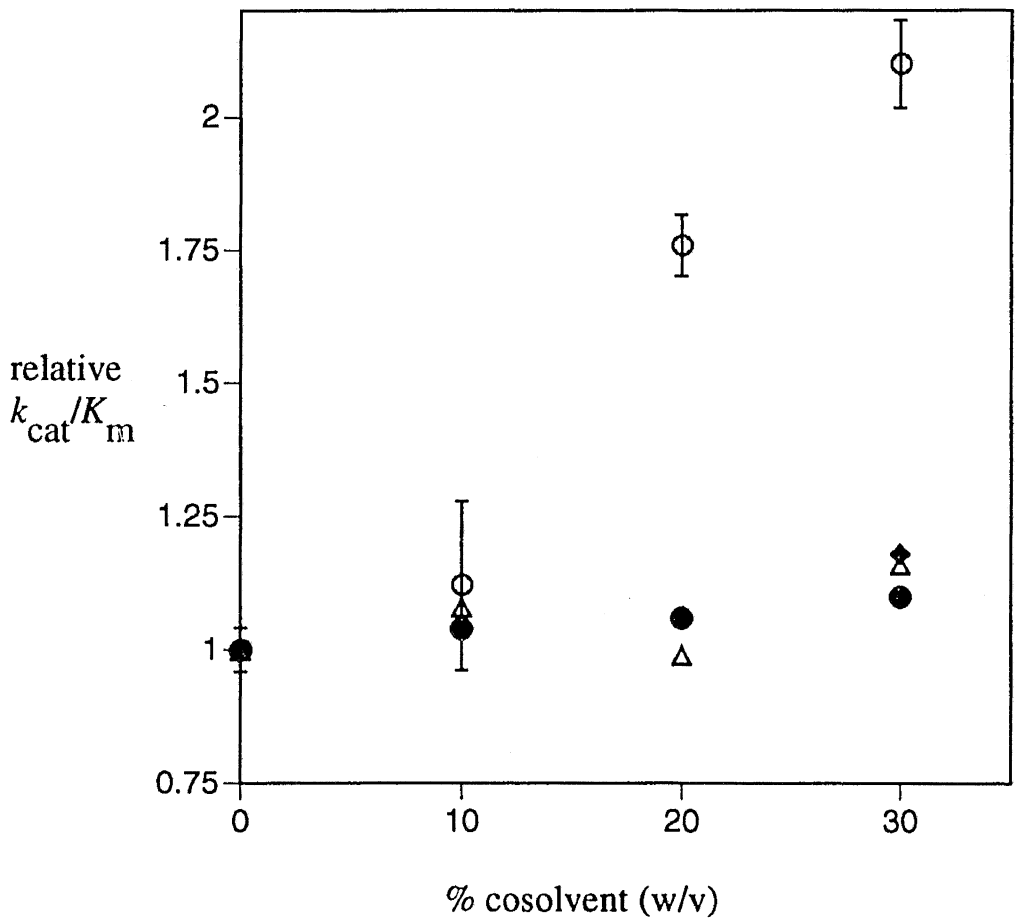
relative
k_{cat}/K_m
2
1.75
1.5
1.25
1
0.75
0
10
20
30
% cosolvent (w/v)

Figure 3.2

Plot of the time-course for the degradation of UpA at pH 6.0 in 50 mM MES-HCl buffer, containing 0.10 M NaCl at 25 °C.

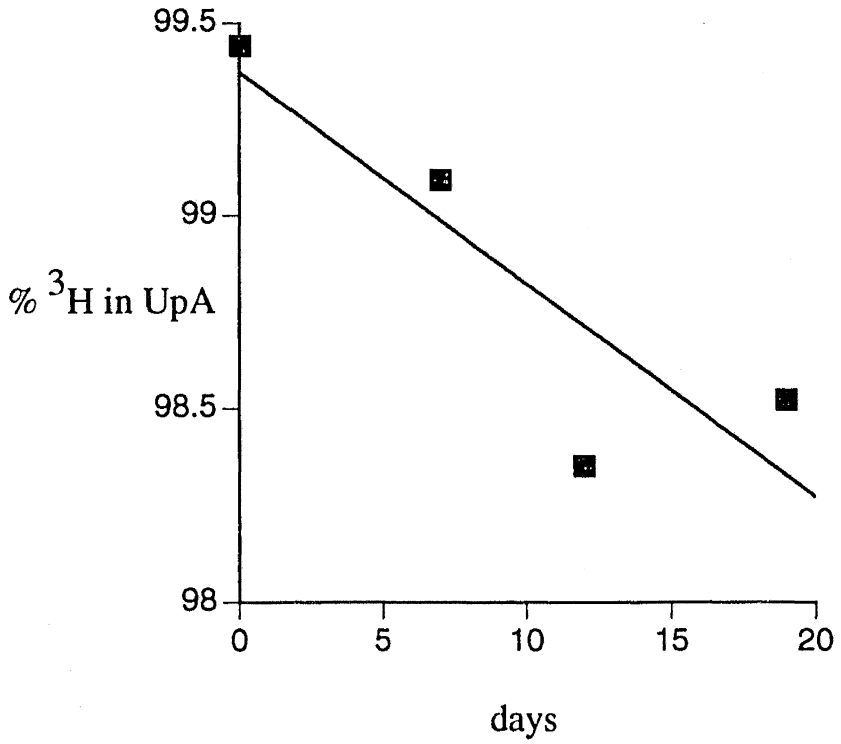
99.5
99
98.5
98
% 3H in UpA
0
5
10
15
20
days

Figure 3.3

Accumulation of cleavage reaction products U>p (X) and A (●) at pH 6.0 and 25 °C in 50 mM MES-HCl buffer containing 0.1 M NaCl. Products other than UpA, U>p and adenosine accounted for <0.1% of the radioactivity at each time point.

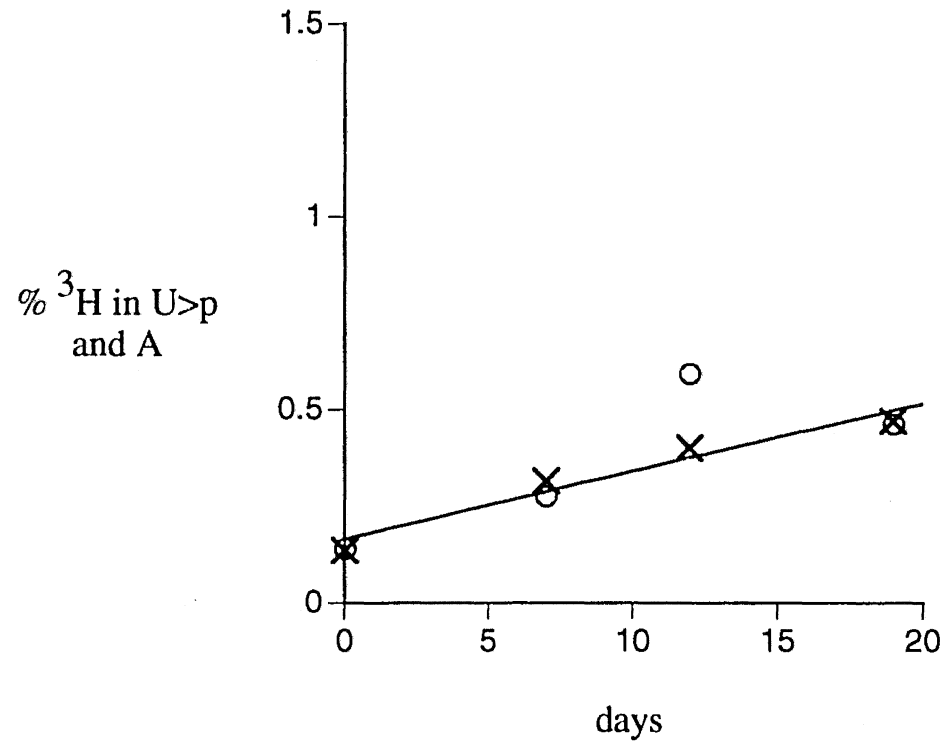
% 3H in U>p and A
1.5
1
0.5
0
0
5
10
15
20
days

Figure 3.4

Loss of UpA (■) and accumulation of 2′ and 3′ UMP (●) and adenosine (▲) in 50 mM sodium phosphate buffer, pH 12.0, containing 0.1 M NaCl at 25 °C.

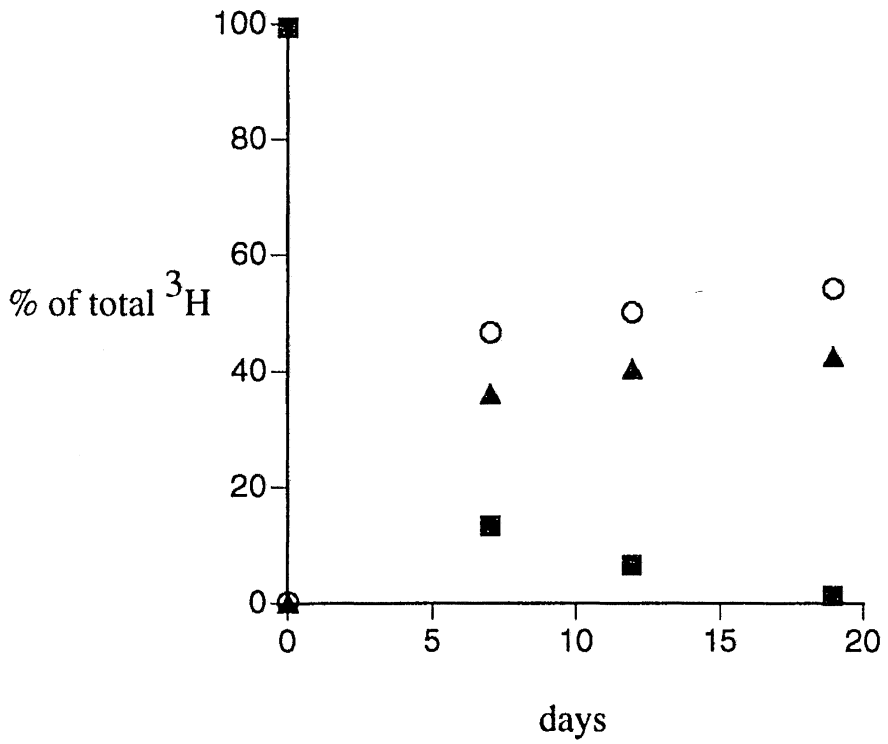
100
80
60
40
20
0
% of total ^{3}H
0
5
10
15
20
days

Scheme 3.1

Scheme for measuring enzymatic affinity for the transition state (taken from (Wolfenden, R. 1976)). $K_E^{\ddagger}$ is the equilibrium constant for achieving the enzymatically bound transition state; $K_{NE}^{\ddagger}$ is the equilibrium constant for achieving the transition state in the absence of catalysts; K_{TX} is the dissociation constant for the enzyme binding to the transition state. Decay of the two transition states is assumed to occur at the same rate.

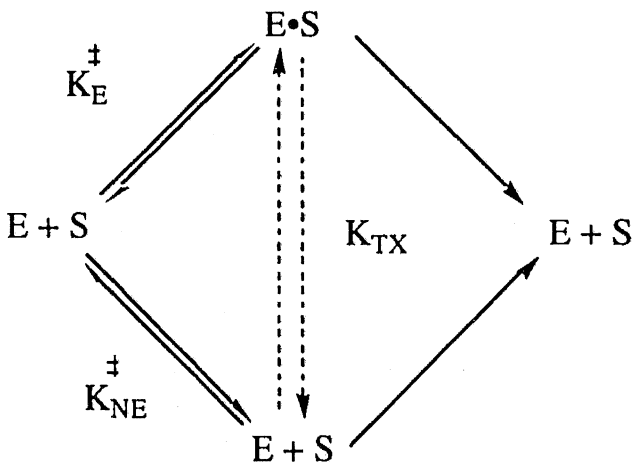
E•S
$K_E^{\ddagger}$
E + S
K_{TX}
E + S
$K_{NE}^{\ddagger}$
E + S

Figure 3.5

Free energy barriers to catalysis by RNase A (solid lines) and the uncatalyzed reactions (dashed lines). Barriers were calculated using eqs 3.1 and 3.2 and the following data. In the case of the enzymatically catalyzed reactions a 1 μM standard state was used. Cleavage reaction: uncatalyzed rate = 5×10^{-9} s^{-1} (this work); k_{cat}/K_m for cleavage of UpA by wild-type RNase = 2×10^{6} $M^{-1}s^{-1}$ (delCardayré, S.B. 1994); k_{cat}/K_m for cleavage of UpA by K41A RNase A = 2×10^{2} $M^{-1}s^{-1}$ (Messmore, J.M. 1995). Hydrolysis reaction: uncatalyzed rate: 4×10^{-9} s^{-1} for C>p (Eftink, M.R. 1983); k_{cat}/K_m for hydrolysis of U>p = 900 $M^{-1}s^{-1}$ (delCardayré, S.B. 1995); the relative free energies of U>p and 3′-UMP were calculated using an equilibrium constant of 1×10^{3} (del Rosario, E.J. 1969). Uncatalyzed hydrolysis of U>p also yields 2′–UMP (not shown).

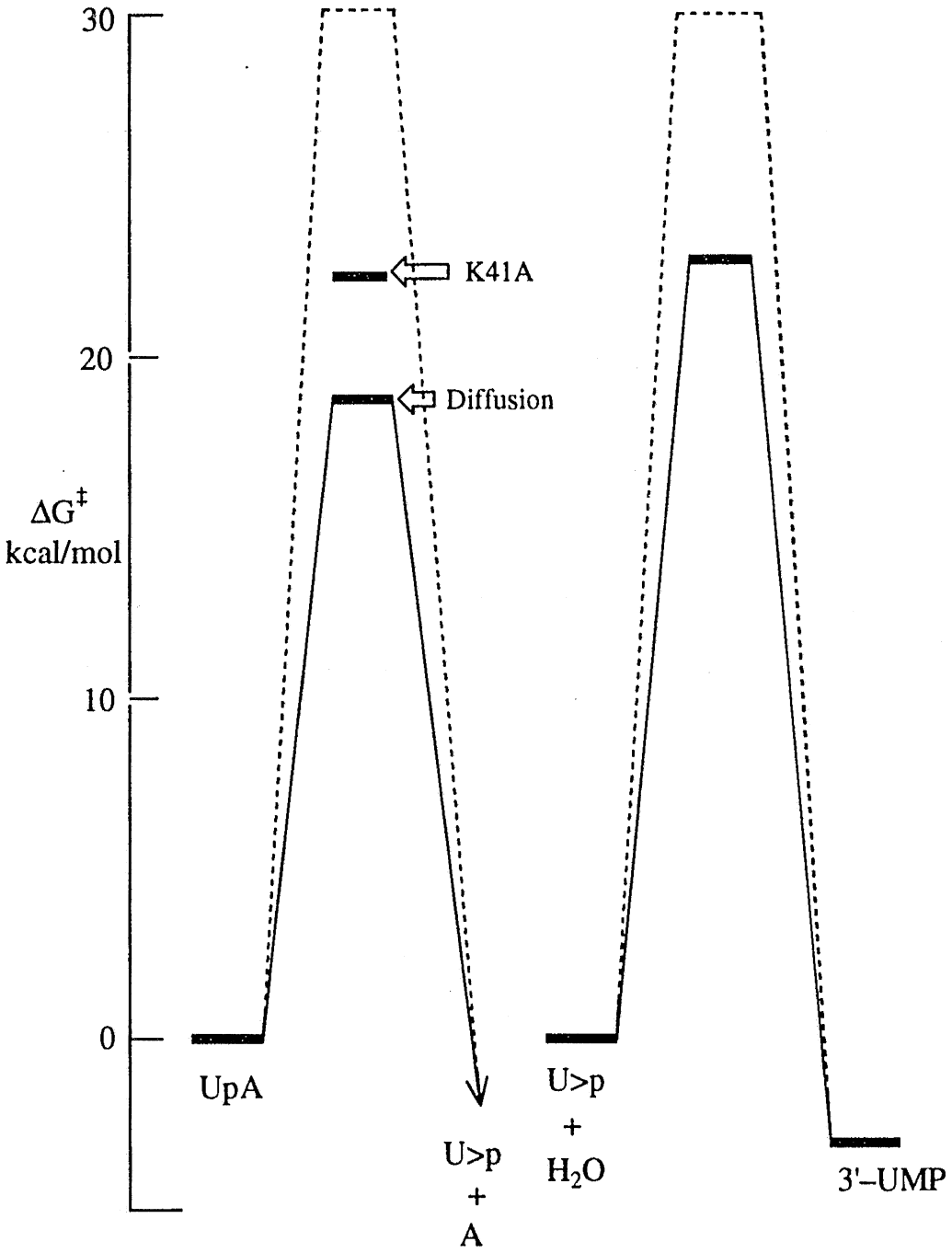
30
20
10
0
ΔG‡
kcal/mol
K41A
Diffusion
UpA
U>p
+
A
U>p
+
H2O
3'-UMP

Chapter 4

Production, purification and characterization of RNase A mutants lacking active-site histidines 12 and 119

Portions of this work published as: Value of general acid–base catalysis to ribonuclease A. J.E. Thompson and R.T. Raines *J. Am. Chem. Soc.* (1995) **116**, 5467–5468.

Summary

The active site of bovine pancreatic ribonuclease A (RNase A) contains two histidines, histidine 12 (H12) and histidine 119 (H119). Site–directed mutagenesis was used to replace either H12 or H119 with an alanine residue. These mutants were expressed in *E. coli* and purified. The mutants' catalytic efficiencies were characterized by measuring their abilities to accelerate the cleavage of three substrates: poly(C), UpA, and Up(4–nitrophenol). The first two substrates have leaving groups pK_a's ~ 14, but Up(4-nitrophenol) has pK_a = 7.14. Replacing either H12 or H119 with alanine resulted in a drop in k_{cat}/K_m of $>10^4$-fold with UpA or poly(C) as a substrate. The mutants' k_{cat}/K_m and k_{cat} are lower limits because both mutants catalyze the cleavage reaction via a different mechanism than does wild–type RNase A. In contrast, when Up(4–nitrophenol) was the substrate, mutating H119 to alanine caused k_{cat}/K_m to drop only five-fold, compared to $>10^4$ –fold on mutating H12 to alanine. The pH–dependence of k_{cat}/K_m showed that H119A RNase A is a better catalyst than the wild-type RNase A when Up(4-nitrophenol) is the substrate and pH > 7. These data provide direct evidence that H119 acts as an acid catalyst during cleavage and indicate that each active-site histidine residue can stabilize the transition state by >5 kcal/mol. pH titration of both mutant enzymes was monitored by ^{1}H NMR, allowing determination of the histidines' pK_a's in the presence and absence of 3′-UMP, a competitive inhibitor. Comparing the microscopic pK_a's in the presence and absence of inhibitor suggests that the histidines' interactions with the phosphoryl group are synergistic. The pK_a's also suggest that the mutants are structurally similar to the wild-type enzyme. The pH dependence of C–2 proton NMR peak width showed that the proton exchange rate of H12 decreased upon elimination of H119. This

result suggests that after reaction, H119 aids in recycling RNase A to its active protonation state. Fluorescence anisotropy was used to measure the K_d of RNase A binding to a substrate analog, d(AUAA). Replacing the histidine residues caused a loss of substrate binding energy of 1.1 kcal/mol (H12) and 1.8 kcal/mol (H119).

Introduction

RNase A catalyzes two kinetically distinct reactions (Figure 1.1). The *cleavage* reaction is a transphosphorylation which yields a 2′,3′-cyclic monophosphate (N>p) and breaks the RNA strand. The *hydrolysis* reaction is an attack of water on the N>p which yields a 3′-monophosphate. The cleavage reaction is catalyzed more efficiently than is the hydrolysis reaction (Chapter 2).

H12 and H119 were identified as catalytically important residues in the early stages of RNase A research. After solving the primary structure of RNase A, Stein and Moore used haloacetates to carboxymethylate the histidines of RNase A and found the modified enzyme to be inactive. They identified H12 and H119 as the modified residues (Barnard, E.A. 1959; Barnard, E.A. 1959; Crestfield, A.M. 1963).

Other researchers used the S-peptide:S-protein interaction to selectively modify H12. S–peptide and S–protein are the products of limited proteolysis by subtilisin (Richards, F.M. 1959). RNase S, the noncovalent complex of S–protein and S–peptide (residues 21–124 and 1–20 respectively) retains nearly full activity and can be disrupted reversibly at low pH. Before recombinant DNA technology made site–directed mutagenesis possible, chemically synthesized S–peptide analogs were complexed with S–protein to study protein structure–function relationships (Richards, F.M. 1971). Hofmann and coworkers synthesized peptides with a variety of specifically substituted histidine analogs at position 12 and studied the modified S–peptides affinities for S–protein (Hofmann, K. 1970). Only the S–peptide containing N_{δ}–carboxymethylated histidine at position 12 showed any ribonuclease activity when complexed to S–protein, and 100–fold molar excesses of peptide were required. Even this result is consistent with the identification of H12 as catalytically important because the N_{δ} of H12 forms a hydrogen bond with the mainchain oxygen of T45 (Wyckoff, H.W. 1967) and is not

accessible to the substrate. Substitution of 4–flourohistidine at position 12 of RNase S was reported to yield an inactive enzyme isostructural with native RNase S (Taylor, H.C. 1981). However, recent studies have disputed the lack of catalytic activity reported for 4-fluorohistidine–substituted RNase S (Jackson, D.Y. 1994).

The bell–shaped pH dependence of catalysis by RNase A is consistent with an active-site that contains two titratable residues of pK_a ~ 6, one protonated and the other unprotonated (Richards, F.M. 1971 Eftink, 1983 #174). The histidines are the only residues that need be invoked to explain the pH dependence of catalysis. Wells and coworkers were able to incorporate 4-fluorohistidine at positions 12 and 119 into RNase A using a combination of chemical and enzymatic techniques (Jackson, D.Y. 1994). The pH dependence of this doubly substituted enzyme was bell–shaped, but was shifted to lower pH. Since 4–fluorohistidine has a lower pK_a than histidine, this perturbation is consistent with both 4-fluorohistidine residues participating in catalysis.

The structural environments of H12 and H119 corroborate the modification data. Uridine vanadate is a putative analog for a pentavalent transition state during U>p hydrolysis, and the structure of wild-type RNase A with uridine vanadate bound in the active-site has been solved (Borah, B. 1985). In this complex, the H12 N_δ forms a hydrogen bond with the backbone carbonyl of T45, and the N_ε forms a hydrogen bond with the 2′ oxygen of the uridine. N_ε of H119 forms a hydrogen bond with the sidechain carboxylate of D121, and the N_δ forms a hydrogen bond with one of the non–bridge oxygens of the vanadate. The sidechain of H119 is found in only one conformation is this complex, but has been reported to be in two positions in complexes of the enzyme with sulfate (Howlin, B. 1992) and cytidine 3′-monophosphate (Zegers, I. 1994). In the free enzyme, H119 is also found in only one position (Nachman, J. 1990). The significance of the multiple positions of H119 is not understood. This complexity not

withstanding, the positions of H12 and H119 in the active-site are consistent with H12 and H119 acting as general base and general acid in the cleavage reaction catalyzed by RNase A (Figure 1.1).

To understand better the contributions of H12 and H119 to catalysis, we have used site–directed mutagenesis to replace each histidine with alanine. This substitution replaces the imidazole functionality of histidine with a proton. We have characterized the contributions of the histidines to transition state stabilization and to the pH dependence of catalysis. We have also characterized the histidines' interactions with each other, and with a ground state analog. These data allow us to better define the mechanistic roles and the energetic importance of both H12 and H119 to catalysis.

Results

Nomenclature. Throughout this chapter kinetic parameters will be given in the general form $parameter^{enzyme}$[substrate]; for example, k_{cat}/K_m^{WT}[UpA] is equivalent to k_{cat}/K_m for the cleavage of UpA catalyzed by wild-type RNase A. Where appropriate, the enzyme or the substrate may not be specified.

Steady–state kinetic measurements. The substrates used for cleavage assays (shown in Figure 4.1) were UpA, poly(C), and Up(4-nitrophenol). The kinetic parameters for cleavage at pH 6 are listed in Table 4.1, and k_{cat}/K_m's for these reactions are plotted in Figure 4.2. The kinetic parameters for cleavage of UpA by wild-type and H119A RNase A as a function of pH are listed in Table 4.2, and the same parameters for cleavage of Up(4-nitrophenol) are listed in Table 4.3. At some pH's it was not possible to saturate the enzymes sufficiently when UpA was the substrate, preventing k_{cat} and K_m from being determined accurately.

Using wild-type and H119A RNase A as catalysts, pH was plotted against log (k_{cat}/K_m[UpA]), log(k_{cat}/K_m[Up(4-nitrophenol)]) (Figures 4.3 and 4.4) and log (V/K^{H12A}[UpA]) (Figure 4.5). Plots of pH vs k_{cat}/K_m^{wt}[UpA], k_{cat}/K_m^{wt}[Up(4-nitrophenol)] were fit to eq 4.1

$$k_{cat}/K_m \text{ (observed)} = (k_{cat}/K_m)^{ind.} * [\ 1 + K_a/[H] + [H]/K_b + K_a/K_b]^{-1} \qquad (4.1)$$

where $(k_{cat}/K_m)^{ind}$ is the pH-independent k_{cat}/K_m, and K_a and K_b are the apparent microscopic acid dissociation constants for groups a and b. This eq describes the case of an enzyme with two titratable groups in its active site, one of which must be unprotonated (group b) and the other of which must be protonated (group a) for catalysis to occur (Segel, I.H. 1975). Plots of pH vs k_{cat}/K_m^{H119A} [Up(4-nitrophenol)] were fit to eq 4.2,

which describes an enzyme with one active-site residue that must be deprotonated for catalysis.

$$k_{cat}/K_m \text{ (observed)} = (k_{cat}/K_m)^{ind.} * (1 + [H]/K_b)^{-1} \qquad (4.2)$$

Plots of pH vs k_{cat}/K_m^{H119A} [UpA] and V/K^{H12A}[UpA] were fit to eq 4.3, where k_1, k_{-1}, and k_2, are the individual microscopic rate constants shown in Scheme 4.1, and K_a= acid dissociation constant of the one active-site residue that takes part in a two-step mechanism. The residue is requires to be unprotonated in one step and protonated in the other.

$$k_{cat}/K_m \text{ (observed)} = \{ k_1 * k_2 [2 + K_a/[H] + [H]/K_a]^{-1} \} / \{k_{-1}(1+ [H]/K_a)^{-1} + k_2(1+ K_a/[H])^{-1}\} \qquad 4.3$$

The parameters from all curve fittings are listed in Table 4.4.

Separation of the mutants from wild–type RNase A. The elution profile from the cation exchange column is shown in Figure 4.6. Since the mutant lacks one positive charge relative to wild–type RNase A at this pH it elutes from the column sooner. Under these conditions, the peak-to-peak separation was 16 mL and the peak duration for H12A RNase was 4.2 mL and that for wild–type RNase A was 3.6 mL. H12A and H119A RNase A were subjected to this purification three times and were assayed for their ability to cleave UpA. The values for k_{cat}/K_m, K_m, and k_{cat} were identical to values obtained previously without the pH 5.0 purification, and the pH-dependence of V/K was bell-shaped (Figure 4.5 for H12A RNase A, H119A RNase A data not shown).

Titration of the enzymic histidines monitored by ^1H NMR. The pK_a values determined from analysis of C–2 proton chemical shift data are listed in Table 4.5. Error analysis from curve fitting suggests that the pK_a values measured have a ± of 0.02 when the pK_a is 6-7 and a ± of about 0.4 when the pK_a is <4.5 and there are fewer data to fit (Quirk, D.J. 1995). However, errors determined from curve fitting of single points are minimal errors that do not account for deviations owing to inaccuracies in pD and chemical shift. It was not possible to do the necessary repetitions to determine the ± pK_a but the variation of the pK_a of H105 provides a measure of the deviation one might expect. Histidine 105 is solvent exposed and its titration curve fits well under all conditions to a model with a single pK_a. The pK_a of His 105 varies between experiments by only 0.08. If one considers only the histidine mutants, the pK_a varies by only 0.03. Multiple pK_a's are listed for various residues because the pK_a values obtained by NMR are true microscopic pK_a's. Also, the titration of nearby groups can perturb the chemical shift of the C–2 proton, and these titrations must also be considered during data analysis.

Wild-type RNase has four histidines, but only three are suitable for pK_a determination. H48 is inaccessible to solvent and its titration curve shows anomalous behavior with pH (Markley, J.M. 1975). H105 is described above. Fitting the titration curve of H12 in the wild-type active-site of the free enzyme requires three pK_a's (Quirk, D.J. 1995). The inflection of the H12 curve at pK_a = 3.99 may owe to the titration of Asp83, which is near H12 and is important for the enzyme's cytidine/uridine preference (delCardayré, S.B. 1995). H12's two pK_a's, 6.12 and 5.74, are thought to be microscopic pK_a values that are dependent on the protonation of H119. A histidine near another protonated histidine will have a depressed pK_a because of the unfavorable interaction of two positive charges. The two pK_a's of H119 can be explained in the same way: the pK_a

of H119 is depressed to 5.94 when H12 is protonated and is increased to 6.32 when H119 is unprotonated (Quirk, D.J. 1995).

Titration of the mutants confirms this model. When one active-site histidine is removed by mutagenesis, the other shows a single pK_a consistent with removal of the other histidine's positive charge. H119 has a pK_a of 6.4 in the H12A active-site; the higher microscopic pK_a measured for H119 in the wild-type active site is 6.32. Similarly, H12 fits to a single pK_a of 6.08 in the active site of the H119A enzyme. This value is in good agreement with the higher pK_a of 6.12 measured for H12 in the wild-type active site. The inflection in the wild-type H12 titration curve which allowed fitting to pK_a 3.99 was seen with H119A, but spectra were not acquired at pD low enough to measure this pK_a.

When the histidine residues of wild-type RNase A were titrated in the presence of saturating 3′-UMP, the pK_a's attributed to the histidines were elevated (Quirk, D.J. 1995). The microscopic pK_a values for H12 increased 0.6 and 0.32 units and those of H119 increased 0.8 and 0.65 units. These elevations in pK_a are consistent with the introduction of a negative charge which interacts favorably with protonated histidine. There is also a third pK_a required to fit the H119 titration curve when 3′-UMP is bound to the enzyme. This new pK_a of 4.06 is thought to be the depressed pK_a of the phosphate monoanion (Quirk, D.J. 1995).

Here, histidine residues of H12A and H119A RNase A were titrated in the presence of saturating 3′-UMP. The chemical shift dispersion of the histidines' C–2 proton signals was identical for the wild-type and mutant enzymes in the presence of 3′-UMP, indicating that the mutant enzymes were saturated with inhibitor (data not shown). When 3′-UMP is bound to the enzyme, the effect of eliminating one active-site histidine on the pK_a of the other active-site histidine is opposite to that in the free enzyme—the

remaining active-site histidine's microscopic pK_a converges on the *lower* of the two wild-type values (Table 4.5). Although the differences in the microscopic pK_a's of the histidines in the wild–type RNase A are only 0.1 in the presence of 3′ UMP, the accuracy of the values is also high (consider that the pK_a of H105 in the presence of 3′-UMP varies by only 0.01)(Table 4.5). Thus we feel that the comparison of the histidine pK_a's of wild–type RNase A and the mutants enzymes is valid, even though the values are close. Low pD inflections in the titration curves were observed when 3′-UMP was bound to the active site of H12A or H119A These low pD inflections probably derive from the same titrations for the wild-type and mutant enzymes: D83 for H12 and the phosphate monoanion for H119. The measured pK_a's for these acidic groups are much less accurate than are the pK_a's of the histidines (Quirk, D.J. 1995). So although the acidic pK_a's of the mutants' H12 and H119 were different from those of wild-type enzyme when 3′-UMP was bound, no comparison can be made.

Peak width data were also collected and analyzed to compare exchange broadening qualitatively. Exchange broadening of the C–2 peak at the pK_a reports on the histidine's rate of proton exchange (Sanders, J.K.M. 1987). The most significant difference in exchange broadening was found between H12 in the active-sites of wild-type and H119A RNase A. This difference is illustrated in Figure 4.7, which shows H12 C–2 peak width plotted against pD for both the wild-type and H119A enzymes. The difference is even more dramatic than the graph suggests, as there are two points near pD 5 where H12 is too broad (> 0.3 ppm) to measure a peak width. This result indicates that the rate of proton transfer to and from H12 is faster in the presence of H119 than it is in its absence.

K_d of d(AUAA) binding determined by fluorescence anisotropy. The K_d for the binding of fluorescein–labeled d(AUAA) to RNase A was measured for the wild-type

(Templer, B. 1995), H119A and H12A enzyme. d(AUAA) is a substrate analog that binds to the active site and distal subsites of RNase A (Fontecilla-Camps, J.C. 1994). The fluorescence polarization data are shown graphically in Figure 4.8 and K_d values (determined by fitting to eq 5.3) listed in Table 4.6. Elimination of either histidine residue from the active-site reduces the affinity of the enzyme for d(AUAA). Wild-type RNase A binds d(AUAA) 12–fold better than does H12A, and 20–fold better than does H119A.

Discussion

H12 and H119 have been known to contribute to the catalytic efficiency of RNase A for many years [for a review of early work see (Richards, F.M. 1971)]. A variety of modification techniques allowed researchers to alter the histidine residues, which was found to inactivate or alter the activity the enzyme (Barnard, E.A. 1959; Barnard, E.A. 1969; Jackson, D.Y. 1994). To date, these techniques have been used only to transform the imidazole side chain into a larger moiety. By use of site–directed mutagenesis, we have made the first RNase A mutants that remove the imidazole functionality of either H12 or H119, replacing it with a proton.

Value of the Histidines to Catalysis: k_{cat}/K_m is proportional to the association constant of an enzyme and the rate–limiting transition state during catalysis (Wolfenden, R. 1976). Comparisons of k_{cat}/K_m^{WT} with k_{cat}/K_m^{H119A} and k_{cat}/K_m^{H12A} yield relative free energies of transition state stabilization using eq 3.2. Figure 4.1 shows that eliminating the imidazole moiety of H12 decreases the affinity for the rate–limiting transition state at least 10^4 when poly(C), UpA or Up(4-nitrophenol) is the substrate. This value converts into a loss of transition state binding energy of >5 kcal/mol. Elimination of the imidazole moiety of H119 decreases the k_{cat}/K_m [poly(C)] by at least 10^4-fold and k_{cat}/K_m [UpA] by almost 10^4-fold. The rate enhancements provided by H119 convert into transition state binding energies of >5 kcal/mol at 25 °C.

The loss of transition state binding energy ($\Delta\Delta G^{\ddagger}$) on mutation of the H12 or H119 is an apparent value, and it is a lower limit of the true value for two reasons. First, the rate cleavage of poly(C) and UpA is not limited by the chemical step (Chapter 3), and it is likely that cleavage by either H119A or H12A *is* limited by the chemistry. Since it is not possible to measure the full rate enhancement of the conversion of bound substrate to bound products by the wild-type enzyme, comparisons with mutants that have different

rate–limiting steps can yield only lower limits for the true loss in transition state binding energy.

Second, individual kinetic parameters suggest that His12 and His119 RNase A may cleave RNA by a different mechanism than the wild–type enzyme. For instance, if titration of the histidines is the source of the bell-shaped pH vs k_{cat}/K_m profile, then mutation of a histidine to alanine should flatten one arm of the profile. However, the bell-shaped pH dependence of k_{cat}/K_m^{H119A} [UpA] is the same as that of wild-type RNase (Figure 4.2). A plot of pH vs log V/K^{H12A}[UpA] is also bell-shaped (Figure 4.5). The pK_a values obtained from these data are different, but too inaccurate to compare quantitatively.

None of these results is consistent with removal of an essential active-site residue of pK_a ~ 6. We were concerned that the results were consistent with a 10^{-4} : 1 mixture of wild-type and mutant RNase A, possibly the result of translational inaccuracy (Schimmel, P. 1989). However, cation exchange treatment of the mutant enzymes in a manner demonstrated to separate them from the wild–type enzyme (Figure 4.6) yielded mutants with the same activity as before purification. Moreover, the pH-dependence of catalysis of the rigorously purified H12A and H119A RNase A is bell-shaped (Figure 4.5, H119A RNase A not shown). The results of the cation exchange purification at pH 5.0 show that the mutants are not contaminated by wild–type RNase A.

The task before us is to explain how a RNase A mutant that has only one active-site histidine can still have a bell-shaped dependence of catalysis on pH. A mechanism that fits available kinetic data on H12A and H119A RNase A is one that has two steps, one of which requires a protonated histidine and the other an unprotonated histidine.

The reaction can be described generally as in Scheme 4.1. This mechanism is kinetically similar to the mechanism described for the cleavage of UpU by imidazole and other buffers proposed by Breslow (Breslow, R. 1989; Breslow, R. 1993).

The chemical mechanism proposed by Breslow involves protonation of the phosphate prior to attack by the 2′-OH (Breslow, R. 1989). The mechanism of the cleavage reaction catalyzed by H12A and H119A RNase A may involve such a step. We propose that the chemical mechanism of cleavage by the mutant enzymes involves protonation of the phosphate in one step, and then general base catalysis of the attack of the 2′-OH (H12A RNase A) or the shuttling of the phosphate proton to the leaving group (H119A RNase A) in another step. This mechanism is illustrated in Figure 4.9. Water may play the role of the missing histidine in each case.

This mechanistic proposal will be tested in the future by using UpU with sulfur in the non-bridge position on phosphorus as a substrate. These compounds have been synthesized and each diastereomer purified to investigate the "thio-effect" on RNase A-catalyzed cleavage of these molecules and to show that RNase A-catalyzed cleavage proceeds by an in-line mechanism (Burgers, P.M.J. 1979; Herschlag, D. 1994). Since protonation of sulfur is more difficult than protonation of oxygen, we may expect effects on the mutants that are different from those seen on the reaction catalyzed by wild–type RNase A, which we presume does not require protonation of the phosphate for reaction to occur. The predicted effects of the sulfur substitution on the rate of cleavage are shown in Table 4.7.

The different mechanisms of cleavage shown by wild–type and the mutant RNase A's make direct comparison of their rates difficult. Despite these limitations, the kinetic data do report on the energetics of catalysis. For example, H12A, H119A and K41A RNase A (Messmore, J.M. 1995) have each lost > 10^4-fold in rate enhancement of the

cleavage reaction relative to wild-type RNase A. In addition, the B2 subsite provides 10^3-fold rate enhancement during the cleavage reaction. The summed total of these rate enhancements is 10^{17}. However, wild-type RNase A enhances the rate of the cleavage reaction 10^{12} (Chapter 3). H12 and H119 may act in a concerted fashion to effect greater acid/base catalysis than either might be capable of singly. Considering that each histidine is pK_a ~ 6 and that their putative proton exchange partners in the cleavage reaction (Figure 1.1) are pK_a ~ 14, a concerted mechanism (Jencks, W.P. 1987) that avoids formation of high energy intermediates like alkoxides is probable. The non-additive contributions to catalysis of H12, H119, K41, and the B2 subsite and the synergistic interactions of wild-type RNase A with 3′-UMP (this work) suggest that eliminating one histidine may impair the other's catalytic function.

Mechanistic roles of H119. The value of H119 to catalysis depends on the pK_a of the conjugate acid of the leaving groups. Poly(C) and UpA have ribonucleoside leaving groups with pK_a's of 14.8, based on the model compound $CH_3OCH_2CH_2OH$ (Ballinger, P. 1960). In contrast to the 10^4 drop in k_{cat}/K_m [UpA, poly(C)] on mutation of H119, k_{cat}/K_m^{H119A} [Up(4-nitrophenol)] is lowered by only 3.4-fold by the mutation. The pK_a of 4-nitrophenol is 7.14 (Fickling, M.M. 1959) and 4-nitrophenolate may not require protonation to leave. Together, these data provide the first direct evidence that the role of H119 is to protonate the leaving group during cleavage of RNA. In other words, when there is no need for an acid catalyst, H119 can be removed with little effect.

Since at pH 6, k_{cat}/K_m^{H119A} [Up(4-nitrophenol)] is 3.4-fold lower than k_{cat}/K_m^{WT} [Up(4-nitrophenol)] (Table 4.1), it follows that H119A is a poorer catalyst of Up(4-nitrophenol) cleavage than is wild-type RNase A at subsaturating substrate concentrations. However, since k_{cat}^{H119A}[Up(4-nitrophenol)] is 2.6-fold greater than k_{cat}^{WT} [Up(4-nitrophenol)], H119A is a better catalyst when saturated (Table 4.1). These data

suggest that H119 aids in forming the enzyme•Up(4-nitrophenol) complex, and then becomes a hindrance to cleavage. Differences in substrate structure (Figure 4.1) provide one explanation for this effect. Up(4-nitrophenol) has a phenyl ring carbon where an RNA substrate has a methylene group. Once the enzyme•Up(4-nitrophenol) complex is formed, a steric clash between H119 and the phenyl ring may hinder proper orientation of the leaving group for cleavage.

The Up(4-nitrophenol) kinetic data also address a recent mechanistic proposal based on model chemistry. This proposal requires that H119 not only act as the acid catalyst during cleavage of RNA, but that it shuttles a proton to a non–bridge oxygen while a stable phosphorane intermediate is formed (Breslow, R. 1989). As noted, however, H119A RNase A is a better catalyst than the wild-type enzyme in terms of k_{cat} at all pH's (Table 4.3) when Up(4-nitrophenol) is the substrate. Thus, our data argue against the participation of H119 in formation of a phosphorane during cleavage of Up(4-nitrophenol); differences between substrates mean that these results may not apply to the mechanism of RNA cleavage.

Finally, on elimination of H119, the exchange broadening of the H12 C–2 proton NMR peak increases markedly (Figure 4.7). This result indicates that H119 speeds the protonation and deprotonation of H12. The proton transfer may occur through a water molecule, as the histidine – histidine distance [6.4 Å, (Nachman, J. 1990)] is too great for direct proton transfer. RNase A is reverse-protonated after it has catalyzed a cleavage reaction (Figure 1.1). Because the cleavage and hydrolysis reactions are kinetically distinct (Chapter 2), RNase A has an iso–mechanism; it must recycle to the correct protonation state before catalyzing another cleavage reaction. H119 accelerates this recycling step.

Mechanistic role of H12. No direct evidence for the mechanistic role of H12 is available from the present kinetic data. However, since H119 has been identified as the general acid catalyst for the cleavage reaction, it seems reasonable to assign H12 the role of the general base. Since H119 must be protonated for catalysis to occur, it is the most probable source of the drop in the pH vs k_{cat}/K_m (UpA) profiles (Figure 4.2) at pH > 6. The pH vs k_{cat}/K_m [Up(4-nitrophenol)] profiles show this unambiguously, but the differences in substrate preclude extension to the catalysis of RNA cleavage (see below). These data leave H12 as the most probable source of the drop in pH vs k_{cat}/K_m at pH< 5.5, which suggests it must be deprotonated for catalysis of cleavage. All the assembled data are consistent with H12 acting as a general base catalyst for RNA cleavage.

Engineering the pH-dependence of catalysis. H119A RNase A is a relatively poor catalyst of RNA cleavage. However, when provided with the right substrate, this sluggish mutant displays novel catalytic properties. Figure 4.4 shows that above pH 7, H119A RNase A is a better catalyst of Up(4-nitrophenol) cleavage than is wild-type RNase A. For reasons noted above, H119A RNase A is a better catalyst of Up(4-nitrophenol) cleavage than is wild-type RNase A at all pH's when Up(4-nitrophenol) is saturating. Above pH 7, where k_{cat}/K_m^{H119A} is greater than k_{cat}/K_m^{WT}, the catalytic activity of H119A RNase A exceeds that of wild-type RNase A at all Up(4-nitrophenol) concentrations. This effect is created by 1) flattening the alkaline drop of the wild-type pH vs k_{cat}/K_m profile by eliminating H119 and 2) lowering the pK_a of the leaving group conjugate acid so that the acid catalyst is not essential for cleavage. However, these changes in substrate and enzyme should yield a catalyst that is an equally efficient catalyst as the wild-type enzyme, not a better one.

In other words, why does the pH vs k_{cat}/K_m^{WT} [Up(4-nitrophenol)] profile drop at pH > 6? The shape of the pH vs k_{cat}/K_m^{WT} [Up(4-nitrophenol)] profile is that of wild-type

RNase A reacting with UpA, and its shape indicates an active site containing two titratable groups, one protonated and one deprotonated. However, comparison of kinetic parameters for Up(4-nitrophenol) cleavage by H119A and wild-type RNase A shows that H119 does not participate in the reaction (Table 4.1), which suggests that the pH vs k_{cat}/K_m^{WT}[Up(4-nitrophenol)] should be flat at pH ≥ 6. The simplest explanation is that wild-type RNase A is incapable of binding to Up(4-nitrophenol) when H119 is deprotonated. H119 does not participate in cleavage of *bound* Up(4-nitrophenol) by wild-type RNase A, but it is required to *bind* Up(4-nitrophenol) because when it is deprotonated, the wild–type enzyme cannot catalyze the cleavage of Up(4-nitrophenol). In contrast, H119A RNase A must bind Up(4-nitrophenol) in a different way, because it can both bind and cleave this substrate in the absence of H119.

Interactions of the histidines with each other. The pK_a's measured for the active-site histidines show that their interactions with each other can be regarded as primarily Coulombic. In the free enzyme, H12 and H119 have two microscopic pK_a's each, suggesting that when one is protonated it lowers the pK_a of the other. The active-site pK_a's of the H119A and H12A RNase A corroborate this model. For instance, H12 has nearly the same pK_a in H119A as it does in wild-type RNase A with H119 deprotonated (Table 4.5). The well-behaved pK_a's of the mutant active-site histidines also suggest that one histidine is structurally unaffected by removal of the other.

It is interesting to note that eliminating a histidine from an active site containing 3′-UMP has an effect opposite to that on the free enzyme. The pK_a of the remaining histidine is depressed, not elevated (Table 4.5). This decrease is not the result expected from a simple Coulombic model of the interactions of inhibitor and enzyme. For example, a Coulombic model predicts that if H12 is eliminated, the negative charge of the phosphoryl group will be more available to interact with H119. Then, the protonated

form of H119 would be more stable in the complex of 3′-UMP with H12A RNase A than with the wild–type enzyme, and the pK_a of H119 would be elevated. Yet, the opposite effect is seen. The loss of one positively charged histidine by either deprotonation or mutagenesis is accompanied by a loss in favorable interactions between the phosphate and the remaining histidine, whose pK_a is depressed (Figure 4.10 a). This result implies that the 3′-UMP negative charges are distributed to both monovalent phosphate oxygens even when a positively charged histidine is on one side of the inhibitor. The two histidines and the inhibitor form a sort of "Coulombic sandwich", wherein the histidines act synergistically to bind the 3′-UMP (Figure 4.10 b).

Value of the histidines to affinity for the ground state. The DNA four-mer d(AUAA) is a substrate analog. The crystal structure of the enzyme with d(ATAA) shows that the δ–nitrogen of H119 is in a hydrogen bond with the 5′–oxygen of the third A, which is analogous to the leaving group oxygen. The ε–nitrogen of H12 is in a hydrogen bond with a nonbridge oxygen (Fontecilla-Camps, J.C. 1994). It is impossible to determine whether the observed loss in binding free energy corresponds to the energy of these hydrogen bonds because neither mutant structure is available. Still, the contributions of H12 (1.5 kcal/mol) and H119 (1.8 kcal/mol) to the binding energy of d(AUAA) suggest that these are either weak hydrogen bonds or that water takes over the hydrogen bond donor/acceptor role in the mutants, diminishing the net loss in binding energy. Alternatively, the structure of the DNA• mutant complex may have a number of differences from the wild-type structure that add up to the net loss in binding energy. Regardless, the interactions of the active-site histidine residues with the ground state (<1.5 kcal/mol) are much weaker than their interactions with the transition state (>5 kcal/mol).

Table 4.1

Kinetic parameters for the cleavage reaction at pH 6.0. Data for cleavage of poly(C) by wild-type RNase A are from (Templer, B. 1995). All reactions with poly(C) and Up(4-nitrophenol) were performed at 25 °C in 50 mM MES-HCl buffer, pH 6.0, containing 0.10 M NaCl. Reactions with UpA were performed at 25° C in 0.1 M cacodylate buffer, pH 6.0, I = 0.20 M. Steady-state kinetic parameters were determined by fitting initial velocity data to a hyperbolic curve v= (V*S)/(K_m+S) using the program HYPERO (Cleland, W.W. 1979), where v is the initial velocity; V is the maximum velocity; S is substrate concentration, and K_m is the Michaelis constant. Cleavage of poly(C) and Up(4-nitrophenol) was monitored at 250 nm ($\Delta\varepsilon_{250}$ = 2380 $M^{-1}cm^{-1}$) and 330 nm ($\Delta\varepsilon_{330}$ = 4560 $M^{-1}cm^{-1}$), respectively; cleavage of UpA was monitored at 286 nm ($\Delta\varepsilon_{286}$ = –670 $M^{-1}cm^{-1}$).

RNase A	substrate	k_{cat} (s^{-1})	K_m (mM)	k_{cat}/K_m ($M^{-1}s^{-1}$)	$(k_{cat}/K_m)^{mutant}/(k_{cat}/K_m)^{wild\text{-}type}$
wild-type	poly(C)	510 ±10	0.089 ± 0.009	$(5.7 \pm 0.5)\times10^{6}$	1.0
H12A	poly(C)	0.073 ± 0.006	0.105 ± 0.025	$(7.3 \pm 1.2)\times10^{2}$	$(1.3 \pm 0.3)\times10^{-4}$
H119A	poly(C)	0.027 ± 0.001	0.052 ± 0.010	$(5.1 \pm 0.7)\times10^{2}$	$(8.9 \pm 1.4)\times10^{-5}$
wild-type	UpA	1350 ±60	0.29 ± 0.03	$(4.5 \pm 0.3)\times10^{6}$	1.0
H12A	UpA	0.18 ± 0.03	0.23 ± 0.14	$(8.0 \pm 2.8)\times10^{2}$	$(1.8 \pm 1.4)\times10^{-4}$
H119A	UpA	0.026 ± 0.003	0.17 ± 0.053	$(1.44 \pm 0.3)\times10^{2}$	$(3.2 \pm 0.7)\times10^{-5}$
wild-type	$UpOC_6H_4pNO_2$	18.8 ± 0.6	0.33 ± 0.05	$(5.7 \pm 0.6)\times10^{4}$	1.0
H12A	$UpOC_6H_4pNO_2$	0.0029 ± 0.0001	0.275 ± 0.041	$(1.1 \pm 0.1)\times10^{1}$	$(1.9 \pm 0.3)\times10^{-4}$
H119A	$UpOC_6H_4pNO_2$	27 ± 1	0.76 ± 0.08	$(3.6 \pm 0.1)\times10^{4}$	0.63 ± 0.11

Table 4.2

Steady-state kinetic parameters for cleavage of UpA by wild-type and H119A RNase A as a function of pH. Dashed lines indicate the value was not measured. All reactions were performed at 25° C. The cleavage of UpA was monitored in the absence of adenosine deaminase at 286 nm (Witzel, H. 1962). $\Delta\varepsilon_{286}$ at each pH is shown in Table 5.2. Assays were carried out at 25° C. For pH 4.0 – 5.5 the buffer was acetate; 6.0 – 7.0 cacodylate; 7.5 – 8.0 *tris*– (hydroxymethyl)aminomethane. At each pH, [buffer] = 0.067 M and I = 0.20. Steady-state kinetic parameters were determined by fitting initial velocity data to a hyperbolic curve (V*S)/(K_m+S) using the program HYPERO (Cleland, W.W. 1979), where V is the maximum velocity; S is substrate concentration, and K_m is the Michaelis constant.

	Wild-type			H119A		
pH	k_{cat} (s^{-1})	k_{cat}/K_m ($M^{-1}s^{-1}$)	K_m (mM)	k_{cat} (s^{-1})	k_{cat}/K_m ($M^{-1}s^{-1}$)	K_m (mM)
3.8	66 ± 1.7	2.40 ± 0.10 x 10^5	0.27 ± 0.07	----	2.2 ± 0.1	----
4.5	163 ± 16	7.8 ± 0.8 x 10^5	0.21 ± 0.04	0.008 ± 0.001	18.0 ± 3.1	0.42 ± 0.14
5.0	421 ± 44	2.52 ± 0.58 x 10^6	0.17 ± 0.05	----	----	----
5.5	822 ± 36	4.75 ± 0.44 x 10^6	0.17 ± 0.02	0.019 ± 0.002	109 ± 25	0.17 ± 0.06
6.0	1349 ± 61	4.56 ± 0.33 x 10^6	0.29 ± 0.03	0.033 ± 0.004	138 ± 28	0.24 ± 0.07
6.5	1219 ± 92	2.19 ± 0.12 x 10^6	0.55 ± 0.07	0.050 ± 0.004	75 ± 5	0.67 ± 0.10
7.0	1645 ± 155	1.29 ± 0.06 x 10^6	1.27 ± 0.18	0.064 ± 0.009	56 ± 5	1.15 ± 0.26
7.5	----	3.2 ± 0.9 x 10^5	----	----	14 ± 2	----
8.0	----	1.28 ± 0.22 x 10^5	----	----	4.7 ± 0.3	----

Table 4.3

Steady-state kinetic parameters for cleavage of Up(4-nitrophenol) by RNase A and H119A as a function of pH. The cleavage of Up(4-nitrophenol) was monitored at 330 nm or 410 nm. $\Delta\varepsilon_{330}$ and $\Delta\varepsilon_{410}$ at each pH are shown in Table 5.2. Assays were carried out at 25° C. For pH 4.0 – 5.5 the buffer was acetate; 6.0 – 7.0, cacodylate; 7.5 – 8.0, *tris*– (hydroxymethyl)aminomethane. At each pH, [buffer] = 0.10 M and I = 0.20. Steady-state kinetic parameters were determined by fitting initial velocity data to a hyperbolic curve (V*S)/(K_m+S) using the program HYPERO (Cleland, W.W. 1979), where V is the maximum velocity; S is substrate concentration, and K_m is the Michaelis constant.

pH	Wild-type			H119A		
	k_{cat} (s^{-1})	k_{cat}/K_m ($M^{-1}s^{-1}$)	K_m (mM)	k_{cat} (s^{-1})	k_{cat}/K_m ($M^{-1}s^{-1}$)	K_m (mM)
4.0	2.93 ± 0.14	5236 ± 74	0.56 ± 0.03	5.04 ± 0.60	720 ± 21	7.00 ± 0.98
4.5	3.13 ± 0.34	14840 ± 550	0.218 ± 0.033	6.99 ± 0.31	2250 ± 45	3.10 ± 0.22
5.0	3.83 ± 0.05	34170 ± 307	0.112 ± 0.002	16.8 ± 0.3	5390 ± 32	3.11 ± 0.06
5.5	5.29 ± 0.21	48080 ± 6250	0.11 ± 0.02	20.52 ± 2.67	10630 ± 744	1.93 ± 0.41
6.0	9.74 ± 0.78	50200 ± 400	0.194 ± 0.029	25.56 ± 0.46	14870 ± 223	1.72 ± 0.07
6.5	24.00 ± 0.43	35725 ± 1429	0.672 ± 0.034	42.7 ± 4.7	15920 ± 748	2.68 ± 0.40
7.0	30.11 ± 2.01	18700 ± 4490	1.61 ± 0.47	46.0 ± 3.7	21210 ± 1210	2.17 ± 0.28
7.5	25.90 ± 1.3	5236 ± 680.68	4.95 ± 0.89	52.7 ± 2.7	17264 ± 310	3.05 ± 0.21
8.0	15.60 ± 0.58	2170 ± 108.5	7.17 ± 0.63	83.7 ± 4.8	15050 ± 150	5.56 ± 0.39

Table 4.4

Kinetic parameters for fits of pH vs k_{cat}/K_m and V/K^{H112A} (UpA). pH vs $k_{cat}/K_m^{wild\text{-}type}$ [UpA} and $k_{cat}/K_m^{wild\text{-}type}$ [Up(4-nitrophenol) were fit to eq 4.1. pH vs k_{cat}/K_m^{H119A}[Up(4-nitrophenol)} was fit to eq 4.2. pH vs k_{cat}/K_m^{H119A}[UpA] and pH vs V/K^{H112A}[UpA] were fit to eq 4.3. k_{cat}/K_m^{ind} is the pH independent k_{cat}/K_m, k_1, k_2, k_{-1}, are the rate constants corresponding to the steps shown in Scheme 4.1. The pK_a values correspond to the pK_a's of the titratable groups involved in catalysis.

Enzyme	Substrate	k_{cat}/K_m^{ind}	pK_a	pK_b		
wild-type	UpA	1.6×10^7	5.7	5.9		
wild-type	Up(4-nitrophenol)	8.43×10^5	5.2	6.3		
H119A	Up(4-nitrophenol)	1.79×10^5	5.35	---		
		$k_1 * k_2$			k_{-1}	k_2
H12A	UpA	----	5.2	----	----	----
H119A	UpA	6100	5.6	----	5.7	28

Table 4.5

pK_a data derived from pD titrations of wild-type (Quirk, D.J. 1995), H12A, and H119A RNases as monitored by ^{1}H NMR. pK_a's were determined by titrating the enzyme in D_2O at 25° C I = 0.20 (with NaCl) and fitting the histidine chemical shift data as a function of pD to eqs 5.2 and 5.3. Experiments with 3′-UMP were performed at 65 mM 3′-UMP and I = 0.20 (with NaCl). No correction for the effect of D_2O on pK_a (Jencks, W.P. 1987) was made.

		Wild-type	H12A	H119A
residue	3′-UMP	pK_a	pK_a	pK_a
His 12	–	6.12 5.74 3.99	–	6.08
His 119	–	6.32 5.94	6.40	–
His 105	–	6.78	6.83	6.84
His 12	+	6.45 6.35 3.77	–	6.31 4.06
His119	+	7.95 7.85 4.06	7.79 4.67	–
His 105	+	6.86	6.86	6.85

Table 4.6

Values of K_d for the binding of fluorescein–labeled d(AUAA) to wild-type (Templer, B. 1995), H12A, and H119A RNase A. Fluorescence polarization was monitored as a function of protein concentration at 25 ± 2° C in MES-HCl buffer (100 mM, pH 6.0, 0.10 M NaCl). K_D was measured by fitting the polarization data to eq 5.3. The free energies were computed using $\Delta G^{\circ}_{relative} = -RT \ln(K_d^{WT} / K_d^{mutant})$.

Enzyme	K_d (mM)	$\Delta G^{\circ}_{relative}$ (kcal/mol)
wild-type	0.090	0.0
H12A	1.1	+1.5
H119A	1.8	+1.8

Table 4.7

Predicted effects of sulfur substitution at the non-bridge oxygen positions of UpU on the rate of cleavage by RNase A. The effects are expressed as the ratio of the rate of the oxygenated compound to the rate of the sulfur substituted compound. The wild-type values are based on the work of Burgers and Eckstein (Burgers, P.M.J. 1979). The mutant values are predicted from the mechanism shown in Figure 4.9.

Diastereomer	wild–type RNase A	H12A RNase A	H119A RNase A
Up(S)U (R_p)	2	>2	2
Up(S)U (S_p)	70	70	>70

Figure 4.1

Substrates used to assay RNA cleavage activity of RNase A and its mutants.

UpA

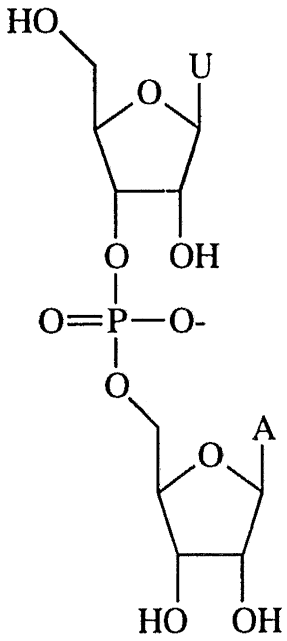

poly(C)

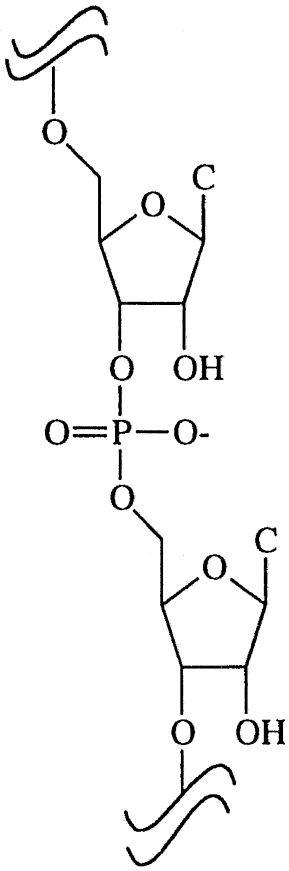

Up(4–nitrophenol)

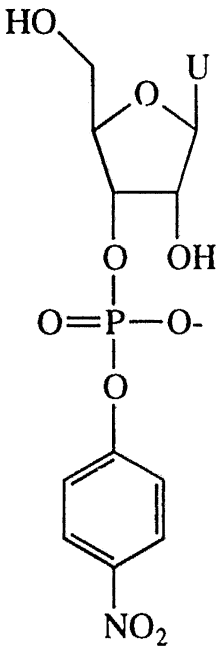

Figure 4.2

Values of k_{cat}/K_m for catalysis of cleavage of poly(C), UpA and Up(4-nitrophenol) by H12A, H119A, and wild-type RNase A.

Figure 4.2 will go here

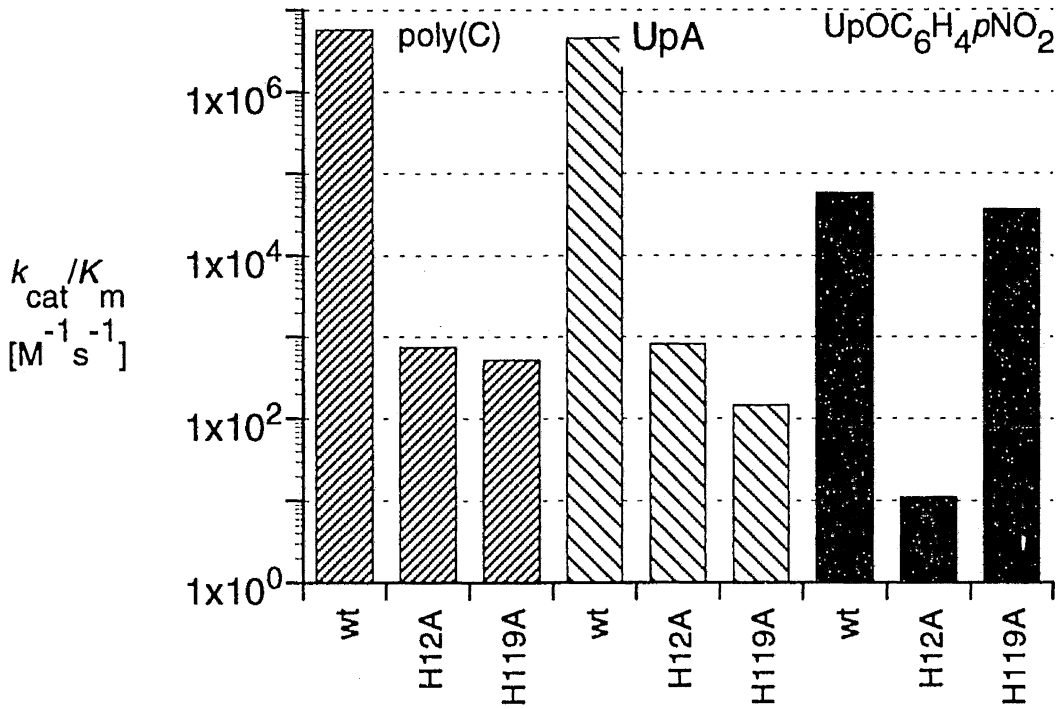
poly(C)
UpA
UpOC6H4pNO2
1x10^6
1x10^4
1x10^2
1x10^0
kcat/Km
[M^-1 s^-1]
wt
H12A
H119A
wt
H12A
H119A
wt
H12A
H119A

Figure 4.3

Dependence of log (k_{cat}/K_m) on pH for UpA cleavage catalyzed by H119A (○) and wild-type (□) RNase A. The solid lines were generated by fitting the data to eq 4.1 for wild-type and 4,3 for H119A RNase A.

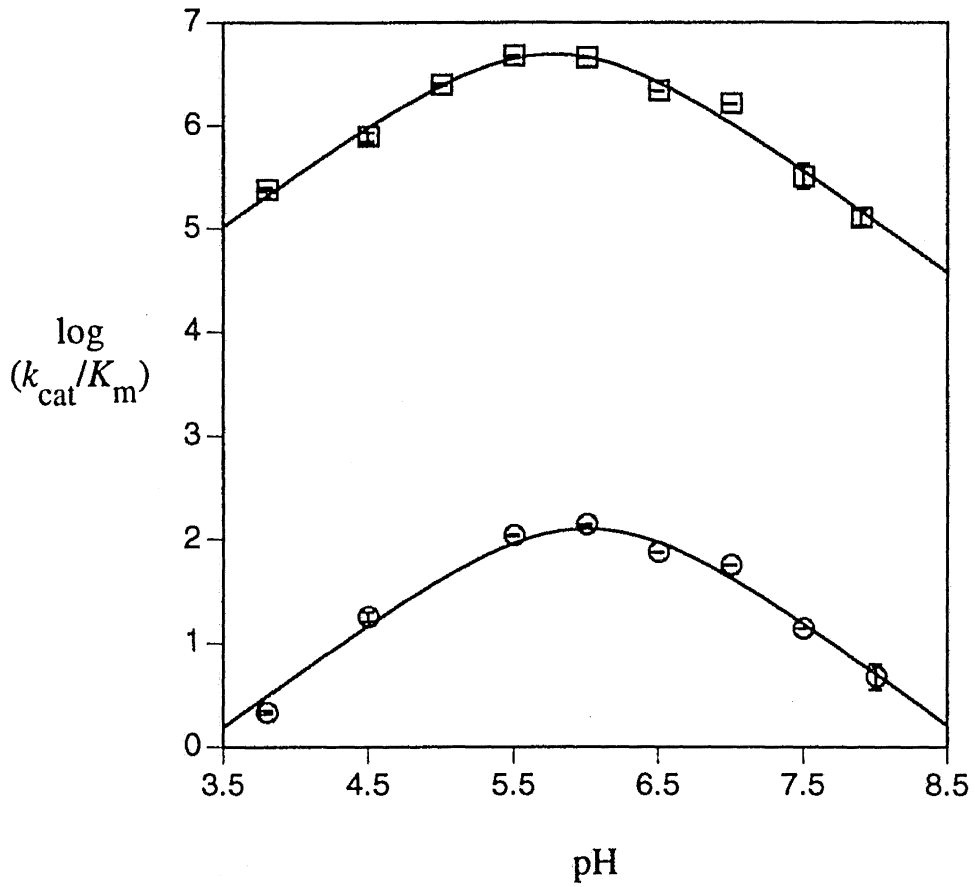
7
6
5
4
3
2
1
0
log
(k_{cat}/K_m)
3.5
4.5
5.5
6.5
7.5
8.5
pH

Figure 4.4

Dependence of $\log(k_{cat}/K_m)$ on pH for Up(4-nitrophenol) cleavage catalyzed by H119A (○) and wild-type (□) RNase A. Solid lines were generated by fitting the data to eq 4.1 (wild-type RNase A) and eq 4.2 (H119A RNase A).

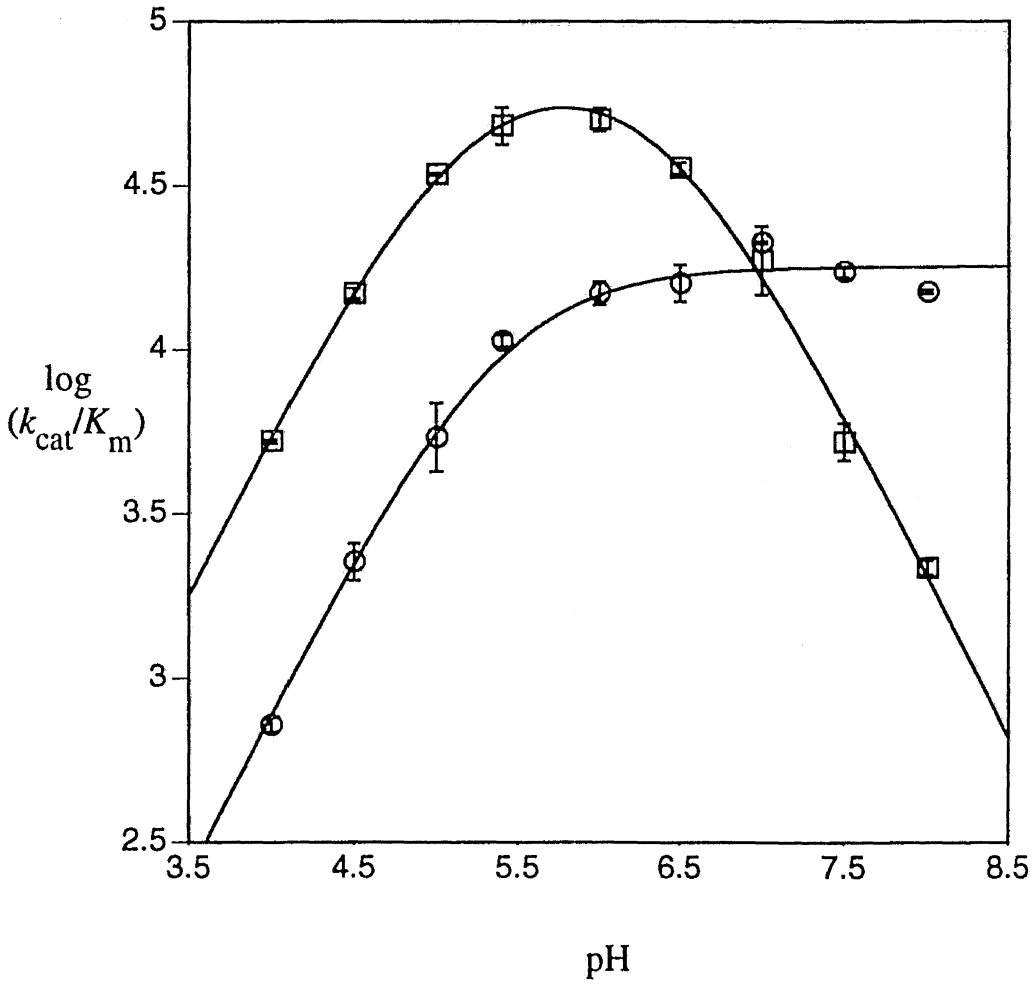
5
4.5
4
3.5
3
2.5
log
(k_{cat}/K_m)
3.5
4.5
5.5
6.5
7.5
8.5
pH

Figure 4.5

pH-dependence of log (V/K*S) of cleavage of UpA by H12A RNase A. Assays were carried out at 25 °C. At pH 4.0, 5.0, the buffer was acetate; 6.0, at pH 7.0, cacodylate; at pH 8.0 *tris*– (hydroxymethyl)aminomethane, [buffer] = 0.10 M and I = 0.20 M. Initial velocity was measured at 0.1 mM UpA, 2.5 μM H12A and taken as equal to V_{max}/K_m*[UpA], except at pH 6, where the initial velocity was taken as equal to $V_{max}/1.5K_m$*[UpA].

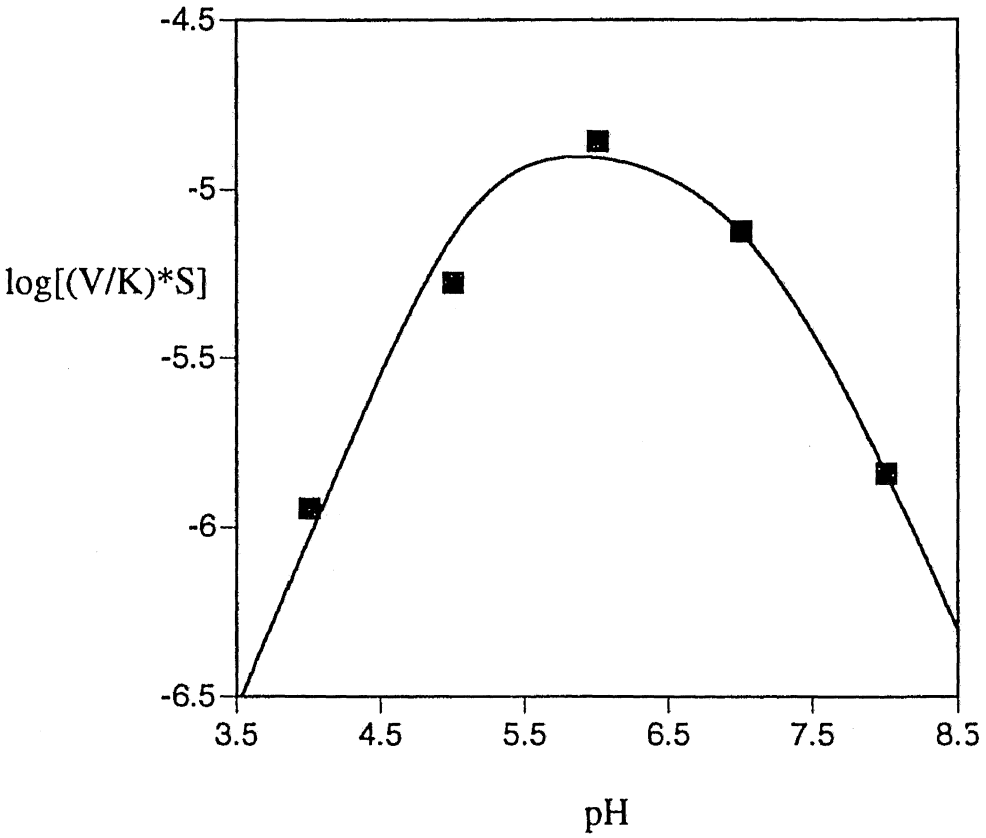
-4.5
-5
-5.5
-6
-6.5
log[(V/K)*S]
3.5
4.5
5.5
6.5
7.5
8.5
pH

Figure 4.6

Elution profile of wild–type and H12A RNase A from a Mono-S cation column at pH 5.0. The proteins were eluted by increasing the concentration of NaCl from 0.20 to 0.28 M over 100 mL.

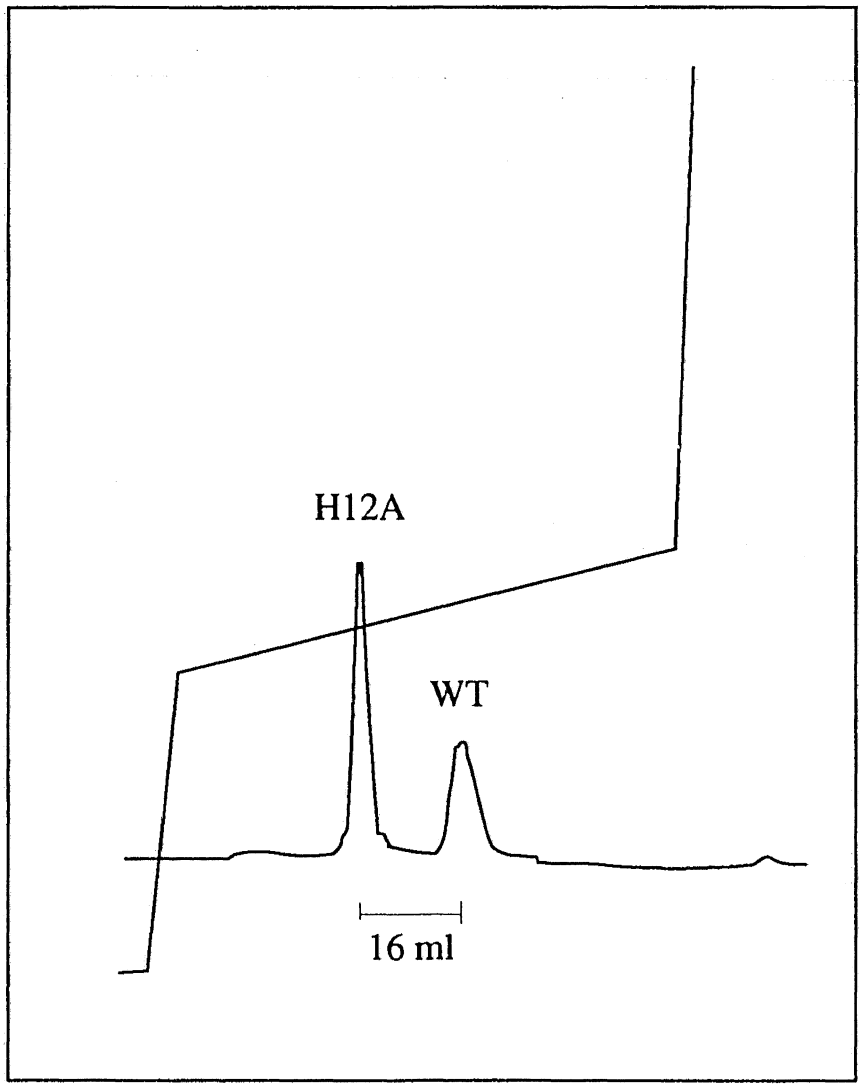
H12A
WT
16 ml

Figure 4.7

Peak width of the H12 C–2 proton in H119A (●) and wild-type (□) RNase A as a function of pD.

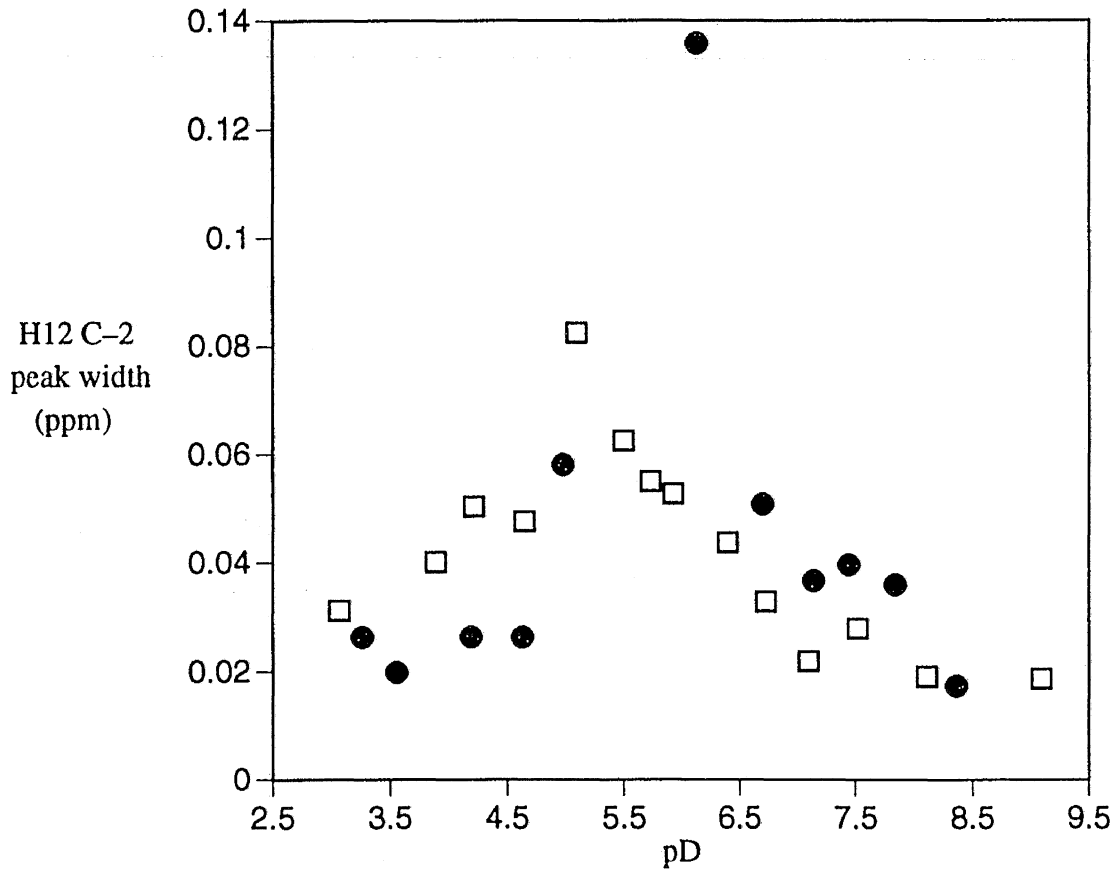
H12 C–2
peak width
(ppm)
0.14
0.12
0.1
0.08
0.06
0.04
0.02
0
2.5
3.5
4.5
5.5
6.5
7.5
8.5
9.5
pD

Figure 4.8

Fluorescence polarization of fluorescein–labeled d(AUAA) as a function of protein concentration for H12A (▲), H119A (●) and wild-type(■) RNase A. The solid lines were generated by fitting the data to eq 5.3.

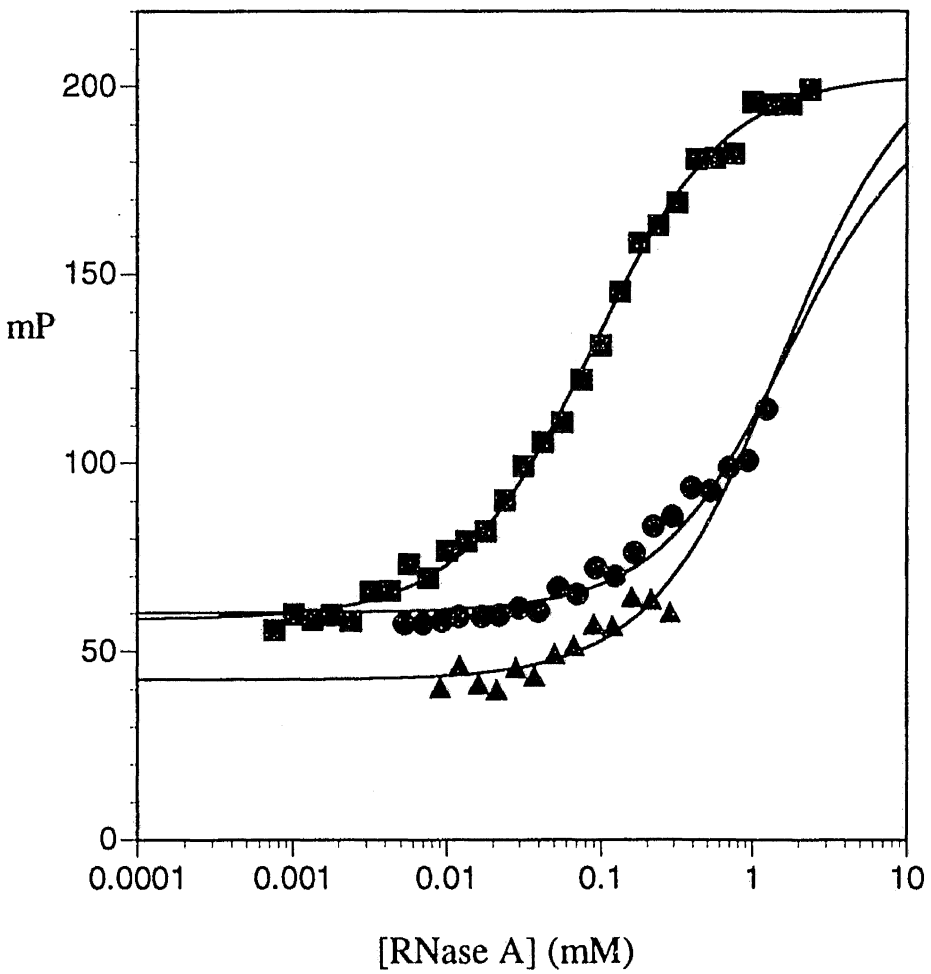
200
150
mP
100
50
0
0.0001
0.001
0.01
0.1
1
10
[RNase A] (mM)

Figure 4.9

Postulated mechanism for cleavage of UpA by H12A RNase A (a) and H119A RNase A (b).

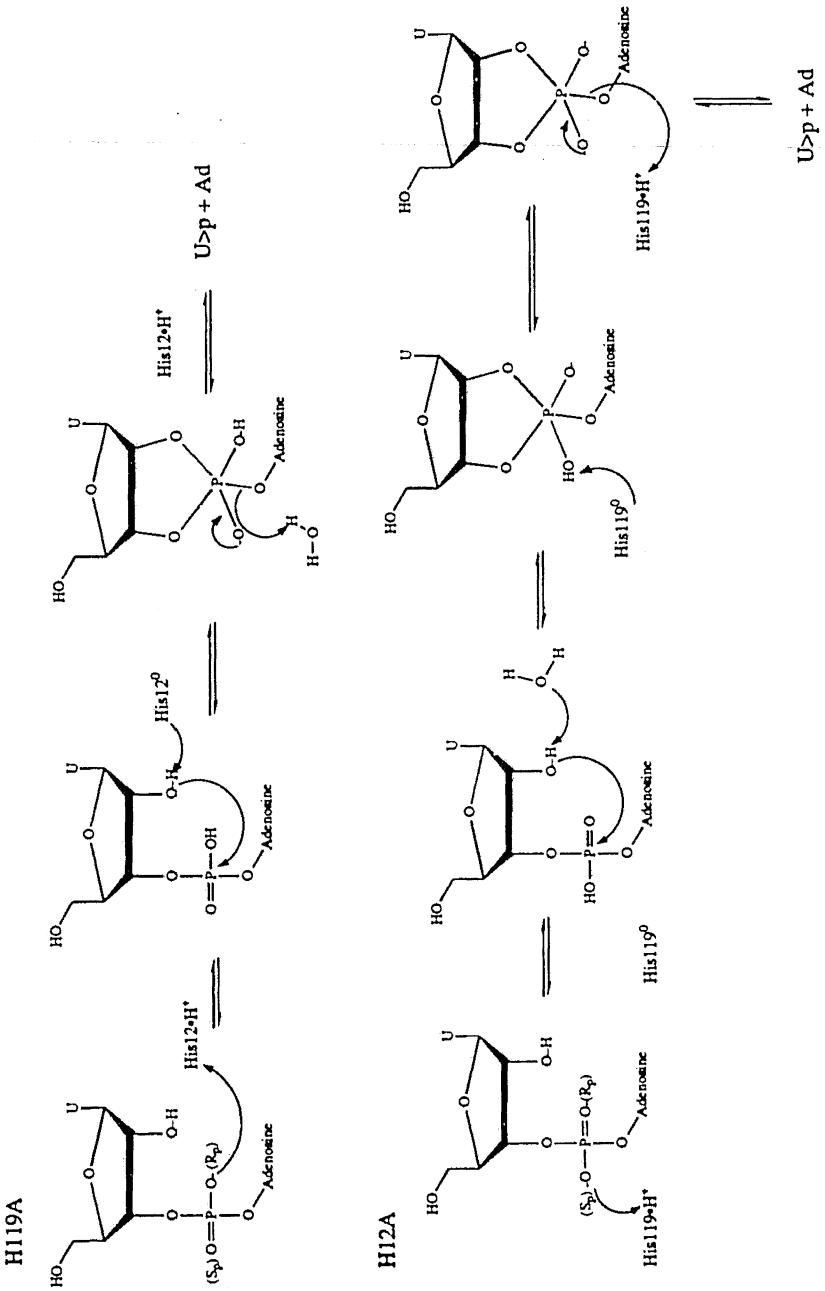
H119A
H12A
U>p + Ad
U>p + Ad
His12•H+
His119•H+
His12⁰
His119⁰
Adenosine
(Sp)O=P—O-(Rp)
(Sp)-O—P=O-(Rp)
O=P—OH
HO—P=O
H—O
HO

Figure 4.10

Qualitative interactions of the phosphate of 3′-UMP with H119A (a) and wild-type(b) RNase A implied by the histidine pK_a's. The loss of H119 *decreases* the strength of interaction between H12 and the phosphate, as measured by the shift in pK_a of H12. The pK_a's of H119 in the active site of H12A RNase A behave similarly.

A

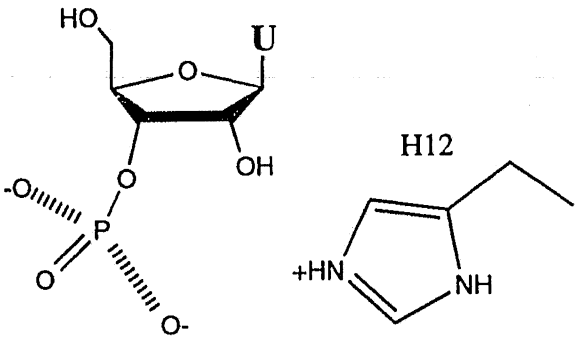

pK_a: 6.31

B

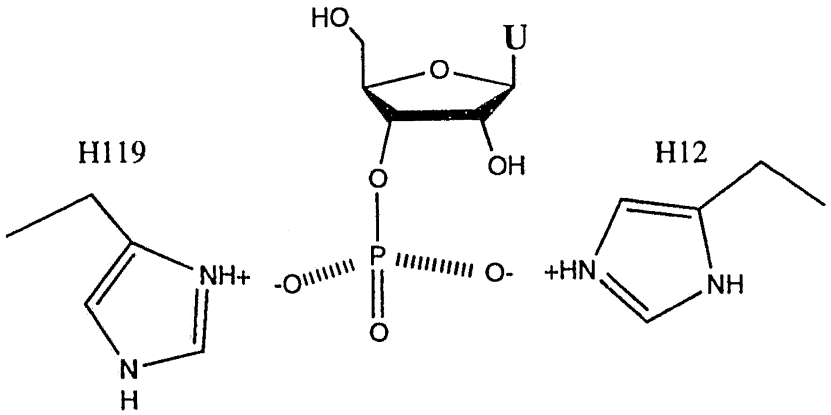

pKa: 7.95

pKa: 6.45

Scheme 4.1 The kinetic scheme for a two-step reaction that requires a histidine protonated in one step and unprotonated in the other.

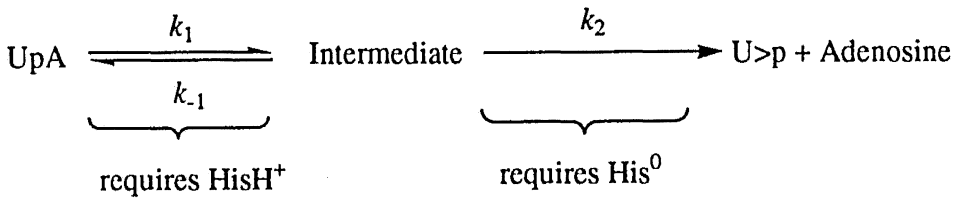
UpA
k_1
k_{-1}
Intermediate
k_2
U>p + Adenosine
requires HisH+
requires His0

Chapter 5

Experimental methods

General Methods

Materials. RNase A (type X–A) was from Sigma Chemical (St. Louis, MO). Poly(U), UpA, U>p, Up, yeast RNA, and salmon sperm DNA were from Sigma Chemical (St. Louis, MO). Polymeric substrates were precipitated from aqueous ethanol (70% v/v) before use.

Spectrophotometric Methods. Ultraviolet absorbance measurements were made on a Cary Model 3 spectrophotometer equipped with a Cary temperature controller. Substrate concentrations were determined by ultraviolet absorption using ε_{260} = 24,600 $M^{-1}cm^{-1}$ at pH 7.0 for UpA (Warshaw, M.M. 1966); ε_{261} = 9,430 $M^{-1}cm^{-1}$ at pH 7.5 for poly (U) (Yakovlev, G.I. 1985); ε_{278} = 6200 $M^{-1}cm^{-1}$ at pH 7.8 for poly(C) (Yakovlev, G.I. 1985); ε_{260} = 9090 $M^{-1}cm^{-1}$ for yeast RNA and ε_{260} = 10,290 $M^{-1}cm^{-1}$ at pH 7.0 for DNA (Ausubel, F.M. 1989) and are given in terms of the molarity of P–$O_{5'}$ bonds. Up (4–nitrophenol) was quantified by dissolving an aliquot of the material in 0.4 N NaOH, measuring absorbance at 408 nm, and using an ε_{408} = 18.3 mM^{-1} cm^{-1}.

Substrate Synthesis

UpA was synthesized by the methods of Ogilvie (Ogilvie, K.K. 1978) and Caruthers (Beaucage, S.L. 1981) (Figure 5.1). UpA was also purchased from Sigma (St. Louis, MO).

Materials. β-Cyanoethyl *N,N*-diisopropylaminochlorophosphoramidite was from Peninsula Research (Belmont, CA). THF was from Aldrich Chemical (Milwaukee, WI), and was freshly-distilled over Na(s) and benzophenone. Pyridine was fractionally distilled from CaH_2 and only the distillate of the boiling temperature 114 °C was used as

a reagent. Authentic UpA was from Sigma Chemical (St. Louis, MO). All other reagents were from Aldrich Chemical, and were used without further purification.

Thin-layer chromatography plates pre-coated with 0.25 mm silica gel (60 F_{254}) were from EM Science (Gibbstown, NJ). Flash chromatography (Still, W.C. 1978) was carried out on silica gel (60-200 mesh) from J.T. Baker (Phillipsburg, NJ). DEAE Sephadex A-25 anion exchange resin was from Pharmacia LKB (Uppsala, Sweden).

Methods. All glassware used was flame-dried, and cooled under N_2(g). All reactions were performed under N_2(g).

2′,5 di-O-(t-butyldimethylsilyl)uridine (**1**). Uridine (2 g, 8 mmol) was dissolved in DMF (20 mL). Imidazole (3 g, 35.2 mmol) and *t*-butyldimethylsilyl chloride (3 g, 18 mmol) were added and the resulting solution was stirred at room temperature for 2 h. The reaction mixture was quenched with brine, and extracted three times with ether. The combined ether extract was dried with $MgSO_4$, and concentrated under reduced pressure to an oil. The products were 2′,5′-; 3′,5′-; and 2′,3′,5′-O-blocked uridine which had R_f's in ether of 0.62, 0.44, and 0.79, respectively. Product **1** was separated by flash chromatography (hexane:ether initially 2:1, then 1:1, and finally 1:2) and was recrystallized from ether and petroleum ether. An alternative method, which proved to yield more of the desired product used a $Ag(NO_3)$ catalyst to direct silylation of the 2′ and 5′ hydroxyl groups (Hakimelahi, G.H. 1981).

Uridine phosphoramidite (**2**). 2′,5′ di-O-(*t*-butyldimethylsilyl)uridine (1.2 g, 2.5 mmol) was dissolved in THF (1 mL). *N,N*-diisopropylethylamine (Hunig's base) was added (1.78 mL, 7.5 mmol), immediately followed by β-cyanoethyl *N,N*-diisopropyl aminochlorophosphoramidite (0.83 mL, 3.75 mmol). The resulting solution was stirred

at room temperature for 3 h, while a white precipitate formed, presumably from salts of Hunig's base. The reaction mixture was quenched with a saturated aqueous solution of NaC_2O_3, and extracted several times with ether. The combined ether extract was dried with $MgSO_4$, concentrated under reduced pressure and subjected to flash chromatography (2:1 ether:hexane, containing triethylamine [1% (v/v)]) to yield product **2** (R_f 0.6, ether). The R_f of **2** was virtually identical to that of **1**, but product **2** stained more quickly with I_2(s) than did **1** and gave two closely-spaced spots, which correspond to different diastereomers.

2′,3′,5′tri-O-(t-butyldimethylsilyl)adenosine (**3**). Adenosine (5.49 g, 20.5 mmol) was suspended in DMF (20 mL). Imidazole (12.2 g, 198 mmol) and *t*-butyldimethylsilyl chloride (13.5 g, 89 mmol) were added, and the resulting suspension (which became homogenous in about 30 min) was stirred for 2 – 24 h. The reaction mixture was quenched with a saturated aqueous solution of NaCl, and extracted three times with ether. The combined ether extract was dried with $MgSO_4$ and concentrated under reduced pressure, and the product subjected to flash chromatography (ether:hexane 1:1 then ether) to yield two products (R_f 0.42, R_f 0.9, ether) that presumably correspond to trisilylated adenosine and tetrasilylated adenosine (also silylated on N^6), respectively. Both products were carried on to **4**.

2′,3′di-O-(t-butyldimethylsilyl)adenosine (**4**). 2′,3′,5′ tri-O-(*t*–butyldimethylsilyl) adenosine was dissolved in aqueous acetic acid [80% (v/v), 10 g per gram of blocked nucleoside], and the resulting solution was stirred at 100 °C for 3 h. The reaction mixture was concentrated under reduced pressure to oil which was dissolved in ether. A saturated aqueous solution of sodium bicarbonate was added to neutralize excess acid, and the

resulting solution was extracted three times with ether. The combined ether extract was dried with $MgSO_4$, and concentrated under reduced pressure to an oil. The product was recrystallized twice, once from ether and petroleum ether, and then from THF and acetonitrile to yield **4** (R_f 0.12, ether; R_f 0.3, ethyl acetate).

Protected UpA (**5**). 2′,3′ di-O-(*t*-butyldimethylsilyl)adenosine (1 eq) was dissolved in the minimum volume of THF and tetrazole (10 eq) was added. The tetrazole did not dissolve completely. This suspension was added to phosphoramidite **2** (1 eq), and the reaction mixture was stirred at room temperature for 6 h. A white solid formed, presumably from precipitation of tetrazolium salts.

I_2(s) (1 eq) was dissolved in aqueous THF [15 mL, 67% (v/v)], and this solution was added dropwise to the reaction mixture. The resulting solution was stirred at room temperature for 15 min. Aqueous sodium bisulfite [10% (w/v), freshly prepared] was added to reduce excess I_2(s), and the resulting solution was extracted three times with CH_2Cl_2. The CH_2Cl_2 extract was dried with $MgSO_4$, concentrated under reduced pressure, and subjected to flash chromatography (CH_2Cl_2 containing methanol [3% (v/v)]) to yield product **5** (R_f 0.24, ethyl acetate).

UpA. 2′,5′ di-O-(*t*-butyldiemethylsilyl) uridylyl (3′→ 5′) 2′,3′ di-O-(*t*-butyldimethylsilyl) adenosine (**5**) was dissolved in ethanolic NH_4OH [20 mL, NH_4OH 75% (v/v) in ethanol] and maintained at 55 °C overnight without stirring. The reaction mixture was then concentrated under reduced pressure to an oil, which was dissolved in 20 mL of a 1.0 M solution of tetrabutyl ammonium fluoride in THF, and stirred at room temperature for 3 to 6 h. The UpA product had R_f 0.8 in 30% (v/v) 0.18 M NaCl in EtOH. The reaction mixture was diluted two-fold with H_2O, the THF was removed

under reduced pressure, and the aqueous solution was extracted once with ether. Any ether dissolved in the aqueous layer was removed under reduced pressure, and this solution maintained at 4 °C overnight. Much of the TBAF crystallized, and these crystals were removed by Buchner filtration.

A column (10 cm x 3.1 cm^2) of A–25 anion exchange resin was equilibrated with 0.5 M triethylammonium bicarbonate buffer, pH 8, and then rinsed with water until the conductivity of the eluant was less than 1 mΩ. The filtrate from the deprotection reaction was diluted until its conductivity was 2 mΩ, and then loaded onto the column. The loaded column was washed with water until the absorbance at 280 nm was 0. The column was eluted with a linear gradient (0 – 0.20 M, 150 mL + 150 mL) of triethylammonium bicarbonate buffer, pH 8. UpA eluted soon after the beginning of the gradient. The fractions containing UpA were concentrated under reduced pressure to an oil, dissolved in methanol and concentrated under reduced pressure to an oil several times, and then dissolved in methanol (5 to 10 mL). Ethylacetate was added until cloudiness persisted, and the resulting solution was incubated at –20 °C to yield UpA as a white solid [R_f 0.8, ethanol containing 0.18 M NaCl (30% v/v)]. The synthetic UpA (40% yield from **2** and **4**) was identical to commercial UpA in its extinction coefficient at 260 nm, ^1H NMR spectrum, and reactivity with RNase A.

Synthesis of Up (4–nitrophenol). Up (4–nitrophenol) was synthesized as described previously (Davis, A.M. 1988) (and references therein) with some modifications (Figure 5.2). Our synthetic protocol is given below for archival purposes.

3´O–Benzoyl uridine (**7**) (Fromageot, H.P.M. 1967) Toluene sulfonic acid monohydrate (1.5 g, 7.9 mmol) was dissolved in trimethylorthobenzoate (15 mL). Uridine (3 g, 12.3 mmol) was added to the solution which was then stirred for 30 min. Acetic acid (50% (v/v), 20 mL) was added, and the reaction stirred for 1 h.

The reaction mixture was concentrated under reduced pressure, dissolved in $CHCl_3$ and filtered. The filtrate was subjected to flash chromatography [$CHCl_3$ containing a gradient of methanol (1-7%)] to yield 3´ O–benzoyl uridine (R_f 0.3, ethyl acetate) as a colorless oil which was and recrystallized from warm ethanol.

2´,5´ di-O–tetrahydropyranyl uridine (**8**). 3´-O benzoyl uridine (2.5 g, 6.8 mmol) was dissolved in anhydrous dioxane (20 mL). Toluene sulfonic acid monohydrate (350 mg, 1.8 mmol) and then dihydropyran (16 mL, 20 mmol) were then added to the resulting solution. The reaction mixture was stirred for 2 h, and then concentrated under reduced pressure to an oil. This oil was dissolved in 1:1 methanol:ammonium hydroxide (50 mL) the resulting solution stirred overnight.

The reaction mixture was concentrated under reduced pressure to yield an oil, which was dissolved in ethyl acetate:hexane (2:1) and subjected to flash choromatography [ethyl acetate: hexane (2:1) and then ethyl acetate] to yield four diastereomers of **8** as a colorless oil (R_f 0.3 in ethylacetate).

2´5´di-O-tetrahydropyranyl 3´O-4-nitrophenylphosphouridine (**9**). 2´5´di-O-tetrahydropyranyl uridine (**8**) (0.6 g, 1.5 mmol) dried overnight under reduced pressure in the presence of phosphorus pentoxide was dissolved in anhydrous dioxane (3 mL). The resulting solution was added dropwise over 20 min to a solution of 4–nitrophenyl phosphodichloridate (0.77g, 3 mmol) and (0.5 mL)pyridine in dioxane (3 mL). The reaction mixture was stirred for 30 min, water (1 mL) and pyridine (3 mL) were added, and the reaction mixture was then stirred at 0 °C for 10 minutes. A saturated aqueous

solution of sodium bicarbonate (saturated) was added dropwise until CO_2 (g) evolution stopped, and the reaction mixture was then stirred for an additional 30 minutes.

The reaction mixture was then dissolved in saturated aqueous sodium bicarbonate. The aqueous layer was extracted three times with chloroform, and the combined chloroform extract was dried over Mg SO_4 and concentrated under reduced pressure. The reaction mixture was subjected to flash chromatography (ethyl acetate:methanol 10:1 to 2:1) to yield **9** (R_f 0.17 ethyl acetate:methanol 3:1).

9 was dissolved in water:methanol 10:1 and applied to a reverse phase silica column equilibrated in the same mobile phase (Kuhler, T.C. 1983). Compound **9** was eluted by increasing the methanol concentration of the mobile phase, and with pure **9** eluting at approximately 50% (v/v) methanol.

Deprotection: Because of the lability of **9**, it must be deprotected on the day of its use. Deprotection was accomplished by the method of (Davis, A.M. 1988) without modification.

Experimental Methods for Chapter 2

Materials. [5, 6-^{3}H]UTP was from Amersham (Arlington Heights, IL). A dimer and trimer of RNase A were prepared by lyophilization of RNase A from aqueous acetic acid (50% v/v) and purified by gel filtration through Sephadex G–75 resin (Crestfield, A.M. 1962; Kim, J.-S. 1993). Dimeric bovine seminal ribonuclease was prepared from bovine seminal plasma (Tamburrini, M. 1986; Kim, J.-S. 1993). Barnase (Hartley, R.W. 1993) and staphylococcal nuclease (Serpersu, E.H. 1986) were prepared from *E. coli* cells expressing genes that code for these enzymes. RNase T_1 was from Boehringer Mannheim (Indianapolis, IN). RNase I and *XhoI* restriction endonuclease were from

Promega (Madison, WI). RNase U_2 and alkaline phosphatase were from United States Biochemical (Cleveland, OH).

DNA oligonucleotides were synthesized on an Applied Biosystems Model 392 DNA/RNA synthesizer by using the β-cyanoethyl phosphoramidite method (Sinha, N.D. 1984) and reagents from Applied Biosystems (Foster City, CA), except for acetonitrile, which was from Baxter Healthcare (McGaw, IL). Run–off transcriptions were performed with the Mega Shortscript Kit (Ambion; Austin, TX). The PCR and other manipulations of DNA were performed as described (Ausubel et al., 1989).

Reactions during preparation and use of [5,6-^{3}H]UpA were monitored by TLC on PEI cellulose plates (Alltech; Waukegan, IL). Mobile phases were 0.5 M LiCl, system A; 0.5 M ammonium bicarbonate, system B; or saturated ammonium sulfate, pH 3.5, system C (Bochner and Ames, 1982). Elution profiles from TLC were constructed by detection of the ^{3}H using a Bioscan System 200 Imaging Scanner (Bioscan; Washington, DC). Samples for radiochemical analysis were dissolved in Biosafe scintillation counting fluid (Research Products International; Mount Prospect, IL) and counted with a TriCarb 1900CA Liquid Scintillation Analyzer (Packard; Meridan, CT). HPLC was performed with a Waters instrument equipped with a Novapak C–8 reverse phase column.

^{31}P NMR Analysis. ^{31}P NMR spectroscopy was used to assess the kinetics of the hydrolysis of RNA as catalyzed by various ribonucleases, staphylococcal nuclease, hydroxide ion, or imidazole buffer. In each reaction, the concentration of P–O_5·· bonds was 3 mM [for poly(U) or UpA] or 10 mM (for yeast RNA).

Reactions catalyzed by ribonucleases were performed at 25 °C in 0.10 M imidazole•HCl buffer, pH 7.0, containing NaCl (0.20 M). These reactions had poly(U) as the substrate for RNase A, dimeric RNase A, trimeric RNase A, or dimeric bovine seminal ribonuclease; yeast RNA as the substrate for RNase T_1, barnase, or RNase I; and

UpA as the substrate for RNase A. The hydrolysis of poly(U) by staphylococcal nuclease was performed in 0.10 M imidazole•HCl buffer, pH 7.0, containing NaCl (0.20 M) and $CaCl_2$ (0.10 M). In each reaction, the concentration of enzyme was such that essentially all of the substrate was transphosphorylated in 1 h.

Reactions catalyzed by small molecules were performed as follows. The hydrolysis of poly(U) by hydroxide ion was performed at 25 °C in 0.2 M NaOH. As a control, DNA was also incubated under these conditions. The hydrolysis of poly(U) by imidazole buffer was performed at 70 °C in 2.5 M imidazole•HCl buffer, pH 7.0. Imidazole buffer has been shown to catalyze the transphosphorylation of RNA (Breslow, R. 1986] and the hydrolysis of ethylene phosphate {Covitz, 1963 #170). Poly(U) was also incubated at 70 °C in 2.5 M NaCl, as a control.

^{31}P NMR spectra were obtained at 161.972 MHz in Fourier transform mode on a Bruker AM400 spectrometer with parameters: pulse width, 13°; acquisition time, 0.28 s; relaxation delay, 3.2 s; line broadening, 5-10 Hz; number of scans, 64 – 100 when following a reaction, 200 when analyzing a static sample. Reactions were carried out in 10 mm NMR tubes with an insert containing D_2O. Chemical shifts were recorded relative to 0.3 M H_3PO_4.

Synthesis of [5,6 -^{3}H]UpA. [5,6-^{3}H]UpA was prepared by a combination of enzymatic and chemical methods, as shown in Figure 5.3. The template for transcription was generated by the PCR using standard conditions (Ausubel, F.M. 1989). Oligonucleotides ATACCGTCGACCTCGAG and CAGTGAGCGCGCGTAAT were used to generate a complementary strand of oligonucleotide CAGTGAGCGCGCGTAATACGACTCACTATAGGGATATATATATATATAT–ATATATATATATATATATACTCGAGGTCGACGGTAT [which contains a T7 RNA polymerase promoter, $[(dA)p(dT)p]_{16}$, and the recognition sequence for *XhoI*

(underlined)] and to amplify the resulting duplex. The product from the PCR was digested with *XhoI*, and the resulting duplex was extracted with phenol:chloroform (1:1 v/v) to remove proteins, and precipitated with aqueous EtOH (70% v/v). This duplex (which contains $[(dA)p(dT)p]_{16}$•$[(dA)p(dT)p]_{16}$) served as a template for run-off transcription.

RNA containing $([5,6\text{-}^3H]UpAp)_{16}$ was prepared by run–off transcription of the duplex template in the presence of [5,6-^{3}H]UTP. Transcription reactions were performed in solutions containing [5,6-^{3}H]UTP (50 μCi, 48 Ci/mmol; R_f 0.33, system B) and unlabeled ATP (0.5 mM), CTP (0.5 mM), GTP (0.5 mM), and UTP (12 μM). The resulting RNA (R_f 0.0, system A or B) was transphosphorylated with RNase U_2 (which cleaves RNA only after adenine residues) to yield [5,6-^{3}H]UpA>p (R_f 0.58, system A). [5,6-^{3}H]UpA>p was hydrolyzed by treatment with 0.6 M $HClO_4$ for 45 min (Shapiro, R. 1986). Precipitate in this solution was removed by centrifugation, and the resulting supernatant was neutralized with saturated $NaHCO_3$ to yield a solution of [5,6-^{3}H]UpAp (R_f 0.25, system A). [5,6-^{3}H]UpAp was hydrolyzed with alkaline phosphatase (which cleaves only phosphomonoesters) to yield [5,6-^{3}H]UpA (R_f 0.56, system A).

[5,6-^{3}H]UpA was purified by extraction with phenol:chloroform (1:1 v/v; to remove proteins) and then by reverse phase HPLC. The impure [5,6-^{3}H]UpA (0.27 μCi, 38 Ci/mmol) was mixed with a small amount of the unlabeled carriers: UpA, U>p, and adenosine. The resulting mixture was injected at a flow rate of 0.8 mL/min on to an HPLC C–8 reverse phase column that had been equilibrated with 0.1 M sodium phosphate buffer, pH 6.0. The loaded column was eluted first with 0.1 M sodium phosphate buffer, pH 6.0 (6.4 mL); then with a linear gradient (0.8 mL + 0.8 mL) of 0.1 M sodium phosphate buffer, pH 6.0, to aqueous methanol (10% v/v); and finally with aqueous methanol (10% v/v; 8.0 mL). Under these conditions, U>p eluted with the void

volume, adenosine eluted at 12 mL, and [5,6-^{3}H]UpA eluted at 12.6 mL. The [5,6-^{3}H]UpA(0.27 μCi, 38 mCi/mmol) was collected, and solvent was removed under vacuum in a rotary centrifuge. The purity of [5,6-^{3}H]UpA was assessed by TLC before and after its treatment with RNase A.

Throughput Experiment. A sample (0.27 μCi, 38 mCi/mmol) of [5,6-^{3}H]UpA was dissolved in 0.1 M imidazole•HCl buffer, pH 7.0 (14 μl), containing U>p (5 mM). RNase A (1 ng in 1 μl of 0.1 M imidazole•HCl buffer, pH 7.0) was then added. At appropriate time intervals, portions (1.0 μl) were withdrawn, spotted onto PEI cellulose plates, and dried. The plates were developed with system C, and elution profiles were constructed with the Bioscan scanner. The regions of the plates corresponding to UpA, U>p, and Up were excised, and the ^{3}H in each of these regions was quantitated by scintillation analysis.

Experimental Methods for Chapter 3

The Lys41Ala RNase A mutant was prepared as described previously {delCardayré, 1995 #115; Messmore, 1995 #521}.

Measurement of cosolvent dependence of k_{cat}/K_m. All reactions contained 50 mM MES-HCl pH 6.0, and 0.1 M NaCl and were carried out at 25° C. The viscogenic buffers contained varying amounts of glycerol. A $\Delta\varepsilon_{286}$ for the cleavage of UpA was measured in each buffer, and this value was used to calculate the initial velocity from the measured change in absorbence with time. When glycerol was the cosolvent initial velocities were measured at five concentrations of substrate in each buffer. The initial velocity data were fitted to the Michaelis–Menten eq using the program HYPERO (Cleland, W.W. 1979) to obtain k_{cat}/K_m. When sucrose was the cosolvent, initial velocity

was measured at 0.1 M UpA and treated as proportional to V_{max}/K_m, which may be plotted on the same axes as k_{cat}/K_m when considered relatively.

Viscosity measurements were made using an Ostwald viscometer from Cannon Instrument Co. (State College, PA) at 25° C. The observed kinematic viscosities were corrected by multiplying by the density of the buffer. Viscosities are reported relative to the corrected viscosity of 50 mM MES-HCl, 0.1M NaCl, 0% glycerol.

Preparation of ^3H UpA. ^{3}H UpA was prepared as described previously (Chapter 5.2) with the following modifications. One hundred μCi [3,5,8–^{3}H] ATP and [5,6–^{3}H] UTP were included in the run–off transcription reaction, and the concentrations of unlabelled UTP and ATP were 12 mM. [5,6–^{3}H]UTP and [3,5,8–^{3}H]ATP were from Amersham (Arlington Heights, IL). HPLC was performed with a Waters instrument equipped with either a Novapak C–8 or a Novapak C–18 column.

^{3}H UpA was purified using HPLC by mixing with a small amount of unlabeled UpA and injecting the mixture onto a C–8 reverse–phase column that had been equilibrated in 0.1 M ammonium acetate. The loaded column was run isocratically at 0.8 mL/min in 0.1 M ammonium acetate, and UpA eluted at 2.6 minutes.

Reaction conditions for measurement of water catalyzed rate of RNA cleavage. Buffers used in experimentation with ^{3}H UpA were stirred with 0.05% diethylpyrocarbonate v/v overnight and autoclaved. Microcentrifuge tubes were soaked overnight in 1% sodium dodecylsulfate and rinsed with absolute ethanol.

Two aliquots of ^{3}H UpA (0.02 mCi) were dissolved, one in 0.5 mL of 50 mM MES-HCl pH 6.0, 0.1 M NaCl, the other in 50 mM phosphate pH 12, 0.1 M NaCl. The reactions were maintained at 25° C.

Separation of ^3H UpA from its degradative products. At timed intervals, 50 mL aliquots were removed and combined with a mixture containing the following cold

carriers: UpA, U>p, 5′ Ap, 2′ Up, 3′ Up, uridine and adenosine. This mixture was injected onto a C–18 reverse phase column that had been equilibrated in 12 mM potassium phosphate pH 7.0, 4 mM tetrabutylammonium phosphate (TBAP). The loaded column was eluted with 18 mL equilibration buffer, then ramped to 50% methanol/water over 2 mL and eluted for an additional 8 mL. Under these conditions retention times were: UpA, 25 minutes; 2′ UMP, 21 minutes; 3′ UMP, 19 minutes; 5′ AMP, 13 minutes; adenosine, 7 minutes, U>p, 4 minutes; uridine, 1minute. These retention times decreased over the course of the experiment, a consequence of long–term use of the TBAP ion–pairing agent. The peak fractions were collected; the 2′ and 3′ UMP's were pooled. The solvent was removed under vacuum in a centrifuge and the samples were taken up in water, diluted ten–fold into Biosafe scintillation counting fluid (Research Products International, Mount Prospect, IL). ^{3}H content was determined with a TriCarb 1900CA liquid scintillation analyzer (Packard, Meridan, CT).

Experimental methods for Chapter 4

Mutagenesis of the RNase A gene. Mutations were introduced into the RNase A gene in the plasmid pBXR (delCardayré, S.B. 1995) by site–directed oligonucleotide-mediated mutagenesis in the case of H12A RNase A and by the PCR (Ausubel, F.M. 1989) with a mutagenic primer in the case of H119A. The oligonucleotide sequences used for mutagenesis are tabulated in Table 5.1. All restriction enzymes were from Promega (Madison, WI). DNA fragments were purified using a GeneClean II kit from Bio–101 (La Jolla, CA).

H12A was produced in pBXR by the method of Kunkel (Kunkel, T.A. 1987). H119A was produced by amplifying the RNase A gene by the PCR using pBXR as a template and the primers listed in Table 5.1. The amplified fragment was digested with

SalI and *PstI* and ligated into pBXR that had been similarly digested. The sequences of both mutant RNase A genes were verified by DNA sequencing using a Sequenase Version 2.0 kit from US Biochemicals (Cleveland OH).

Expression and purification of H12A and H119A RNase A. H12A and H119A RNase A were expressed in *E.coli* strain BL21 (DE3) as described (delCardayré, S.B. 1995) with the following modifications. The RNase A inclusion bodies were solubilized using 6 M guanidine•HCl, 20 mM Tris–acetate pH 7.8, 1 mM EDTA. After purification by cation exchange chromatography at pH 7.5 using fast flow-Sepharose from Pharmacia LKB (Uppsala, Sweden) eluting with a [NaCl] gradient from 0 - 0.35 M, the enzymes were further purified by cation exchange chromatography on a mono S column equipped with FPLC fluidics from Pharmacia LKB (Uppsala, Sweden).

Separation of H12A and H119A RNase A from wild–type RNase A. Samples of the mutant enzymes were eluted from a Mono S cation exchange column using gradient of [NaCl] from 0.2 to 0.28 M over 80 mL in pH 5.0 acetate buffer. Fractions containing the protein of interest were reloaded onto the column and repurified using the same gradient. This was repeated, for a total of three elutions of the mutant enzyme from the cation column.

Steady state kinetic parameters at pH 6. All reactions were performed at 25 °C in 50 mM MES-HCl buffer, pH 6.0, containing 0.1 M NaCl. Steady-state kinetic parameters were determined by fitting initial velocity data to a hyperbolic curve $(V*S)/(K_m+S)$ using the program HYPERO (Cleland, W.W. 1979), where V is the maximum velocity; S is substrate concentration, and K_m is the Michaelis constant. Cleavage of poly(C) and Up(4-nitrophenol) were monitored at 250 nm ($\Delta\varepsilon_{250}$ = 2380 $M^{-1}cm^{-1}$) and 330 nm ($\Delta\varepsilon_{330}$ = 4560 $M^{-1}cm^{-1}$), respectively; cleavage of UpA was

monitored at 265 nm in the presence of excess adenosine deaminase (Ipata, P.L. 1968) ($\Delta\varepsilon_{265} = -6000\ M^{-1}cm^{-1}$).

pH–kinetic parameter profiles: Steady–state kinetic data were collected and analyzed as above with the following exceptions. The cleavage of UpA was monitored in the absence of adenosine deaminase at 286 nm (Witzel, H. 1962). $\Delta\varepsilon_{286}$ at each pH is shown in Table 5.2. The cleavage of Up(4-nitrophenol) was monitored at 330 nm or 410 nm. $\Delta\varepsilon_{330}$ and $\Delta\varepsilon_{410}$ at each pH are shown in Table 5.2. When UpA was the substrate, buffers were prepared such that I = 0.20 and [buffer] = 0.067 M. For pH 4.0 – 5.5 the buffer was acetate; 6.0 – 7.0 cacodylate; 7.5 – 8.0 *tris*– (hydroxymethyl)aminomethane. When Up(4-nitrophenol) was the substrate the same buffers were used except that [buffer] = 0.1 M and I = 0.2. When H12A RNase A was the enzyme, initial velocity was measured at 0.1 mM UpA and 2.5 μM H12A and taken as equal to V_{max}/K_m*[UpA], except at pH 6, where the initial velocity was taken as equal to $V_{max}/1.5K_m$ * [UpA]. This treatment was necessary because the K_m for cleavage of UpA catalyzed by H12A is 0.2 M at pH 6 (this work).

The background rate of Up(4-nitrophenol) cleavage was significant at pH 7.5 and 8.0. A pseudo–first order rate constant (k_{OH}) for the base catalyzed cleavage reaction was measured at each pH and used to calculate a correction for the initial velocity data, shown in eq 5.1.

$$v = v_{obs} - k_{OH}\,[\text{Up(4-nitrophenol)}] \qquad (5.1)$$

The values of k_{OH} at were $7.32 \times 10^{-7}\ s^{-1}$ at pH 7.5 and $1.47 \times 10^{-6}\ s^{-1}$ at pH 8.0.

Titration of the enzymic histidines followed by ^1H NMR: The protonation state of the enzymic histidines was monitored by determining the chemical shift of the C–2

proton of histidine as a function of pD (Markley, J.M. 1975). ^{1}H NMR spectra were acquired in 1D mode on a Bruker AM400 NMR spectrometer at 25 ℃. Spectral parameters were as follows; sweep width: 5384 Hz; number of scans: 128; pulse width: 5 μs; relaxation delay: 1 s; total data: 8,192 or 16,384 points; dummy scans: 4. All chemical shift data are reported relative to 3–(trimethylsilyl)–1–propanesulfonic acid.

Before acquisition of spectra, enzyme samples were exchanged against D_2O in order to deuterate the backbone amides (Markley, J.M. 1975). H12A or H119A RNase A (15 – 25 mg) was dialyzed exhaustively against H_2O and lyophilized; this was followed by two lyophilizations from D_2O. The enzyme was taken up in 0.5 mL D_2O and the pD brought to 3.0 with DCl. This sample was incubated at 60 ℃ for 1 h, and adjusted to 0.2 M NaCl or to 65 mM 3′-UMP and 130 mM NaCl. After aquisition of a spectrum, the pD was measured and adjusted for the next measurement with NaOD.

At least fifteen ^{1}H NMR spectra were obtained for H12A and H119A RNase A from pD 3 – 8 in the presence and absence of saturating 3′-UMP. Assignments were taken from the work of Markley (Markley, J.M. 1975) and the data for the wild-type RNase A come from the work of Quirk (Quirk, D.J. 1995). Chemical shift data were acquired for the C–2 protons of the three histidine residues of each mutant enzyme. These data were fitted to eq 5.2 when only one pK_a was needed to fit the data (δ_{down} = the downfield limit for the chemical shift; δ_{up} = the upfield limit).

$$\delta_{obs} = \delta_{down} * \delta_{up} [(10^{pKa} + 10^{pD})/(\delta_{down} * 10^{pD} + \delta_{up} * 10^{pKa})] \qquad (5.2)$$

If two pK_a's were required to fit the data the eq 5.3 was used, which is essentially a sum of two titration curves (δ_{down1} = the downfield limit for the chemical shift owing to pK_{a1}; δ_{up1} = the upfield limit for the chemical shift change owing to pK_{a1}; δ_{down2} = the downfield

limit the chemical shift owing to pK_{a2} ; δ_{up2} = the upfield limit for the chemical shift change owing to pK_{a2}).

$$\delta_{obs} = \{\delta_{down\,1} * \delta_{up\,1} [\,(10^{pK\,a1} + 10^{pD})/(\,\delta_{down1} * 10^{pD} + \delta_{up1} * 10^{pKa1})]\} +$$
$$\{\delta_{down\,2} * \delta_{up\,2} [\,(10^{pK\,a2} + 10^{pD})/(\,\delta_{down2} * 10^{pD} + \delta_{up2} * 10^{pKa2})] - \delta_{down\,1}\} \qquad (5.3)$$

Wild-type data sometimes required that the data be fit to a model with three pK_a's, in which case one more term like the second in eq 4.4 was included (Quirk, D.J. 1995).

Fluorescence polarization assay for d(AUAA) binding: Fluorescence polarization anisotropy assays were based on the increase of the rotational correlation time of a fluorescein–labeled oligonucleotide on binding to RNase A (LeTilly, V. 1993). The protein•DNA complex tumbles more slowly than free DNA. The ensuing reduction in the rotational correlation time of the fluorophore causes an increase in polarization, which allows the binding to be monitored (LeTilly, V. 1993). The DNA had the sequence AUAA and the fluorescein was linked to the 5′ end of the oligonucleotide by a six–carbon spacer. Fluorescence polarization was measured at room temperature [(25±2) ℃] on a Beacon Fluorescence Polarization System (Pan Vera; Madison WI), with excitation at 488 nm and emission at 520 nm.

To measure polarization was lyophilized enzyme was dissolved in 2 mL 100 mM MES-HCl buffer, pH 6.0, containing 0.10 M NaCl and divided into two 1 mL samples. One sample was used as a blank, the other mixed with d(AUAA) to a final DNA concentration of 2.5 nM. Concentration was varied by diluting the sample by a factor of 0.75 with MES-HCl buffer + 2.5 nM d(AUAA), and by diluting the blank in the same manner into buffer alone. At least four measurements were made at each protein concentration. These data were fitted to the eq 5.4 where *B* is the amount of bound DNA

as measured by observed polarization, B_{max} is the maximum polarization, F is free protein, K_d is the dissociation constant and C is the polarization arising from free DNA.

$$B = [(B_{max} F)/ (K_d + F)] + C \quad (5.4)$$

B_{max} could not be measured directly with the mutant enzymes, so it was assumed that B_{max} did not vary from that of wild-type RNase A. B_{max} was measured using a 1 mM sample of wild-type RNase A and 2.5 nM d(AUAA) before each binding curve was determined.

Table 5.1

Oligonucleotides used for mutagenesis in this work.

Sequence (5′→3′)	Function
CGGAAGTGCTCGAGTCCATGGCCTGCCGCTCA	H12A; silent *Xho*I site
CGCAAGCTTGTCGACTACACGCTAGCATCAAAGGCGAC TGGCACG	H119A; silent *Nhe*I PCR primer
CCAAGGAAACTGCAGCAGCC	PCR primer; also known as (SD20)

Table 5.2

Values of $\Delta\varepsilon$ for cleavage of UpA and Up(4-nitrophenol) used to determine the initial velocities.

pH	$\Delta\varepsilon_{286}$ for UpA ($M^{-1}cm^{-1}$)	$\Delta\varepsilon$ for Up(4-nitrophenol) ($M^{-1}cm^{-1}$)	λ (nm) for Up(4-nitrophenol)
4.0	-685	5390	330
4.5	-660	5880	330
5.0	-625	5740	330
5.5	-645	5660	330
6.0	-670	5330	330
6.5	-675	4560	330
7.0	-640	7250	410
7.5	-700	12260	410
8.0	-695	14100	410

Figure 5.1

Scheme for synthesis of UpA.

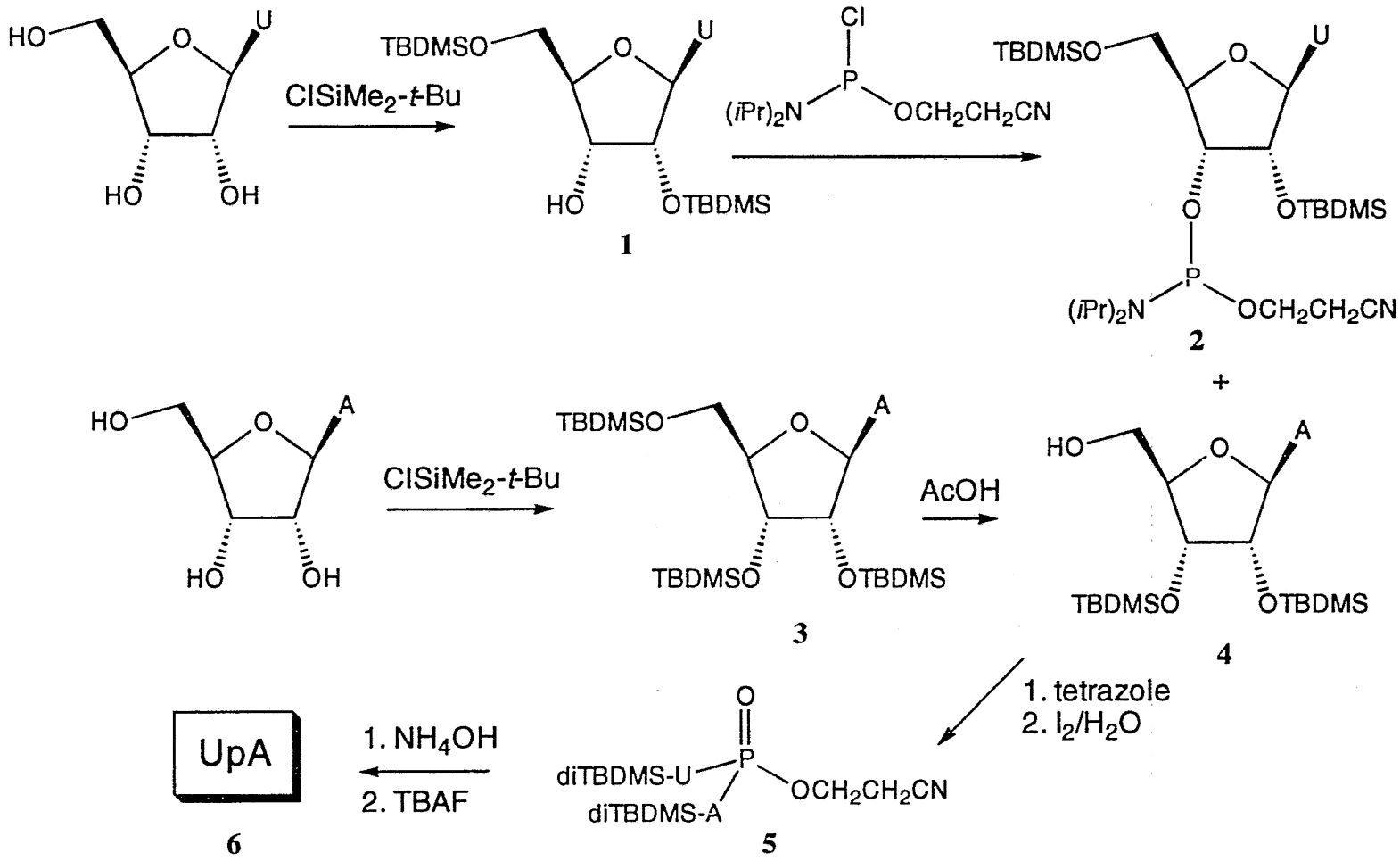
HO
U
O
HO
OH
ClSiMe2-t-Bu
TBDMSO
HO
OTBDMS
1
Cl
P
(iPr)2N
OCH2CH2CN
TBDMSO
OTBDMS
(iPr)2N
OCH2CH2CN
2
+
HO
A
ClSiMe2-t-Bu
TBDMSO
TBDMSO
OTBDMS
3
AcOH
HO
TBDMSO
OTBDMS
4
1. tetrazole
2. I2/H2O
O
diTBDMS-U
diTBDMS-A
OCH2CH2CN
5
1. NH4OH
2. TBAF
UpA
6

Figure 5.2

Synthetic scheme for Up(4-nitrophenol).

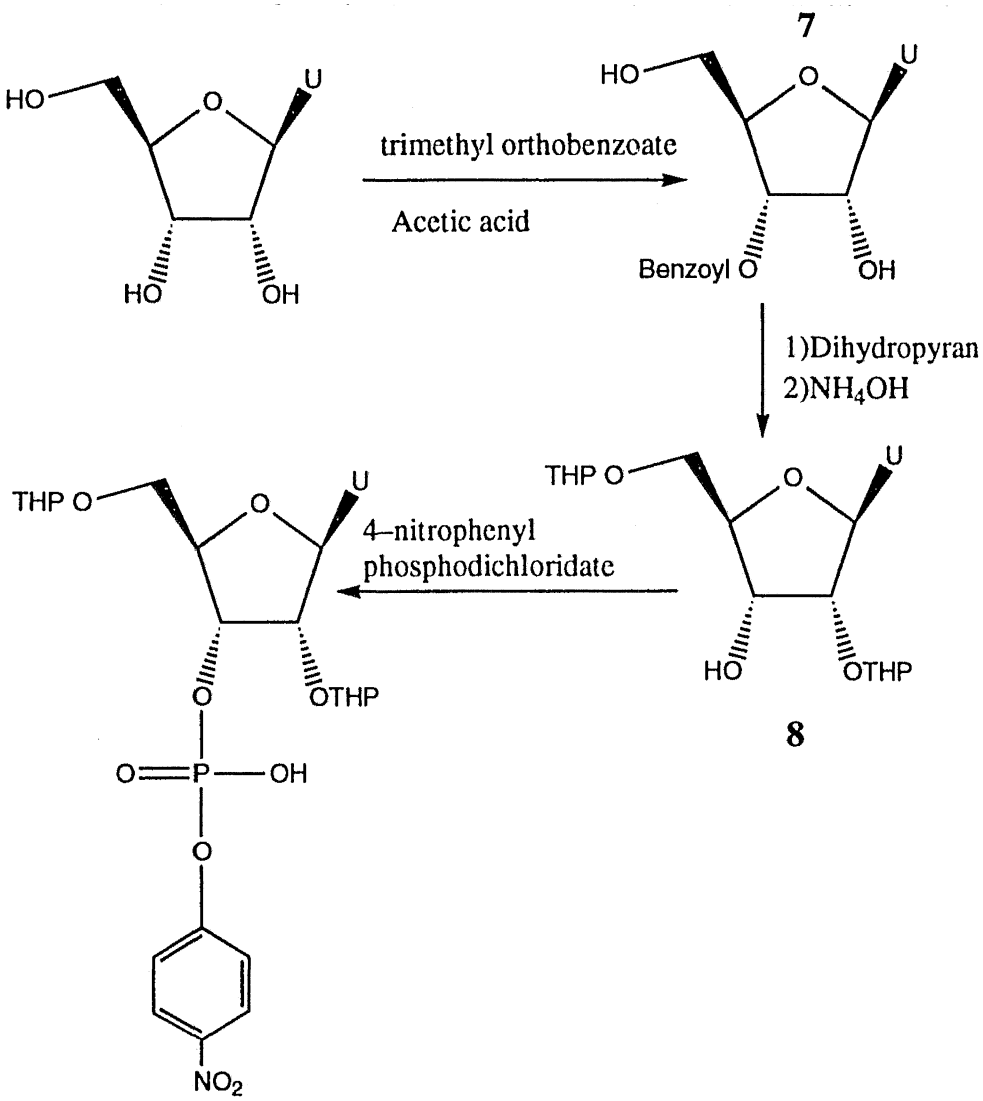
HO
O
U
HO
OH
trimethyl orthobenzoate
Acetic acid
7
HO
O
U
Benzoyl O
OH
1)Dihydropyran
2)NH4OH
THP O
O
U
HO
OTHP
8
4–nitrophenyl
phosphodichloridate
THP O
O
U
O
OTHP
O=P—OH
O
NO2
9

Figure 5.3

Scheme for synthesis of [5,6 ^{3}H] UpA

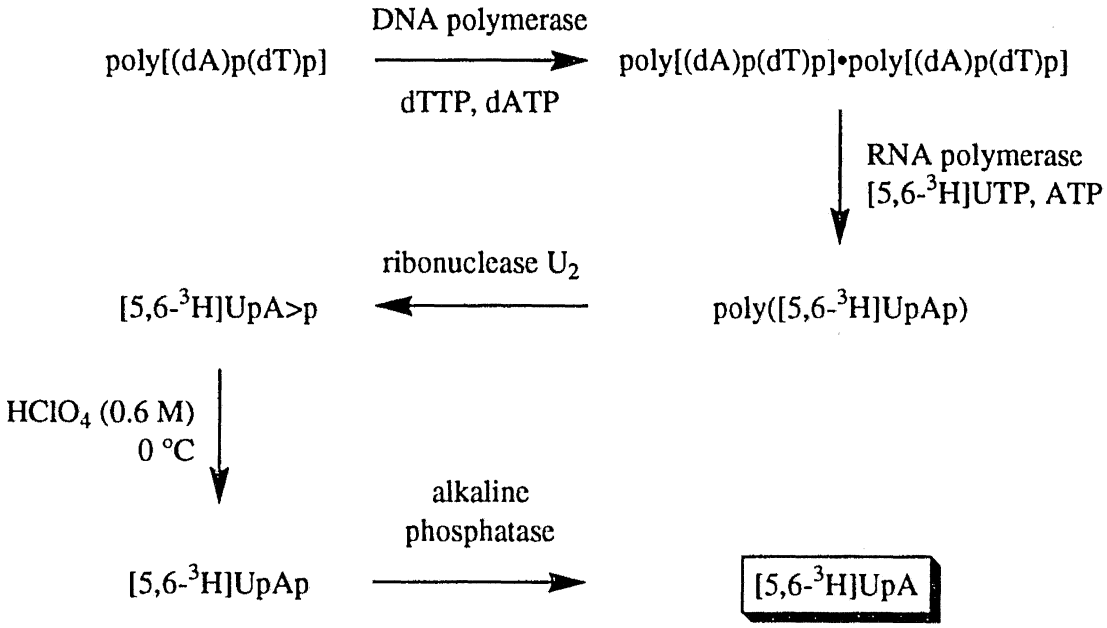
poly[(dA)p(dT)p]
DNA polymerase
dTTP, dATP
poly[(dA)p(dT)p]•poly[(dA)p(dT)p]
RNA polymerase
[5,6-3H]UTP, ATP
poly([5,6-3H]UpAp)
ribonuclease U2
[5,6-3H]UpA>p
HClO4 (0.6 M)
0 °C
alkaline
phosphatase
[5,6-3H]UpAp
[5,6-3H]UpA

Appendix

The following are mass-spectral and ^{1}H NMR spectra of the indicated compounds

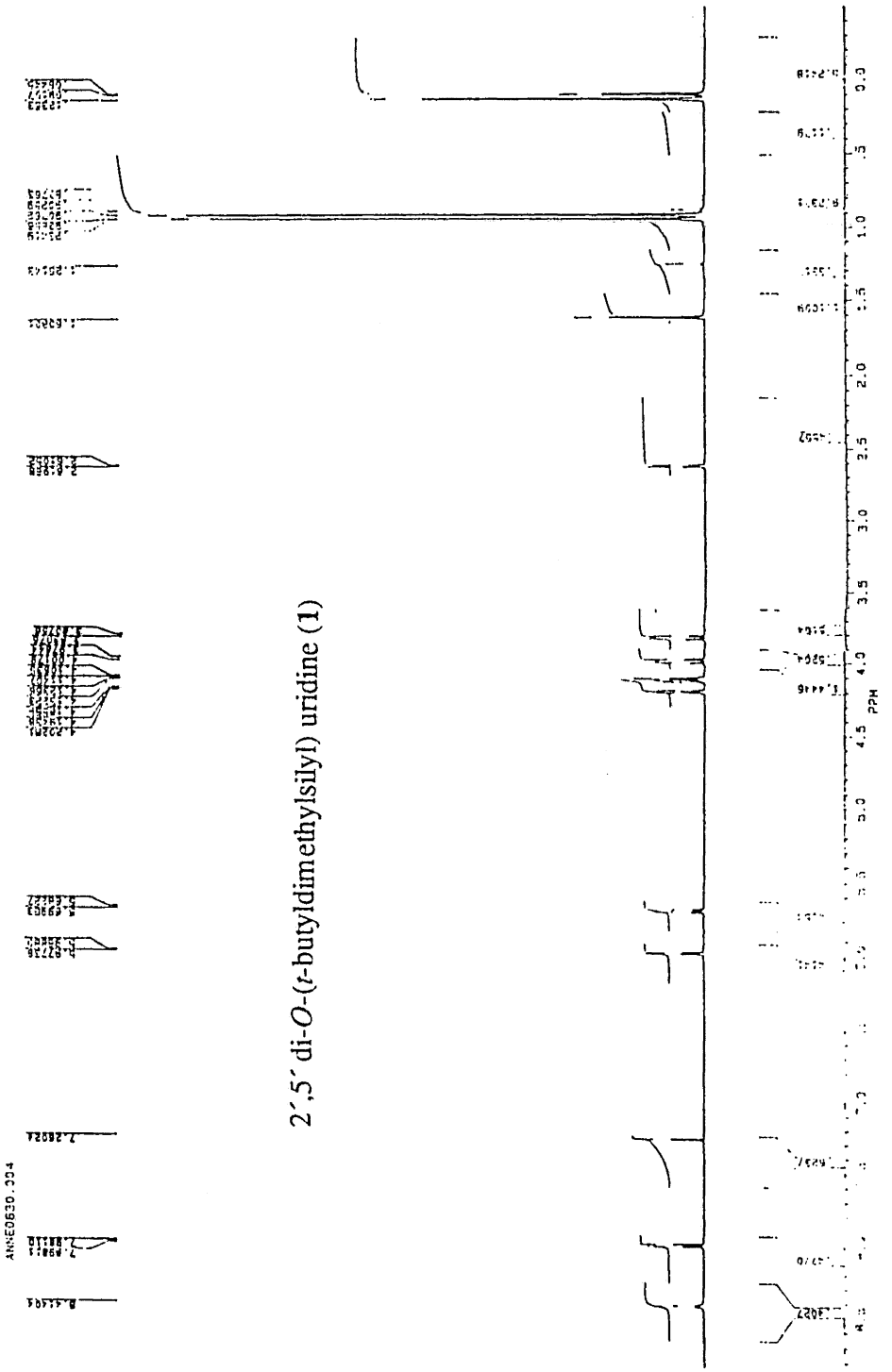

2′,5′ di-*O*-(*t*-butyldimethylsilyl) uridine (**1**)

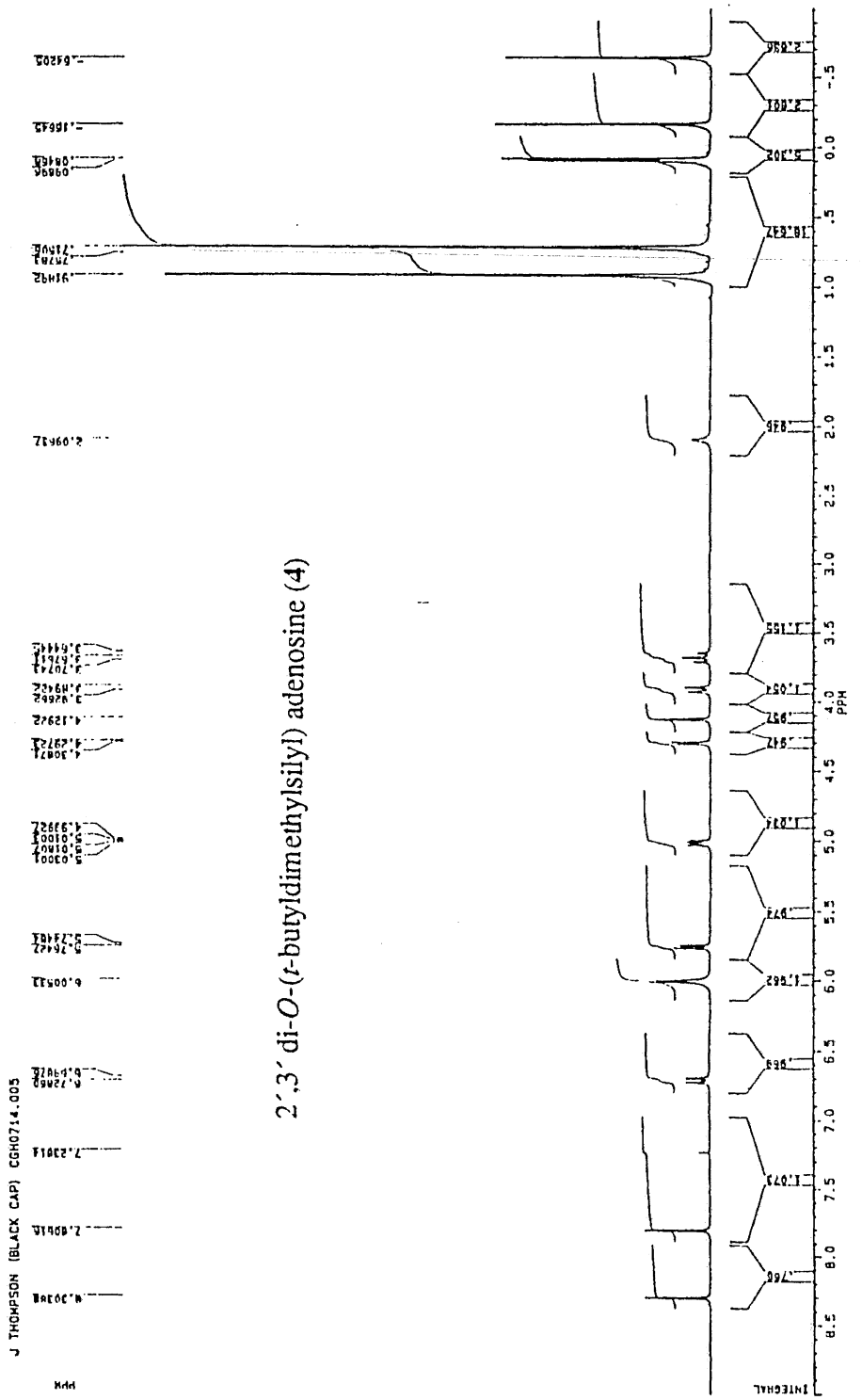

2′,3′ di-*O*-(*t*-butyldimethylsilyl) adenosine (**4**)

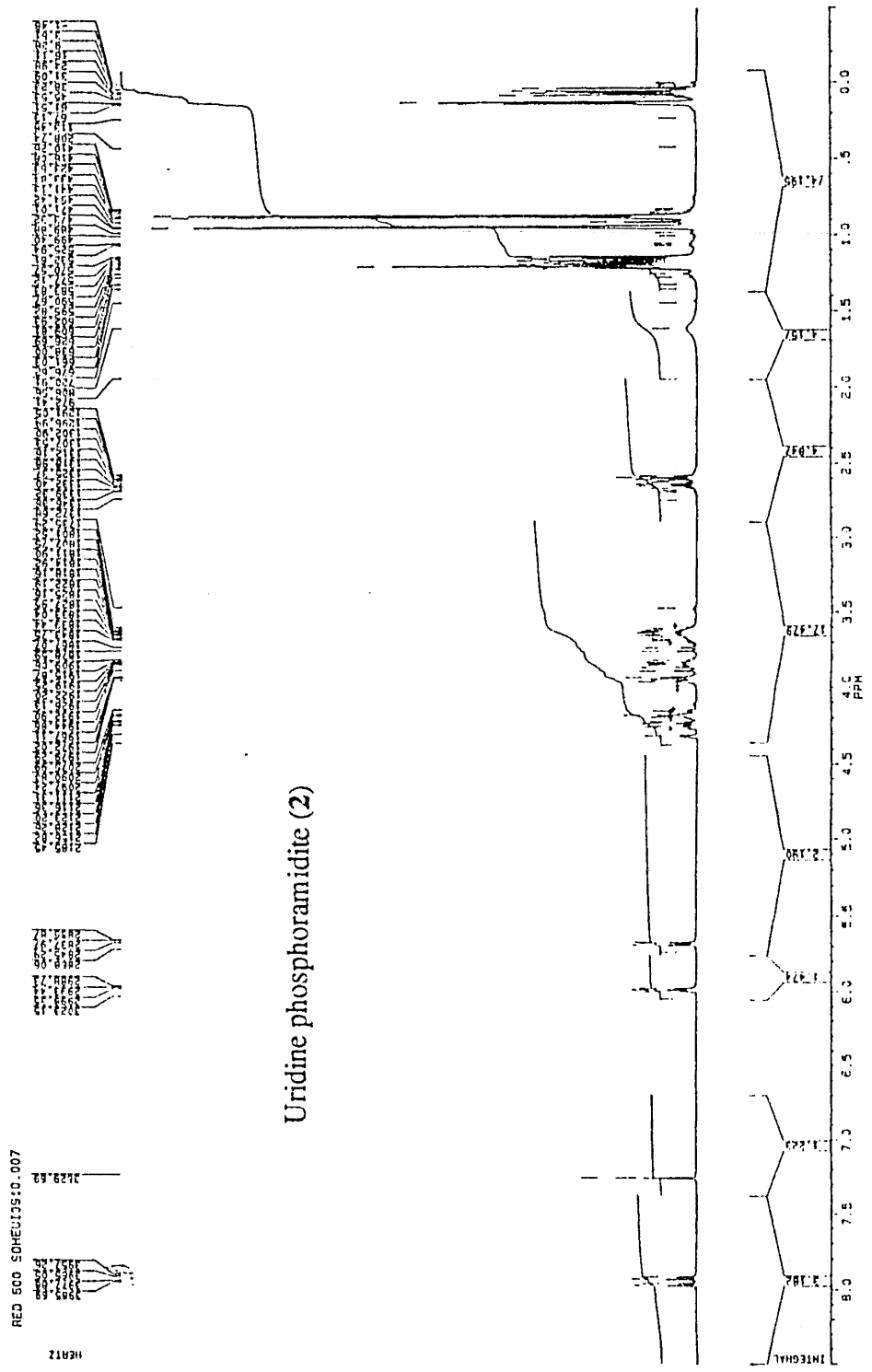

Uridine phosphoramidite (2)

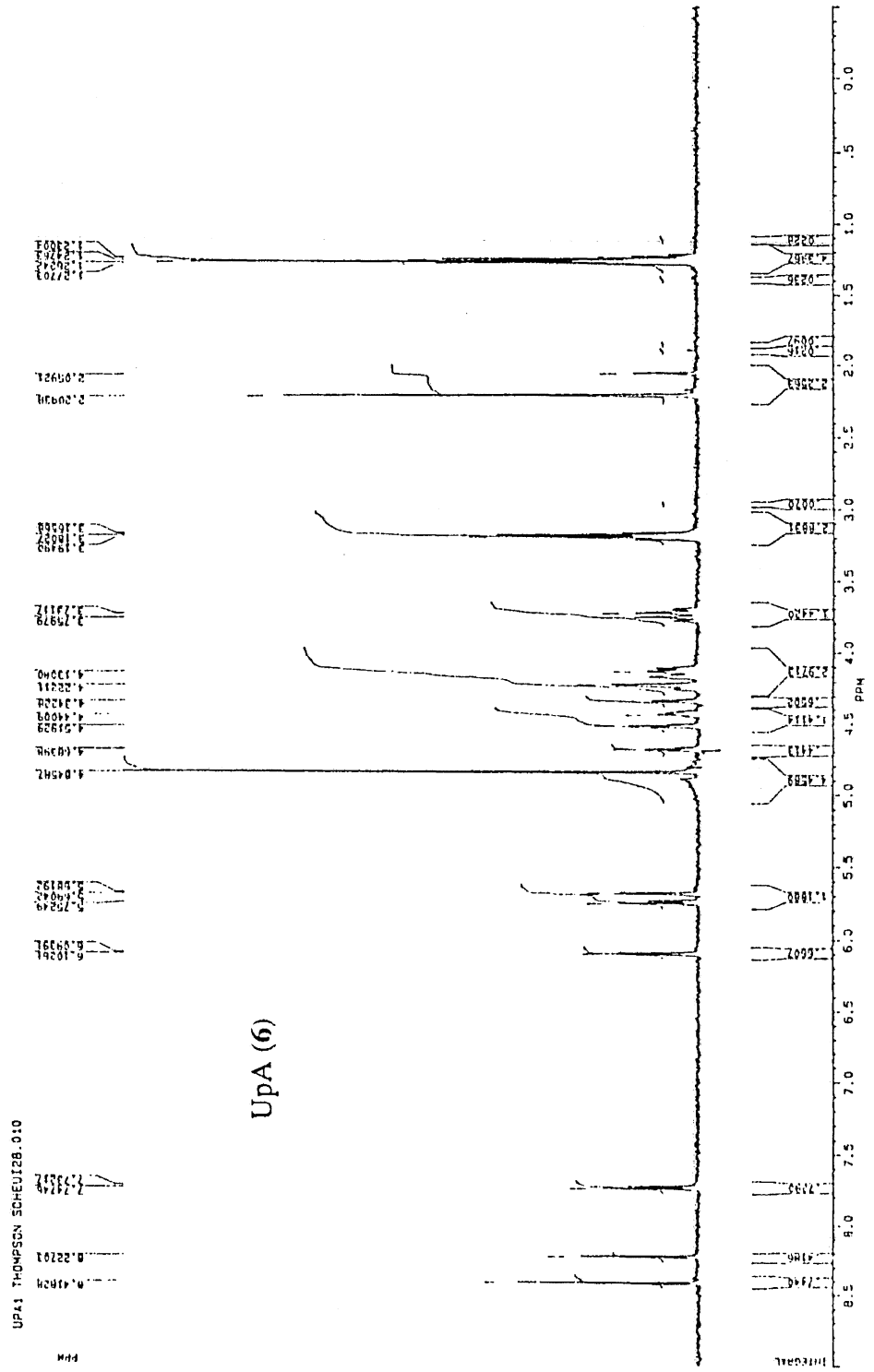
UpA (6)
UPA1 THOMPSON SCHEUI28.010
PPM

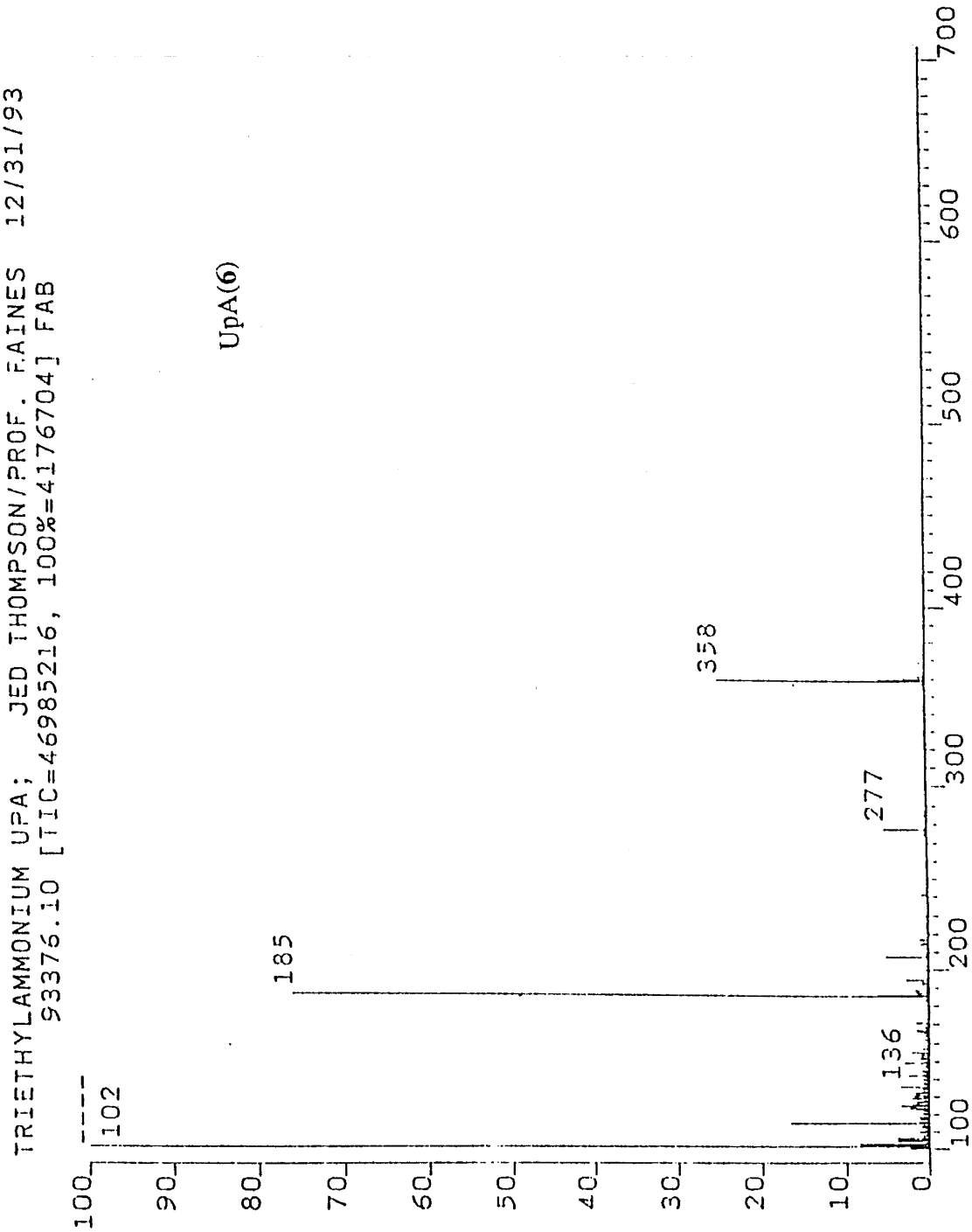
TRIETHYLAMMONIUM UPA; JED THOMPSON/PROF. FAINES 12/31/93
93376.10 [TIC=46985216, 100%=41767041] FAB
UpA(6)
102
136
185
277
358
100
90
80
70
60
50
40
30
20
10
0
100
200
300
400
500
600
700

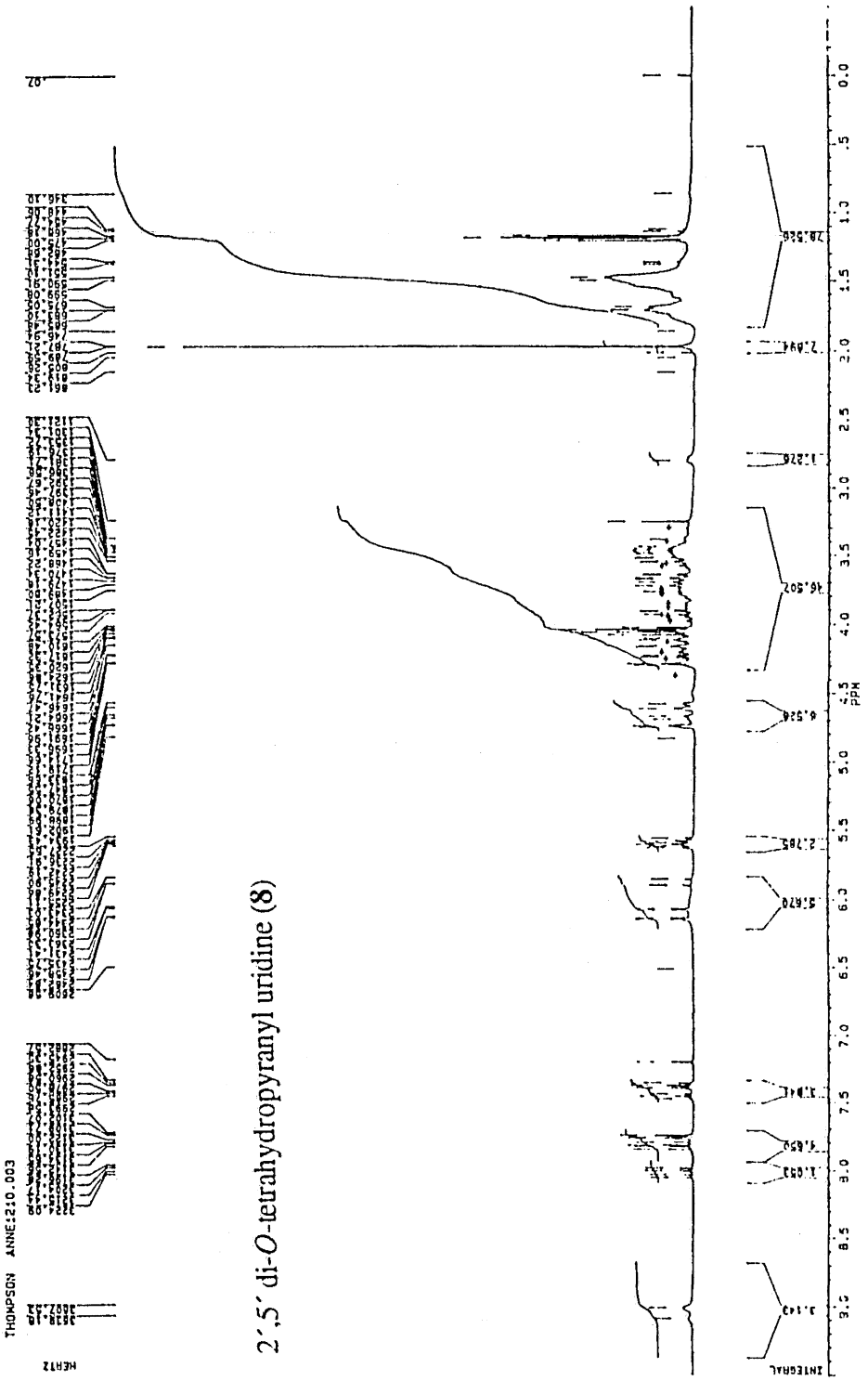

2′,5′ di-*O*-tetrahydropyranyl uridine (8)

2′,5′ di-*O*- tetrahydropyranyl 3′ *O*-4-nitrophenylphosphouridine (**9**)

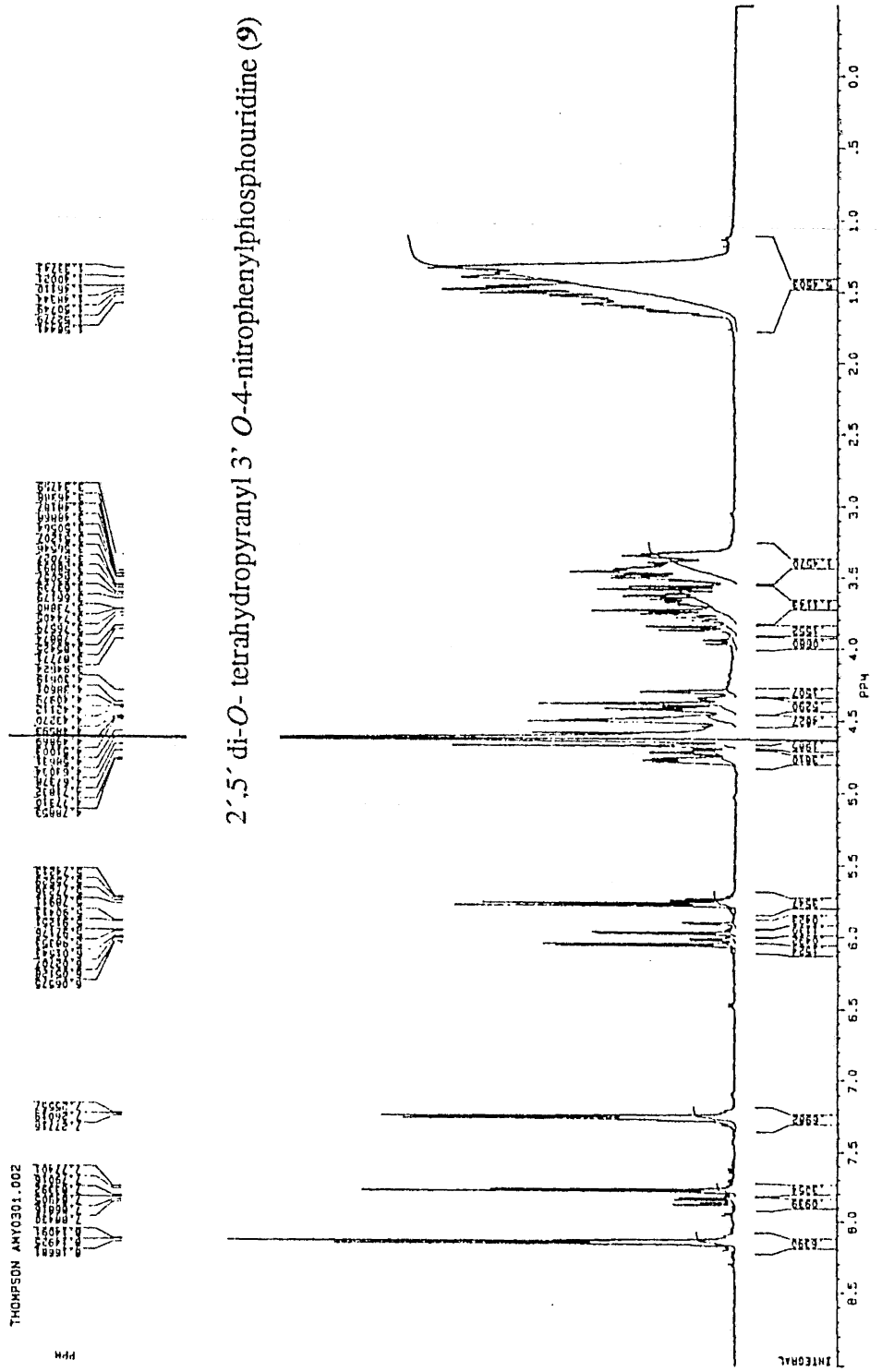

References

Aguilar, C.F., Thomas, P.J., MIlls, A., Moss, D.S. and Palmer, R.A. (1992). "Newly observed binding mode in pancreatic ribonuclease." J. Mol. Biol. **224**: 265-.

Anfinsen, C.B. (1973). "Principles that govern the folding of protein chains." Science **181**: 223-230.

Ausubel, F.M., Brent, R., Kingston, R.E., Moore, D.D., Seidman, J.G., Smith, J.A. and Struhl, K. (1989). Current Protocols in Molecular Biology. New York, Wiley.

Ballinger, P. and Long, F.A. (1960). "Acid ionization constants of alcohols II: Acidities of some substituted methanols and related compounds." J Am. Chem. Soc. **82**: 795–798.

Barnard, E.A. (1969). "Biological function of pancreatic ribonuclease." Nature **221**: 340-344.

Barnard, E.A. and Stein, W.D. (1959). "The histidine in the active centre of ribonuclease I. A specific reaction with bromoacetic acid." J. Mol. Biol. **1**: 339-349.

Barnard, E.A. and Stein, W.D. (1959). "The histidine residue in the active centre of ribonuclease II. Position of this residue in primary protein chain." J. Mol. Biol **1**: 350-358.

Beaucage, S.L. and Caruthers, M.H. (1981). "Deoxynucleoside phosphoramidites—a new class of key intermediates for deoxypolynucleotide synthesis." Tetrahedron Lett. **22**: 1859-1862.

Blacklow, S.C., Raines, R.T., Lim, W.A., Zamore, P.D. and Knowles, J.R. (1988). "Triosephosphate isomerase catalysis is diffusion controlled." Biochemistry **27**: 1158-1167.

Borah, B., Chen, C., Egan, W., Miller, M., Wlodawer, A. and Cohen, J.S. (1985). "Nuclear magnetic resonance and neutron diffraction studies of the complex of ribonuclease A with uridine vanadate, a transition-state analogue." Biochemistry **24**: 2058-2067.

Breslow, R. (1995). personal communication.

Breslow, R., Huang, D.L. and Anslyn, E. (1989). "On the mechanism of action of ribonucleases: Dinucleotide cleavage catayzed by imidazole and Zn^{2+}." Proc. Natl. Acad. Sci. USA **86**: 1746-1750.

Breslow, R. and Labelle, M. (1986). "Sequential general base acid catalysis in the hydrolysis of RNA by imidazole." J. Am. Chem. Soc. **108**: 2655-2659.

Breslow, R. and Xu, R. (1993). "Quantitative evidence for the mechanism of RNA cleavage by enzyme mimics. Cleavage and isomerization of UpU by morpholine buffers." J. Am. Chem. Soc. **115**: 10705-10713.

Brown, D.M. and Todd, A.R. (1953). "Nucleotides. Part XXI The action of ribonuclease on simple esters of the monoribonucleotides." J. Chem. Soc. (London): 2040-2052.

Bunton, C.A., Mhala, M.M., Oldham, K.G. and Vernon, C.A. (1960). "The reactions of organic phosphates III. The hydrolysis of dimethyl phosphate." J. Chem. Soc.: 3293-3301.

Burbaum, J.J., Raines, R.T., Albery, W.J. and Knowles, J.R. (1989). "Evolutionary optimization of the catalytic effectiveness of an enzyme." Biochemistry **28**: 9293-9305.

Burgers, P.M.J. and Eckstein, F. (1979). "Diastereomers of 5'-O-adenosyl 3'-O-uridyl phosphorothioate: chemical synthesis and enzymatic properties." Biochem **18**: 592-596.

Chou, K.C. and Zhou, G.P. (1982). J. Am. Chem. Soc. **104**: 1409-1413.

Cleland, W.W. (1975). "What limits the rate of an enzyme-catalyzed reaction?" Acc. Chem. Res. **8**: 145-151.

Cleland, W.W. (1979). "Statistical analysis of enzyme kinetic data." Methods Enzymol. **63**: 103-138.

Cleland, W.W. (1979). "Statistical analysis of kinetic data." Methods Enzymol. **63**: 103-138.

Cotton, F.A., E.E. Hazen, J. and Legg, M.J. (1979). Proc. Natl. Acad. Sci. USA **76**: 2551-2555.

Cozzone, P.J. and Jardetsky, O. (1977). "The mechanism of purine polynucleotide hydrolysis by ribonuclease A." FEBS Lett. **73**: 77-79.

Crestfield, A.M., Stein, W.H. and Moore, S. (1962). "On the aggregation of bovine pancreatic ribonuclease." Arch. Biochem. Biophys. **Supplement 1**: 217-222.

Crestfield, A.M., Stein, W.H. and Moore, S. (1963). "Alkylation and identification of the histidine residues at the active site of ribonuclease." J. Biol. Chem. **238**: 2413.

Cuchillo, C.M., Parés, X., Guasch, A., Barman, T., Travers, F. and Nogués, M.V. (1993). "The role of 2',3'-cyclic phosphodiesters in the bovine pancreatic ribonuclease A catalysed cleavage of RNA: intermediates or products?" FEBS Lett. **333**: 207-210.

Davis, A.M., Regan, A.C. and Williams, A. (1988). "Experimental charge measurement at leaving oxygen in the bovine ribonuclease A catalyzed cyclization of uridine 3'-phosphate aryl esters." Biochemistry **27**: 9042-9047.

Davis, A.M., Regan, A.C. and Williams, A. (1988). "Experimental charge measurement at leaving oxygen in the bovine ribonuclease A catalyzed cyclization of Uridine 3′–phosphate aryl esters." Biochem **27**: 9042-9047.

Day, A.G., Parsonage, D., Ebel, S., Brown, T. and Fersht, A.R. (1992). "Barnase has subsites that give rise to large rate enhancements." Biochemistry **31**: 6390-6395.

Dejaegere, A. and Karplus, M. (1993). "Hydrolysis rate difference between cyclic and acyclic phosphate esters: solvation versus strain." J. Am. Chem. Soc. **115**: 5316-5317.

del Rosario, E.J. and Hammes, G.G. (1969). "Kinetic and equilibrium studies of the ribonuclease-catalyzed hydrolysis of uridine 2',3'-cyclic phosphate." Biochemistry **8**: 1884-1889.

del Rosario, E.J. and Hammes, G.G. (1970). "Relaxation spectra of RNase VII The interaction of RNase with uridine 2',3' cyclic monphosphate." J. Am. Chem. Soc. **92**: 1750-1753.

delCardayré, S.B. and Raines, R.T. (1994). "Stuctural determinants of enzymatic processivity." Biochemistry **33**: 6031-6037.

delCardayré, S.B. and Raines, R.T. (1995). "A residue – residue hydrogen bond mediates the specificity of ribonuclease A." J. Mol. Biol.: In Press.

delCardayré, S.B., Ribó, M., Yokel, E.M., Quirk, D.J., Rutter, W.J. and Raines, R.T. (1995). "Engineering ribonuclease A: production, purification, and characterization of wild-type enzyme and mutants at Gln11." Protein Engng. **8**: 261-273.

delCardayré, S.B., Thompson, J.T. and Raines, R.T. (1994). Altering substrate specificity and detecting processivity in nucleases. Techniques in Protein Chemistry V. J. W. Crabb. San Diego, CA, Academic Press: 313-320.

Eftink, M.R. and Biltonen, R.L. (1983). "Energetics of ribonuclease A catalysis. 1. pH, ionic strength, and solvent isotope dependence of the hydrolysis of cytidine cyclic 2',3'–phosphate." Biochemistry **22**: 5123-5134.

Eftink, M.R. and Biltonen, R.L. (1983). "Energetics of ribonuclease A catalysis. 2. Nonenzymatic hydrolysis of cytidine cyclic 2',3'-phosphate." Biochemistry **22**: 5134-5140.

Erman, J.E. and Hammes, G.G. (1966). "Relaxation spectra of Ribonuclease. IV. The interaction of Ribonuclease with cytidine 2′,3′-cyclic phosphate." J. Am. Chem. Soc. **88**: 5607-5614.

Fersht, A. (1985). Enzyme Structure and Mechanism. New York, Freeman.

Fickling, M.M., Fischer, A., Mann, B.R., Packer, J. and Vaughan, J. (1959). "Hammet substituent constants for electron withdrawing substituents: Dissociation of phenols, anilinium ions and dimethyl anilinium ions." J. Am. Chem. Soc. **81**: 4226–4230.

Findlay, D., Herries, D.G., Mathias, A.P., Rabin, B.R. and Ross, C.A. (1961). "The active site and mechanism of action of bovine pancreatic ribonuclease." Nature **190**: 781-784.

Fontecilla-Camps, J.C., de Llorens, R., le Du, M.H. and Cuchillo, C.M. (1994). "Crystal structure of ribonuclease A•d(ApTpApApG) complex." J. Biol. Chem. **269**: 21526-21531.

Fontecilla–Camps, J.C., Llorens, R.d., Du, M.H.L. and Cuchillo, C.M. (1995). "Crystal structure of the ribonuclease A d(ApTpApApG) complex: Direct evidence for extended subsite recognition." manuscript in preparation.

Fromageot, H.P.M., Griffin, B.E., Reese, C.B. and Sulston (1967). "The synthesis of oligoribonucleotides-III Monoacylation of ribonucleosides and derivatives *via* orthoester exchange." Tetrahedron **23**: 2315-2331.

Ganguly, S. and Kundu, K.K. (1993). "Transfer energetics of some DNA and RNA bases in mixtures of urea and glycerol." J. Phys. Chem. **97**: 10862-10867.

Gerlt, J.A. and Gassman, P.G. (1993). "Understanding the rates of certain enzyme-catalyzed reactions: proton abstraction from carbon acids, acyl-transfer reactions, and displacement reactions of phosphodiesters." Biochemistry **32**: 11943-11952.

Hakimelahi, G.H., Proba, Z.A. and Ogilvie, K.K. (1981). "New catalysts and procedures for the demethoxytritylation and selective silylation of ribonucleosides." Can. J. Chem. **60**: 1106-1113.

Hartley, R.W. (1993). "Directed mutagenesis and barnase-barstar recognition." Biochemistry **32**: 5978-5984.

Herschlag, D. (1994). "Ribonuclease revisited: Catalysis via the classical general acid-base mechanism or a triester-like mechanism?" J. Am. Chem. Soc. **116**: 11633-11635.

Hochachka, P.W. and Somero, G.N. (1984). Biochemical Adaptation. Princeton, NJ, Princeton University Press.

Hofmann, K., Visser, J.P. and Finn, F.M. (1970). "Studies on polypepties XLIV. Potent synthetic S–peptide antagonists." J. Am. Chem. Soc. **92**: 2900-2910.

Howlin, B., Moss, D.S., Harris, G.W. and Palmer, R.A. (1992). "Manuscript in preparation." .

Ipata, P.L. and Felicioli, R.A. (1968). "A spectrophotometric assay for ribonuclease activity using Cytidyl-(3',5')-Adenosine and uridyl-(3',5')-adenosine as substrates." FEBS Lett. **1**(1): 29-31.

Jackson, D.Y., Burnier, J., Quan, C., Stanley, M., Tom, J. and Wells, J.A. (1994). "A designed peptide ligase for total synthesis of ribonuclease A with unnatural catalytic residues." Science **266**: 243–247.

Jencks, W.P. (1987). Catalysis in Chemistry and Enzymology. Mineola, NY, Dover.

Kahne, D. and Still, W.C. (1988). "Hydrolysis of a peptide bond in neutral water." J. Am. Chem. Soc. **110**: 7529-7534.

Kim, J.-S. and Raines, R.T. (1993). "Bovine seminal ribonuclease produced from a synthetic gene." J. Biol. Chem. **268**: 17392-17396.

Kluger, R. and Taylor, S.D. (1990). "On the origins of enhanced reactivity of five-membered cyclic phosphate esters. The relative contributions of enthalpic and entropic factors." J. Am. Chem. Soc. **112**: 6669-6671.

Knowles, J.R. (1987). "Tinkering with enzymes: What are we learning?" Science **236**: 1252-1258.

Kuhler, T.C. and Lindsten, G.R. (1983). "Preparative reversed–phase flash chromatography, a convenient method for workup of reaction mixtures." J. Org. Chem. **48**: 3589–3591.

Kumamoto, J., Cox, J.R. and Westheimer, F.H. (1956). "Barium ethylene phosphate." J. Am. Chem. Soc. **78**: 4858-4860.

Kunitz, M. (1939). "Isolation from beef pancreas of a crystalline protein possessing ribonuclease activity." Science **90**: 112-113.

Kunkel, T.A., Roberts, J.D. and Zakour, R.A. (1987). "Rapid and efficient site-specific mutagenesis without phenotypic selection." Methods Enzymol. **154**: 367-382.

LeTilly, V. and Royer, C.A. (1993). "Fluorescence anisotropy assays implicate protein–protein interactions in regulating *trp* repressor DNA binding." Biochemistry **32**: 7753-7758.

Markham, R. and Smith, J.D. (1952). "The structure of ribonucleic acids I Cyclic nucleotides produced by ribonuclease and by alkaline hydrolysis." Biochem. J. **52**: 552-557.

Markley, J.M. (1975). "Observation of histidine residues in proteins by means of nuclear magnetic resonance spectroscopy." Acc. Chem. Res. **8**: 70-79.

McGeehan, G.M. and Benner, S.A. (1989). "An improved system for expressing pancreatic ribonuclease in *Escherichia coli*." FEBS Lett. **247**(1): 55-56.

Medwedew, G. (1937). Enzymologia **2**: 53-72.

Menger, F.M. (1991). "The negative rate constants of Breslow and Huang." J. Org. Chem. **56**: 6251-6252.

Messmore, J.M., Fuchs, D.N. and Raines, R.T. (1995). "Ribonuclease A: revealing structure – function relationships with semisynthesis." J. Am. Chem. Soc. **117**(31): 8507-8060.

Messmore, J.M. and Raines, R.T. (1995). : manuscript in preparation.

Nachman, J., Miller, M., Gilliland, G., Carty, R., Pincus, M. and Wlodawer, A. (1990). "Crystal structures of two nucleoside derivatives of RNase A." Biochemistry: 928-937.

Northrop, D.B. and Rebholz, K.L. (1994). "Kinetics of enzymes with iso-mechanisms: analysis and display of progress curves." Anal. Biochem. **216**: 285-290.

Ogilvie, K.K., Beaucage, S.L., Schifman, A.L., Theriault, N.Y. and Sadana, K.L. (1978). "The synthesis of oligoribonucleotides. II. The use of silyl protecting groups in nucleoside and nucleotide chemistry. VII." Can. J. Chem. **56**: 2768-2780.

Parés, X., Nogués, M.V., de Llorens, R. and Cuchillo, C.M. (1991). "Structure and function of ribonuclease A binding subsites." Essays Biochem. **26**: 89-103.

Quirk, D.J. and Raines, R.T. (1995). "Catalytic dyad of ribonuclease A: role of Asp121 in catalysis." Biochemistry: Submitted.

Quirk, D.J. and Raines, R.T. (1995). "Role of aspartate 121 in catalysis by RNase A." Biophys. J.: manuscript in preparation.

Radzicka, A. and Wolfenden, R. (1995). "A proficient enzyme." Science **267**: 90-92.

Raines, R.T. and Hansen, D.E. (1988). "An intuitive approach to steady-state kinetics." J. Chem. Ed. **65**: 757-759.

Rebholz, K.L., Thompson, J.E., Raines, R.T. and Northrup, D.B. (1993). "unpublished results." .

Richards, F.M. and Vithayathil, P.J. (1959). "The preparation of subtilisin-modified ribonuclease and the separation of the peptide and protein components." J. Biol. Chem. **234**: 1459-1465.

Richards, F.M. and Wyckoff, H.W. (1971). "Bovine pancreatic ribonuclease." The Enzymes **IV**: 647-806.

Sanders, J.K.M. and Hunter, B.K. (1987). . Modern NMR Spectroscopy – a guide for chemists. Tiptree, UK, Courier International Ltd.

Schimmel, P. (1989). "Hazards of deducing enzyme structure–activity relationships on the basis of chemical applications of molecular biology." Acc. Chem. Res. **22**: 232-233.

Segel, I.H. (1975). Enzyme Kinetics. New York, Wiley.

Serpersu, E.H., Shortle, D. and Mildvan, A.S. (1986). "Kinetic and magnetic resonance studies of effects of genetic substitutions of a Ca^{2+}-liganding amino acid in staphylococcal nuclease." Biochemistry **25**: 68-77.

Shapiro, R., Fett, J.W., Strydom, D.J. and Vallee, B.L. (1986). "Isolation and characterization of a human colon carcinoma-secreted enzyme with pancreatic ribonuclease-like activity." Biochemistry **25**: 7255-7264.

Sinha, N.D., Biernat, J. and Koster, H. (1984). "Polymer support oligonucleotide synthesis XVIII: Use of β-cyanoethyl-*N*,*N*-dialkylamino-/*N*-morpholino phosphoramidite of deosynuclosides for the synthesis of DNA fragments simplifying deporotection and isolation of the final product." Nucleic Acids Res. **12**: 4539-4557.

Still, W.C., Kahy, M. and Mitra, A. (1978). J. Org. Chem. **43**: 2923-2925.

Tamburrini, M., Piccoli, R., De Prisco, R., Di Donato, A. and D'Alessio, G. (1986). "Fast and high-yielding procedures for the isolation of bovine seminal RNAase." Ital. J. Biochem. **35**: 22-32.

Taylor, H.C., Richardson, D.C., Richardson, J.S., Wlodawer, A., Komoriya, A. and Chaiken, I.M. (1981). "Active" conformation of an inactive semi-synthetic ribonuclease-S." J. Mol. Biol. **149**: 313-317.

Templer, B. (1995). Biochemistry: manuscript in preparation.

Thompson, J.E. and Raines, R.T. (1994). "Value of general acid-base catalysis to ribonuclease A." J. Am. Chem. Soc. **116**: 5467-5468.

Warshaw, M.M. and Tinoco, I. (1966). "Optical properties of sixteen dinucleoside phosphates." J. Mol. Biol. **20**: 29-38.

Witzel, H. (1963). "The function of the pyrimidine base in the ribonuclease reaction." Progr. Nucleic Acid Res. **2**: 221-258.

Witzel, H. and Barnard, E.A. (1962). "Mechanism and binding sites in the ribonuclease reaction II. Kinetic studies of the first step of the reaction." Biochem. Biophys. Res. Com. **7**(4): 295-299.

Wlodawer, A. and Sjolin, L. (1981). "Orientation of histidine residues in RNase A." Proc. Nat. Acad. Sci. **78**(2853-2855).

Wolfenden, R. (1976). "Transition state analog inhibitors and enzyme catalysis." Annu. Rev. Biophys. Bioeng. **5**: 271-306.

Wyckoff, H.W., Hardman, K.D., Allewell, N.M., Inagami, T., Tsernoglou, D., Johnson, L.N. and Richards, F.M. (1967). "The structure of ribonuclease-S at 6 Å resolution." J. Biol. Chem. **242**: 3749-3753.

Yakovlev, G.I., Bocharov, A.L., Moiseyev, G.P. and Mikhaylov, S.N. (1985). FEBS Lett. **179**: 217-220.

Zegers, I., Maes, D., Dao-thi, M.H., Wyns, L., Poortmans, F. and Palmer, R. (1994). "manuscript in preparation." .